Ontario Geological Survey
Study 55

Chromite Deposits in Ontario

by
Peter J. Whittaker

1986

Ontario
Ministry of
Northern Development
and Mines

©1986 Government of Ontario
ISSN 0704-2590
Printed in Ontario, Canada
ISBN 0-7729-1640-3

Publications of the Ontario Geological Survey, Ministry of Northern Development and Mines, are available from the following sources. Orders for publications should be accompanied by cheque or money order payable to the *Treasurer of Ontario*.

Reports, maps, and price lists (personal shopping or mail order):

Public Information Centre, Ministry of Natural Resources
Room 1640, Whitney Block, Queen's Park
Toronto, Ontario M7A 1W3

Reports and accompanying maps only (personal shopping):

Ontario Government Bookstore
Main Floor, 880 Bay Street
Toronto, Ontario M7A 1N8

Reports and accompanying maps (mail order or telephone orders):

Publications Services Section, Ministry of Government Services
5th Floor, 880 Bay Street
Toronto, Ontario M7A 1N8
Telephone (local calls) 965-6015
Toll-free long distance 1-800-268-7540
Toll-free from Area Code 807 0-ZENITH-67200

Canadian Cataloguing in Publication Data

Whittaker, Peter J.

Chromite deposits in Ontario

(Ontario Geological study, ISSN 0704-2590; 55)

Includes index.

ISBN 0-7729-1640-3

1. Chromite--Ontario. I. Ontario. Ministry of Northern Development and Mines. II. Ontario Geological Survey. III. Title. IV. Series

TN490.C4W48 1986 549'.526 C86-099687-5

Every possible effort is made to ensure the accuracy of the information contained in this report, but the Ministry of Northern Development and Mines does not assume any liability for errors that may occur. Source references are included in the report and users may wish to verify critical information.

Parts of this publication may be quoted if credit is given. It is recommended that reference be made in the following form:

Whittaker, Peter J.
1986: Chromite Deposits in Ontario; Ontario Geological Survey, Study 55, 97p.

If you wish to reproduce any of the text, tables or illustrations in this report, please write for permission to the Director, Ontario Geological Survey, Ministry of Northern Development and Mines, 11th floor, 77 Grenville Street, Toronto, Ontario, M7A 1W4.

Critical Reader: J.A. Robertson

Scientific Editor: M.L.T. Stuart

1500-86-Twin Offset

Foreword

Chromium, which is important in the production of hardened steels and corrosion-resistant alloys, occurs in nature primarily as the oxide mineral chromite. Mineable accumulations of chromite are known from mafic and ultramafic intrusions; disseminated chromite occurs in extrusive equivalents of these rock types, and secondary accumulations are known from sedimentary rocks.

This report reviews the geology of known chromite occurrences in Ontario, and discusses the significance of the petrology and chemistry of chromite in these occurrences as they pertain to the exploitation of this potential resource.

This information will aid in defining exploration targets for chromite in Ontario.

V.G. Milne

Director

Ontario Geological Survey

Contents

Abstract 2
Résumé 2
Introduction 2
  Acknowledgments 3
Mineralogical Characteristics of Chromite 3
  Rocks of Komatiitic Affinity 5
  Middle Precambrian Gabbroic Anorthosites 6
  Nipissing Diabase 7
  Metasedimentary Rocks 7
  Ultramafic Intrusions 9
  Rocks of Mafic Composition 9
Puddy-Chrome Lakes Deposit 9
  Location and Access 11
  Previous Work 11
  General Geology 11
  Detailed Geology 11
  Alteration 11
  Chromite Occurrences 11
  Disseminated and Layered Chromite 15
  Petrography 15
  Chromite 17
  Magnetite 18
  Lizardite 21
  Antigorite 21
  Chlorite 25
  Chromite Compositional Variation 26
  Major Element Chemistry 26
  Trace Element Chemistry 28
  Summary 30
Big Trout Lake Deposit 31
  Location and Access 37
  Previous Work 37
  General Geology 37
  Anorthositic Rocks 37
  Serpentinized Ultramafic Rocks 40
  Serpentinite 43
  Lizardite and Antigorite 43
  Chromite 44
Major and Trace Element Chemistry 44
  Chromite Chemistry 52
  Summary 52
Crystal Lake Gabbro 52
  Location and Access 62
  Previous Work 62
  General Geology 62
  Crystal Lake Gabbro 62
  Layering 70
  Pegmatitic Patches 70
  Chromite 70
  Petrography 71
    Feldspar 71
    Olivine and Pyroxene 71
    Opaques 71
  Major Element Chemistry 71
  Trace Element Chemistry 72
  Summary 72

Other Chromite Occurrences 82
Shebandowan Mine 82
Chromite Zone 82
Chromite in the Extrusive Environment 82
Summary and Conclusions 86
References 89

FIGURES

1. Chromite occurrences in Ontario 3
2. Median Cr values of various mafic-ultramafic rocks, Ontario 4
3. Percentage frequency distribution vs. ppm Cr for rocks of komatiitic affinity 7
4. Percentage frequency distribution vs. ppm Cr for Nipissing Diabase 8
5. Percentage frequency distribution vs. ppm Cr for dunites, peridotites, and their serpentinized equivalents 8
6. Percentage frequency distribution vs. ppm Cr for gabbroic and basaltic rocks, exclusive of Nipissing Diabase 10
7. General Geology of Puddy and Chrome Lakes 12
8. Disseminated and layered chromite occurrences, Chrome Lake 13
9. Mine shaft area chromite occurrence, Chrome Lake 14
10. Schematic diagram of the temperature regimes of the observed assemblages 16
11. Magnetic anomalies at Puddy Lake and high Ni zone 22
12. Composition of Puddy-Chrome Lakes chromite grains 27
13. Plot of Cr and Mg ratios for Puddy-Chrome Lakes chromite grains 27
14. Plot of Fe^{+3} and Mg ratios for Puddy-Chrome Lakes chromite grains 28
15. Plot of Puddy-Chrome Lakes chromite analyses 29
16. Plot of Puddy-Chrome Lakes ultramafic rocks, SiO_2 vs. FeO/MgO 30
17. AFM plot of whole rock analyses from the Puddy-Chrome Lakes area 31
18. Ternary diagrams $CaO-MgO-Al_2O_3$ and $Fe_2O_3-MgO-Al_2O_3$ 32
19. Ni vs. Cr plot of chromites from the Puddy-Chrome Lakes area 34
20. Plot of Cr-Ni-Co and Cr-Ni-Cu, Puddy-Chrome Lakes area 35
21. Variation of Cr_2O_3, NiO, and TiO_2 with MgO in the Puddy-Chrome Lakes serpentinite 36
22. Location map, Big Trout Lake, Ontario 37
23. General geology of the Big Trout Lake area 38
24. Features of an ultramafic xenolith 40
25. Drill sections through magnetic anomaly 41
26. Stratigraphic section, hole 57321, section 20000 N, Big Trout Lake 45
27. Stratigraphic section, hole 57320, section 20000 N, Big Trout Lake 46
28. Stratigraphic section, hole 57314, section 800 S, Big Trout Lake 47
29. Stratigraphic section, hole 57310, line 800 S, Big Trout Lake 48
30. Stratigraphic section, hole 57313, line 800 S, Big Trout Lake 49
31. AFM plot of serpentinite and anorthosite rocks from Big Trout Lake 54
32. Plot of SiO_2 vs. FeO/MgO 54
33. Compositional plots of chromite rims and cores from Big Trout Lake 55
34. Plot of NiO (weight percent) vs. Cr_2O_3 (weight percent), Big Trout Lake 58
35. Plot of Cr_2O_3, NiO, and TiO_2 vs. MgO for Big Trout Lake samples 58
36. Cr/Fe ratios vs. MgO (weight percent) of chromites from Big Trout Lake 59

37. Plot of 100 Cr/(Al+Cr) vs. 100 Mg/(Mg+Fe^{+2}), of chromites from Big Trout Lake 61
38. Location map showing the Crystal Lake Gabbro 62
39. The Crystal Lake Gabbro showing location of drill holes 63
40. Distribution of disseminated chromite, Crystal Lake Gabbro 64
41. AFM plot of Crystal Lake Gabbro samples 69
42. Plot of MgO-CaO-Al_2O_3 and MgO-Fe_2O_3-Al_2O_3 from the Crystal Lake Gabbro 73
43. Plot of SiO_2 vs. FeO/MgO, Crystal Lake Gabbro 74
44. FeO/MgO ratios in chromitiferous anorthositic gabbro, Crystal Lake Gabbro 75
45. Cr and Ni values for samples from chromitiferous anorthositic gabbro, Crystal Lake Gabbro 76
46. Cu and Co values for samples from chromitiferous anorthositic gabbro, Crystal Lake Gabbro 77
47. Pb and Zn values for samples from chromitiferous anorthositic gabbro, Crystal Lake Gabbro 78
48. Plot of Ni-Cr-Co and Cu, Crystal Lake Gabbro 80
49. Plot of Cr_2O_3, NiO, and TiO_2 vs. MgO, Crystal Lake Gabbro 81
50. NiO vs. Cr_2O_3, Crystal Lake Gabbro 81
51. Simplified plan of ultramafics and ore at Shebandowan Mine 83
52. Section A-A′ looking west, Shebandowan Mine 84
53. Section B-B′ looking west, Shebandowan Mine 85

TABLES

1. Specifications for chromite ores or concentrates required by industry 5
2. Modal analyses of serpentinites from Chrome Lake 16
3. Microprobe analyses of chromite in peridotite from Puddy-Chrome Lake 26
4. Cr/Fe ratios from Puddy-Chrome Lakes 29
5. Major and trace element analyses from Puddy-Chrome Lakes area 33
6. Cr values from Puddy-Chrome Lakes chromite occurrences 36
7. Modal analyses of serpentinites from Big Trout Lake 42
8. Major and trace element analyses from Big Trout Lake 53
9. Microprobe analyses of chromite from Big Trout Lake 56
10. Cr/Fe ratios from Big Trout Lake 60
11. Major and trace element analyses from the Crystal Lake Gabbro 67
12. Summary of chromite-bearing deposits in Ontario 87

PHOTOGRAPHS

1. Subhedral disseminated chromite 17
2. Euhedral and subhedral chromite, Chrome Lake 18
3. Highly fractured and inclusion-rich chromite, Chrome Lake 19
4. Inclusion-filled chromite 19
5. Massive chromite with intercumulus lizardite and magnetite 20
6. Relict chromite boundaries 21
7. Secondary magnetite in anastomosing fractures 23
8. Lizardite bastite defining pseudomorphic texture after clinopyroxene 23
9. Columnar fracture modifying lizardite mesh texture 24
10. Antigorite rimming relict olivine 24
11. Interlocking antigorite developed in random orientation 25

12. Porphyritic gabbroic anorthosite, Big Trout Lake 39
13. Layered gabbro and anorthositic gabbro at Leopard Point 39
14. Serpentinized olivine with lizardite cores and antigorite rims 42
15. Serrated edges on corroded chromite grains, Big Trout Lake 50
16. Silicate inclusion zones and negative crystal cavity fillings in chromite, Big Trout Lake 51
17. Sulphide trapped between chromite grains, Big Trout Lake 51
18. Three- to five-centimetre layering in upper anorthositic gabbro zone, Crystal Lake Gabbro 65
19. Half-metre layering, Crystal Lake Gabbro 65
20. Chromite poikilitically included within plagioclase, Crystal Lake Gabbro 66

CONVERSION FACTORS FOR MEASUREMENTS IN ONTARIO GEOLOGICAL SURVEY PUBLICATIONS

If the reader wishes to convert imperial units to SI (metric) units or SI units to imperial units the following multipliers should be used:

CONVERSION FROM SI TO IMPERIAL			CONVERSION FROM IMPERIAL TO SI		
SI Unit	*Multiplied by*	*Gives*	*Imperial Unit*	*Multiplied by*	*Gives*
		LENGTH			
1 mm	0.039 37	inches	1 inch	**25.4**	mm
1 cm	0.393 70	inches	1 inch	**2.54**	cm
1 m	3.280 84	feet	1 foot	**0.304 8**	m
1 m	0.049 709 7	chains	1 chain	20.116 8	m
1 km	0.621 371	miles (statute)	1 mile (statute)	1.609 344	km
		AREA			
1 cm²	0.155 0	square inches	1 square inch	**6.451 6**	cm²
1 m²	10.763 9	square feet	1 square foot	**0.092 903 04**	m²
1 km²	0.386 10	square miles	1 square mile	2.589 988	km²
1 ha	2.471 054	acres	1 acre	0.404 685 6	ha
		VOLUME			
1 cm³	0.061 02	cubic inches	1 cubic inch	16.387 064	cm³
1 m³	35.314 7	cubic feet	1 cubic foot	0.028 316 85	m³
1 m³	1.308 0	cubic yards	1 cubic yard	0.764 555	m³
		CAPACITY			
1 L	1.759 755	pints	1 pint	0.568 261	L
1 L	0.879 877	quarts	1 quart	1.136 522	L
1 L	0.219 969	gallons	1 gallon	4.546 090	L
		MASS			
1 g	0.035 273 96	ounces (avdp)	1 ounce (avdp)	28.349 523	g
1 g	0.032 150 75	ounces (troy)	1 ounce (troy)	31.103 476 8	g
1 kg	2.204 62	pounds (avdp)	1 pound (avdp)	0.453 592 37	kg
1 kg	0.001 102 3	tons (short)	1 ton (short)	907.184 74	kg
1 t	1.102 311	tons (short)	1 ton (short)	0.907 184 74	t
1 kg	0.000 984 21	tons (long)	1 ton (long)	1016.046 908 8	kg
1 t	0.984 206 5	tons (long)	1 ton (long)	1.016 046 908 8	t
		CONCENTRATION			
1 g/t	0.029 166 6	ounce (troy)/ ton (short)	1 ounce (troy)/ ton (short)	34.285 714 2	g/t
1 g/t	0.583 333 33	pennyweights/ ton (short)	1 pennyweight/ ton (short)	1.714 285 7	g/t

OTHER USEFUL CONVERSION FACTORS

1 ounce (troy)/ton (short)	20.0	pennyweights/ton (short)
1 pennyweight/ton (short)	0.05	ounce (troy)/ton (short)

NOTE–Conversion factors which are in bold type are exact. The conversion factors have been taken from or have been derived from factors given in the Metric Practice Guide for the Canadian Mining and Metallurgical Industries published by The Mining Association of Canada in co-operation with the Coal Association of Canada.

Chromite Deposits in Ontario

by
Peter J. Whittaker

Geologist, Mineral Deposits Section, Ontario Geological Survey, Toronto.

Manuscript approved for publication June 24, 1980, by J.A. Robertson, Chief, Mineral Deposits Section, Ontario Geological Survey, Toronto. This report is published with the permission of V.G. Milne, Diractor, Ontario Geological Survey.

Abstract

Chromite in Ontario occurs in three crystallization environments: plutonic, hypabyssal, and extrusive. In these, three modes of chromite mineralization are represented. Within the framework of environment and mode of mineralization, the exploration potential for each situation is examined for the deposits dealt with in this study.

Mafic to ultramafic rocks or their serpentinized equivalents host chromite mineralization which occurs most commonly in disseminated and layered form and less frequently in podiform style. The layered and disseminated chromite is developed in ultramafic to mafic Archean fractionated hypabyssal (subvolcanic) sills as represented by the deposits at Big Trout Lake and Shebandowan. The Crystal Lake Gabbro is a fractionated chromitiferous hypabyssal sill of Proterozoic age which intrudes older Proterozoic metasedimentary rocks. Podiform chromite in the Puddy-Chrome Lakes ultramafic body occurs in conjunction with disseminated and layered chromite. Disseminated chromite occurs as an accessory mineral in extrusive komatiitic Archean metavolcanic rocks and minor chromite concentrations occur as placer deposits in sedimentary rocks.

Results from work on Ontario chromite suggest that potential for layered chromite deposits lies in large-volume, Archean, fractionated, ultramafic to anorthositic intrusions similar to the Big Trout Lake Occurrence. Smaller intrusions, such as the Puddy-Chrome Lakes body, hold potential for less extensive but higher grade podiform chromite mineralization.

Résumé

A l'Ontario, la chromite survient dans trois milieux de cristallisation: plutonique, hypabyssal, et extrusive. Dans ces environements trois modes de minéralisation de chromite sont présentes. Dans le cadre des milieux et les modes de minéralisation, le potentiel d'exploration pour chaque situation, pour tous les gisements inclus dans cette étude, est examiné.

Les roches mafiques et ultramafiques ou leurs équivalentes serpentinisées hôtent la minéralisation de chromite qui survient ordinairement comme disséminée et stratifiée et peu fréquemment comme masse minéralisée allongée. La chromite stratifiée et disséminée s'est developé dans des filons-couches mafiques et ultramafiques fractionnés hypabyssaux (sous-volcaniques) et se représent aux gisements de Big Trout Lake et Shebandowan. Le pluton gabbroïque de Crystal Lake est un filon-couche chromifère, hypabyssal fractionné de Protérozoïque qui s'introduit dans les roches métasédimentaires de Protérozoïque inférieur. Dans les roches ultramafiques de Puddy-Chrome Lakes, la chromite à masse allongée est accompaniée par la chromite disséminée et stratifiée. Chromite disséminée survient comme un minéral accessoire dans les roches extrusives komatiitiques d'Archéen et quelques concentrations mineures de chromite surviennent dans les gisements alluviaux dans les roches sédimentaires.

Les résultats du travail sur les gisements de chromite de l'Ontario suggérent que le potentiel pour des gisements stratifiés peut se trouver dans les grands intrusions ultramafiques à anorthositiques fractionnés d'Archéen comme les gisements de Big Trout Lake. Des intrusions plus petits, comme Puddy-Chrome Lakes soutiennent le potentiel pour des gisements à masse minéralisée allongée plus petits mais à teneurs plus fortes.

Chromite Deposits in Ontario, by Peter J. Whittaker, Ontario Geological Survey, Study 55, 97p. Published 1986. ISBN 0-7729-1640-3.

Introduction

A two-year program to examine chromite mineralization in Ontario was initiated by the Mineral Deposits Section, Ontario Geological Survey (Ministry of Northern Development and Mines, formerly Ministry of Natural Resources) in May 1978. This work (Figure 1) was aimed at classifying the style of chromite mineralization, identifying the crystallization environment, and assessing Ontario's potential for economic chromite deposits. Field and analytical work was undertaken to investigate known chromite deposits and to establish background Cr concentrations in various rock types as well as to examine the Cr content in chromite. Chromium analyses from Ontario Geological Survey reports dating back to 1965 were collected, and from these data, average Cr values were established for various mafic and ultramafic rock types, and anomalous occurrences were thus identified. Figure 2 illustrates the Cr values which were determined as upper limits of average concentrations for these mafic and ultramafic rocks.

ACKNOWLEDGMENTS

The author would like to gratefully acknowledge D.G. Innes (Geologist, Mineral Deposits Section, Ontario Geological Survey, Sudbury) for his assistance, and for critically reviewing the manuscript along with J.A. Robertson (Chief, Mineral Deposits Section, Ontario Geological Survey, Toronto) and F.J. Wicks (Geologist, Royal Ontario Museum, Toronto). Discussions on the Puddy Lake area with C. Kustra

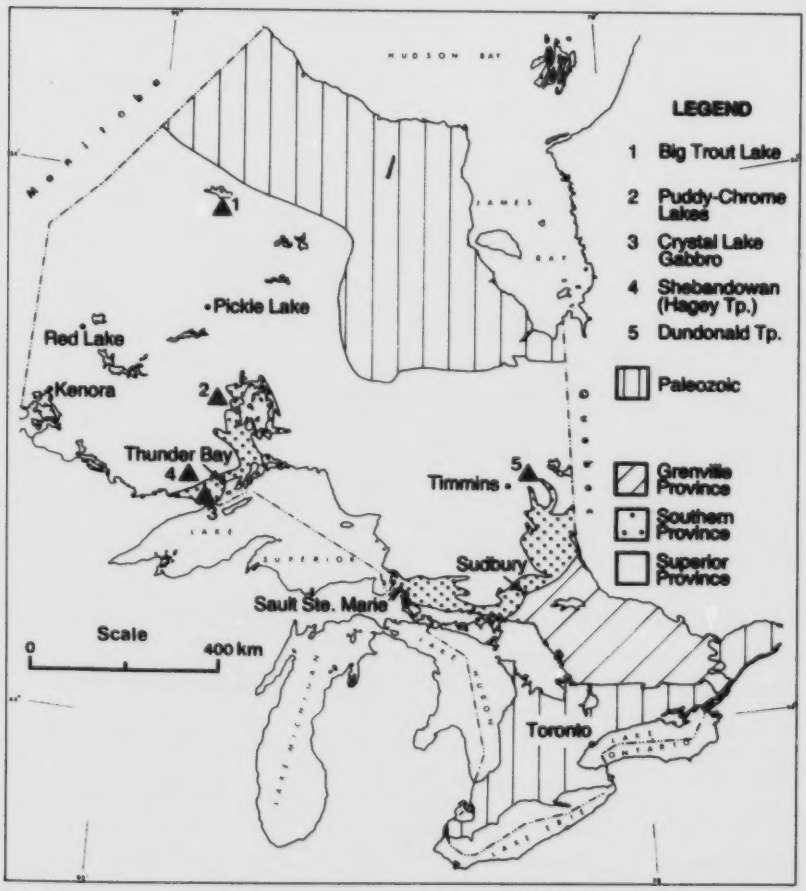

Figure 1. *Chromite occurrences in Ontario.*

(Regional Liaison Geologist, Ontario Geological Survey, Toronto) were helpful. R. Morin and J. Weaver provided capable field assistance. Drill core samples for the work on the Big Trout Lake serpentinite and sections showing chromite at Shebandowan were freely provided by the Canadian Nickel Company Limited and their help is gratefully acknowledged. Great Lakes Nickel Limited cooperated by providing access to drill core sections through the Crystal Lake Gabbro. Microprobe analyses of chromite from Big Trout Lake and from the Puddy-Chrome Lakes areas were provided by D.H. Watkinson (Professor, Carleton University, Ottawa) and P. Mainwaring (Research Associate, Carleton University, Ottawa).

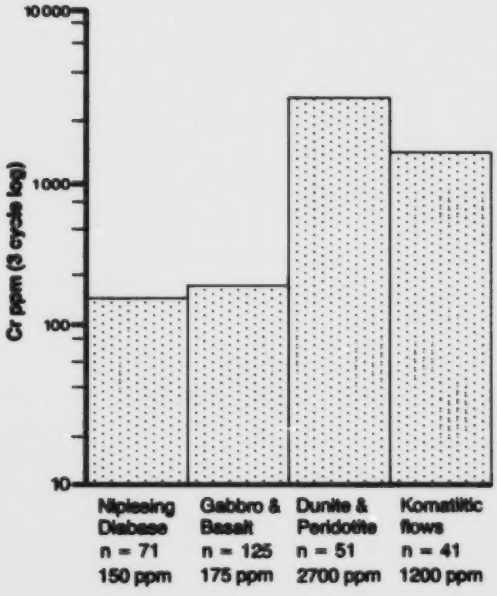

Figure 2. Median Cr values of various mafic-ultramafic rocks, Ontario.

Mineralogical Characteristics of Chromite

Chromite occurs most commonly as an accessory mineral in mafic and ultramafic rocks; under appropriate circumstances, it becomes concentrated to form ore grade mineralization. Chromite belongs to a solid solution series, with the end members spinel and magnesiochromite, which involves the main substitution of Al^{+3} for Cr^{+3} in the octahedral sites. The octahedral radius of Cr^{+3} is 0.615 angstrom (Shannon and Prewitt 1969) which is similar to the octahedral radii of Al^{+3} (0.53 angstrom), Fe^{+3} (0.645 angstrom), Ti^{+4} (0.68 angstrom), and Mg^{+2} (0.72 angstrom) (Burns and Burns 1975). Consequently, Cr^{+3} can be substituted into the octahedral sites of several silicate minerals apart from those in the spinel-magnesiochromite solid solution series.

Chromite is categorized as either metallurgical, chemical, or refractory grade, primarily by its Cr:Fe ratio. In addition, the amount of SiO_2, Al_2O_3, CaO, and 0 in the gangue material affects the grading of the ore. Table 1 presents the characteristics which are used to classify chromite ores or concentrates (Raicevic 1977). Metallurgical grade chromite, with a Cr:Fe ratio of 2.8, is used for production of chromium metal and ferrochromium alloys; refractory grade material is used for furnace bricks and other refractories; and chemical grade chromite, with a Cr:Fe ratio of 1.6:1, finds uses in the production of chromium chemicals. Hard lumpy ore produces a chromium metal with a low level of carbon. Friable ore is finer grained, reacting at lower temperatures to produce higher carbon alloys (Downing 1971).

Apart from the industrial uses of chromite, which are primarily for the hardening of steel and the development of highly corrosion resistant alloys, chromium is of interest to petrology. Chromium is the tenth most abundant element and chromite, its main mineral, is an important indicator of physical-chemical conditions under which ultramafic and mafic rocks were formed. The multiple valency of Cr in chromite, from Cr^{+2} to Cr^{+6}, and the variety of elements with similar ionic radii which can substitute for Cr, make it a sensitive petrogenetic indicator.

Chromite is found primarily in ultramafic rocks in various geologic environments, including: continental stratiform layered intrusions, ophiolitic suites and associated alpine-type peridotites, and ultramafic extrusive komatiitic volcanic rocks. Chromite also occurs to a lesser extent as placer-type deposits in sedimentary rocks.

The major world supply of chromium is produced from the Bushveld Complex in South Africa (Buchanan 1979). The Bushveld Complex is a continental layered intrusion which fractionated from ultramafic rocks, primarily peridotite, to a granophyre end product. Recent age determinations by Coertze *et al.* (1978), using U-Pb determinations, indicate an approximate age of 1950 million years (m.y.) for the Bushveld granite and ages about 100 m.y. older for the basic portions of the complex. The mafic rocks are approximately 8 km thick and have been subdivided into five zones with the appearance of chromite marking the boundaries of the upper zones (Hunter 1978). The various zones form repeated cyclic units. An idealized cyclic unit, as described by Hunter (1978), would begin with chromite and be followed by successive layers in which the predominant minerals are olivine, pyroxene, and finally plagioclase, which forms an upper anorthosite layer.

TABLE 1. SPECIFICATIONS FOR CHROMITE ORES OR CONCENTRATES REQUIRED BY INDUSTRY (RAICEVIC 1977, p. 62).

Metallurgical grade	Refractory grade	Chemical grade
>48% Cr_2O_3	Approx. 31% Cr_2O_3	Approx. 45% Cr_2O_3
>2.8 Cr:Fe ratio	12% Fe	Cr:Fe = 1.6:1
<3% SiO_2	<6% SiO_2	<5% SiO_2
<25% $MgO + Al_2O_3 + CaO$	25% Al_2O_3	<15% Al_2O_3
Preferably hard and lumpy ore	Preferably hard and lumpy ore	Friable ores acceptable

In the western part of the complex, the main chromite seam, known as the LG6 or the Main Seam, has been outlined over a strike length of 70 km. In the eastern part of the complex, the main chromite seam, the Steelport bed, has been traced over a strike length of 90 km. Ore reserves, in the eastern and western lobes of the complex, total 1 094 150 000 metric tonnes of chromite. In some areas where the Cr:Fe ratio is low, platinum group element (PGE) values are sufficient to produce ore grade material, with chromite produced as a by-product (Buchanan 1979).

North American chromite-bearing equivalents of the Bushveld Complex occur on a smaller scale and include the Stillwater and Muskox Intrusions. Chromite in the Precambrian Stillwater Complex occurs in planar cumulate layers which form part of 15 cyclic units in the Ultramafic Zone (Page *et al.* 1976). The chromite-bearing units are traceable over a distance of about 32 km with some fault interruption. The Muskox Intrusion, approximately 1200 m.y. old, is a layered continental intrusion with chromitiferous layers in the mafic to ultramafic parts of the complex (Irvine and Smith 1967). The chromite occurs in both disseminated and layered forms predominantly in the ultramafic component. Disseminated chromite forms from 1% to 3% of the dunite, peridotite, and feldspathic peridotite while layered chromite occurs near the top of the main ultramafic zone. The chromite layers occur in peridotite immediately below orthopyroxenite. The lower chromite zone consists of a 1 to 2 m thick unit of disseminated mineralization with a 9 cm thick band of 50% to 70% chromite (Irvine and Smith 1967).

Chromite is produced from the ultramafic parts of ophiolite complexes, one of which is the Tertiary Troodos complex in Cyprus (Spooner *et al.* 1974). Chromite concentrations in the ultramafic portion of ophiolite complexes are typically podiform in shape, and random in distribution (Panayiotou 1978). The chromite which occurs in both disseminated and concentrated form develops chromitite pods in dunite. Podiform chromitite displays primary features (such as net texture) and schlieren structure developed by deformation (Greenbaum 1977). Chromite pods are developed as isolated cumulate patches near the base of the cumulate dunite. Later deformation served to further displace the pods resulting in their random distribution. Cr/Fe ratios range from 2.23 to 4.08 with the chromite being mostly chemical and metallurgical grade. The podiform type of chromite generally has a higher Cr/Fe ratio than chromite from stratified continental intrusions.

Podiform-type chromite is mined from ultramafic rocks in Pakistan where it forms irregular lenses and pods and has Cr/Fe ratios from 2.06 to 2.53 (Ahmed 1978). Similarly in Turkey, chromite is produced from podiform deposits some of which are mined by small scale private developments; however, most is produced by the state-owned mining company, Etibank. Turkish chromite reserves are estimated at 100 000 000 metric tonnes (Ethem 1979).

The production of chromite from various world sources leaves the Bushveld Complex as the single largest producer of chromite. Apart from the Bushveld Complex, the remainder of the world's chromium production is from chromite contained in podiform-type deposits, many of which represent the lower parts of ophiolite complexes.

In Ontario, several Cr deposits are known, representing various styles of Cr mineralization. At the present time, Cr is not mined in Ontario; however, minor production has come from a layered and podiform-type deposit in the Puddy-Chrome Lakes area.

ROCKS OF KOMATIITIC AFFINITY

Rocks of komatiitic affinity considered in this study include ultramafic komatiites and basaltic komatiites. The range in chromium values is from 200 to 2500 ppm. The median chromium concentration is 1200 ppm. The distribution of percent frequency chromium concentrations (Figure 3) reveals three peaks. The interval 600 to 700 ppm Cr represents 12% of the analyses, the interval 1200 to 1300 ppm Cr represents 10% of the analyses, and the interval 2300 to 2400 represents 7% of the analyses. Additional analyses to the 41 plotted must be collected to verify the validity of the Cr median for komatiitic rocks.

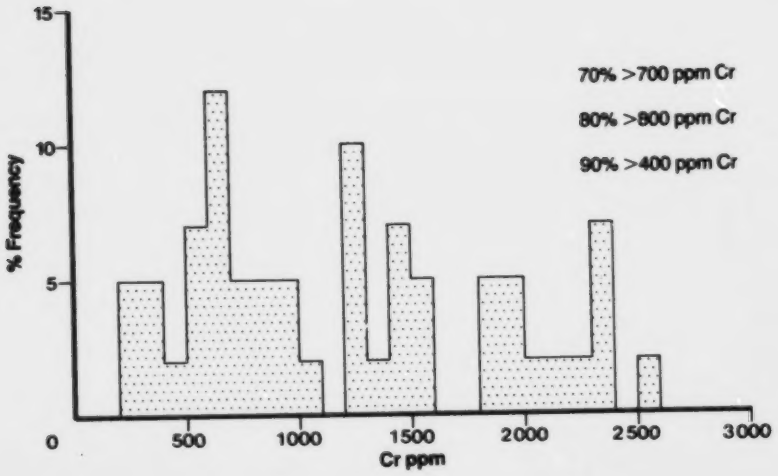

Figure 3. *Percentage frequency distribution vs. ppm Cr for rocks of komatiitic affinity (41 analyses).*

MIDDLE PRECAMBRIAN GABBROIC ANORTHOSITES

Gabbroic-anorthositic rocks of Middle Precambrian age, exposed at the base of the Huronian Supergroup between Sault Ste. Marie and Sudbury, do not exhibit extensive ultramafic units (Card and Palonen 1976). Gabbro occurs as layers in intrusions such as the Dunlop-Shakespeare body, where chromite is unreported and the chromium value of 250 ppm is normal for a mafic rock (Card and Palonen 1976). Gabbroic anorthosite from the East Bull Lake Intrusion was sampled for this study and returned Cr values ranging from 110 to 387 ppm.

Anorthositic suite intrusive rocks mapped by Lumbers (1975) in the Grenville Province near Burwash, Ontario, contain 1 m thick mafic and ultramafic layers. Analysis of these mafic rocks indicates a normal Cr concentration of 150 ppm Cr.

A brief survey of Middle Precambrian gabbro-anorthosite suites indicates that ultramafic units are rare. Metapyroxenite is described from the East Bull Lake Complex by Born and James (1978) as xenoliths in the main layered gabbro to anorthositic-gabbro intrusion. The available analyses of mafic rocks from these gabbro-anorthosite complexes suggest only normal chromium concentrations.

The chromite deposits identified for detailed work in this study (Figure 1) include: 1) the Big Trout Lake Deposit, 2) the Puddy-Chrome Lake Deposit, 3) the Crystal Lake Gabbro, 4) the Shebandowan Deposit, and 5) komatiitic lavas from the Timmins area.

NIPISSING DIABASE

Seventy-one Cr analyses of samples of Nipissing Diabase were plotted, resulting in a median Cr value of approximately 125 ppm (Figure 4). Although gabbroic in bulk composition, Nipissing Diabase appears to have slightly lower Cr contents than other mafic rocks. Additional analyses of gabbro, basalt, and Nipissing Diabase are required to further characterize the Cr contents of these rocks and to verify if the lower Cr content in Nipissing Diabase is representative.

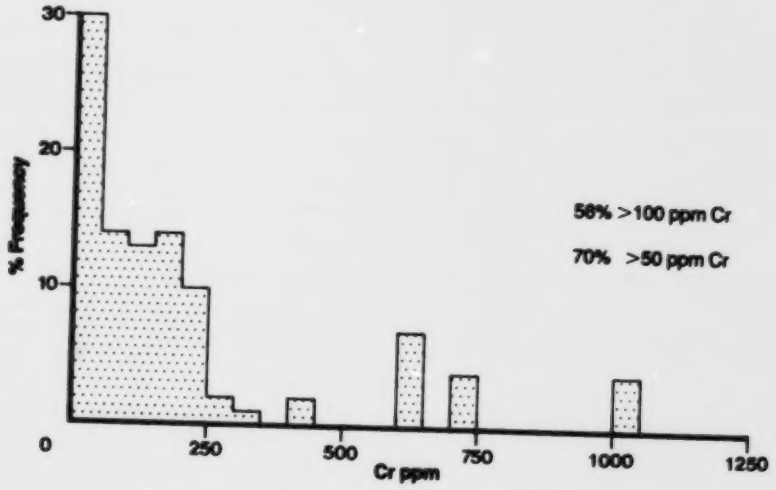

Figure 4. Percentage frequency distribution vs. ppm Cr for Nipissing Diabase (71 analyses).

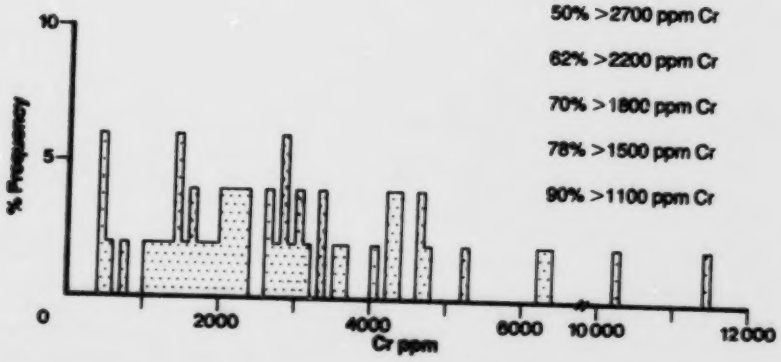

Figure 5. Percentage frequency distribution vs. ppm Cr for dunites, peridotites, and their serpentinized equivalents (51 analyses).

METASEDIMENTARY ROCKS

During the compilation of data, it was evident that sedimentary rocks from shales to quartzites exhibited significant chrome values. Many Cr values in sedimentary rocks were equal to or greater than the median Cr values for the Nipissing Diabase and gabbro-basalt groups. A metapelite of the McKim Formation of the Huronian Supergroup has 200 ppm Cr (Card 1978; Robertson 1976) while a metasiltstone of the same formation contains 250 ppm Cr (Card 1978). Both are greater than the median Cr values of mafic rocks and of Nipissing Diabase, 175 ppm and 125 ppm Cr respectively. Metasiltstones of the Mississagi Formation of the Huronian Supergroup have been described as containing 3100 ppm Cr (Meyn 1979).

ULTRAMAFIC INTRUSIONS

The rocks considered for the ultramafic intrusive category include dunites and peridotites (Figure 5) plus their serpentinized equivalents. Their range in chromium concentrations extends from 400 to 11 400 ppm, a much broader range than komatiitic rocks. The Cr median value is 2700 ppm, significantly higher than for komatiites. There are weak peaks at 400 to 500 ppm Cr, 1400 to 1500 ppm Cr, and at 2800 to 2900 ppm Cr. Each of these Cr concentration intervals represents 6% of the analyses. The apparent scatter of data suggests that additional analyses there are required.

ROCKS OF MAFIC COMPOSITION

Analyses of gabbro and basalt were considered for this category (Figure 6). Nipissing Diabase, although gabbroic, was dealt with separately because of its restricted distribution to the Southern Province. The range of Cr concentrations in gabbros and basalts is from <50 ppm to 1850 ppm, with the median Cr value being approximately 175 ppm. The Cr interval with the highest frequency of analyses is 150 ppm to 200 ppm, representing 21% of the analyses plotted. Chromium in the mafic rocks exhibits a more restricted range of values when compared to komatiitic flows and ultramafic intrusive rocks. Out of 125 analyses plotted, 90% fall in the interval from 0 to 500 ppm Cr, which is a more concentrated grouping of Cr values than is shown by ultramafic extrusive and intrusive rocks.

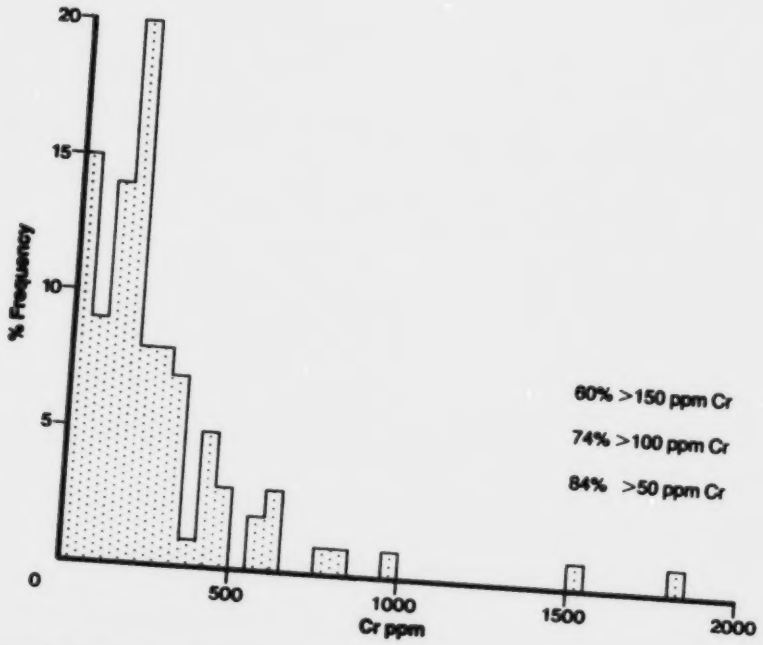

Figure 6. Percentage frequency distribution vs. ppm Cr for gabbroic and basaltic rocks exclusive of Nipissing Diabase (125 analyses).

Puddy–Chrome Lakes Deposit

LOCATION AND ACCESS

The Puddy-Chrome Lakes area is located 175 km northwest of Thunder Bay, Ontario, and 50 km west of Lake Nipigon (Figure 7).

Access is by float-equipped aircraft based in either Thunder Bay or Armstrong, Ontario.

PREVIOUS WORK

Early mapping was carried out by Graham (1931), Hurst (1931), and Kidd (1933). This was followed by detailed mapping by Kustra (1966) and additional mineralogical work by Simpson and Chamberlain (1967).

An exploration shaft was sunk by Chromium Mining and Smelting Corporation Limited in the early 1930s to 110 m, providing access to three levels. Diamond drilling outlined 25 000 tons averaging 12% chromite (Canadian Mines Handbook 1966-1967, p.78). Bulk samples were run for concentrate testing, resulting in an average concentrate grade of 40.0 to 41.5 weight percent Cr_2O_3 (Parsons 1937). The mine has been inactive since 1937.

GENERAL GEOLOGY

The serpentinized ultramafic intrusion at Puddy and Chrome Lakes (Figure 7) is exposed for 7 km along strike and is approximately 1 km in width. The intrusive body is emplaced at the contact between Archean quartzofeldspathic paragneisses and Archean volcanogenic metasediments. A stock of porphyritic quartz monzonite, intruding both the paragneiss and the metasediments, forms part of the southwest contact. Magnetic data indicate a southerly dip.

Rocks of the intrusion include dunite, peridotite, and minor pyroxenite, all of which are serpentinized. North-striking and east-striking dikes of probable Late Precambrian age cut the intrusion. Faulting, indicated by intense shearing of the ultramafic rocks, is evident at the west end of Puddy Lake and at the north end of Chrome Lake. Country rock xenoliths of paragneiss occur along the north contact of the intrusion at Puddy Lake (Figure 8). The xenoliths are elongate slabs aligned parallel to the contact.

DETAILED GEOLOGY

Serpentinite in the Puddy-Chrome Lakes area exhibits extremely variable outcrop characteristics. Relict textures indicate that peridotite is most common with pyroxenite and dunite present in minor amounts. All of these rock types have been thoroughly serpentinized and relict textures have been destroyed where shearing has been active. In hand specimens, serpentinized dunite can be recognized by medium-grained olivine phenocrysts which form a massive cumulate texture. The olivine grains are generally outlined by very fine grained magnetite which also develops along fractures cutting olivines. Serpentinized peridotite exhibits medium-grained intercumulate patches of fibrous minerals (amphibole) replacing fine-grained pyroxenes. A peridotite outcrop on Puddy Lake contains less altered, resistant pyroxenes which form a knotty (maculose) weathered surface.

ALTERATION

Alteration in the form of serpentinization involves the addition of water, CO_2, and other volatiles to the primary ultramafic assemblage. At Puddy-Chrome Lakes, the ultramafic body has been pervasively serpentinized in a heterogeneous manner, resulting in outcrop ranging in colour from red and purple, to green and grey. A variegated effect results where single outcrops exhibit irregular red or purple patches in primarily greenish grey outcrop. The variation from red to grey shades could reflect sharp local differences in oxygen fugacity (fO_2), affecting the oxidation state of iron.

Iron redistribution associated with the serpentinization process results in the formation of complex magnetite veining. Iron, released from the breakdown of

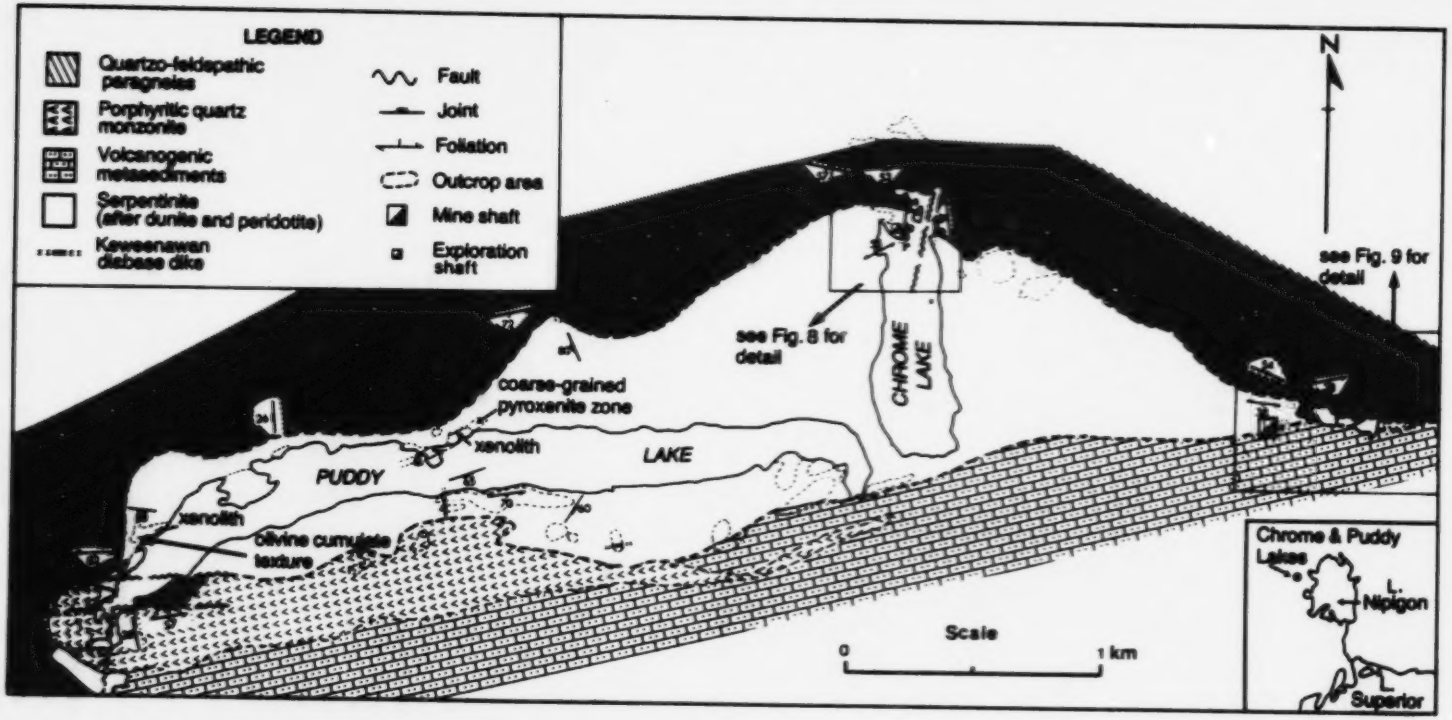

Figure 7. General geology of Puddy and Chrome Lakes (modified after Kustra 1966).

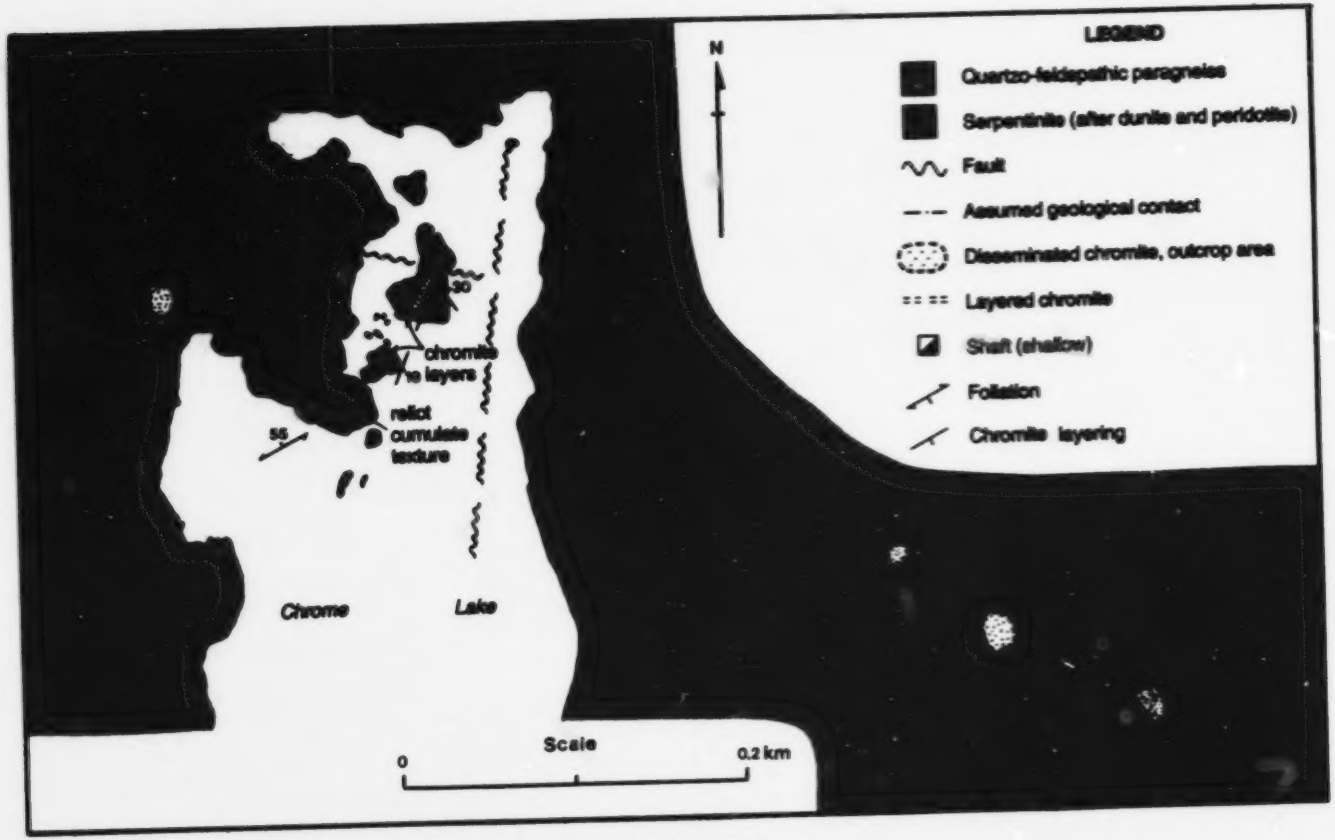

Figure 8. *Disseminated and layered chromite occurrences at Chrome Lake.*

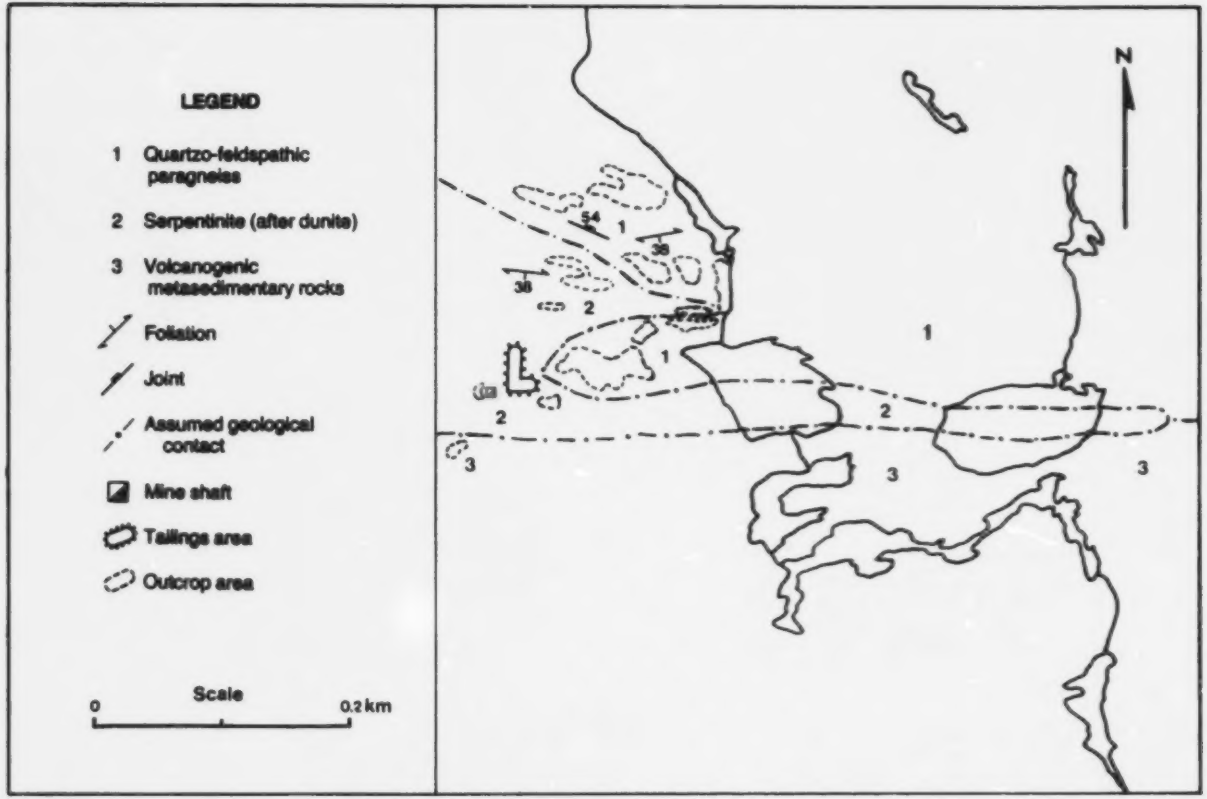

Figure 9. Mine shaft area chromite occurrence, Chrome Lake.

olivine and pyroxene to serpentine minerals, migrates to fractures where fO_2 conditions were favourable to magnetite (Fe_3O_4) crystallization. Veins of magnetite range from 1 mm to 1 cm thick and display ladder-like to dendritic morphology (*see* Photo 7). With progressive loss of Fe to form increasingly larger magnetite veins, the remaining serpentinite exhibits paler shades of green and eventually becomes chalky white with maximum iron loss.

Alteration in the northeast end of the ultramafic body, in the area of the chromite occurrences, is less variable. Uniformly black-green to grey-green serpentinite is predominant.

Variegated alteration at Puddy Lake may represent the collection of volatiles in an upper or central part of the intrusion where crystallization was slowest. If the collection of volatiles were patchy and with minimal diffusion, then variegated serpentinite would be expected.

CHROMITE OCCURRENCES

Chromite is exposed along the northeastern contact of the Puddy-Chrome Lakes serpentinite in a zone from the north end of Chrome Lake to the east end of the intrusion (Figure 7). The chromite mineralization occurs in three forms: layered, disseminated, and podiform.

DISSEMINATED AND LAYERED CHROMITE

Disseminated chromite is the most widely distributed style of chromite mineralization and it occurs along with layered and massive chromitite (>75% chromite). Chromite, in disseminated form, is very fine grained to fine grained and forms 5 to 15 modal percent of the serpentinite. At the north end of Chrome Lake (Figure 8), disseminated chromite has been redistributed by shearing into wispy schlieren-type concentrations 0.5 cm thick and up to 4 cm long, separated by black-green, strongly foliated serpentinite.

Chromite in layered form is best exposed at the north end of Chrome Lake (Figure 8) where the layered zone is approximately 0.5 m thick, strikes north, and dips easterly. The layers are deflected to a northwesterly strike as the east-striking fault contact with paragneisses to the north is approached. Individual chromite layers vary from 1 to 6 cm thick, and are cumulate concentrations of fine- to medium-grained subhedral chromite. A representative sequence is described as follows:

Top 15.5 cm

Serpentinized olivine phenocrysts become gradationally more abundant and form approximately 90 modal percent of the rock. Patchy areas with about 20 modal percent chromite occur irregularly through the dunite.

11.5 cm

Massive chromitite with approximately 10 modal percent medium-grained serpentinized olivine phenocrysts. Olivine is serpentinized to lizardite and antigorite.

7.5 cm

Serpentinite in sharp contact with fine-grained massive chromitite layer. Chromite is equigranular and anhedral, and generally ovoid or spherical in shape.

5.0 cm

Fine- to medium-grained serpentinite which may exhibit a cumulate olivine texture. Where the serpentinite has been sheared, talc and magnesite are developed.

Base 0.0 cm

Shearing has modified the thinner (1 cm) chromitite layers by breaking them into stretched fragments which are 1 to 3 cm in length and exhibit angular to cuspate ends. All fragments are aligned parallel to the foliation. Folding is pre-

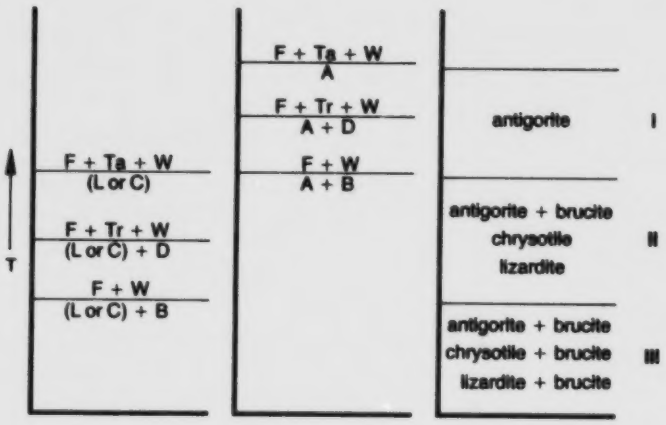

Figure 10. Schematic diagram of the temperature regimes of the observed assemblages. Abbreviations for minerals in the equilibria: A=antigorite, B=brucite, C=chrysotile, D=diopside, F=forsterite, L=lizardite, Ta=talc, Tr=tremolite, W=water. The three temperature regimes are denoted I, II, and III on the extreme right of the diagram (Wicks and Whittaker 1977).

TABLE 2. MODAL ANALYSES OF SERPENTINITES FROM CHROME LAKE (1000 POINTS PER THIN SECTION).

Sample Number	Lizardite	Antigorite	Mica*	Chromite	Magnetite	Total
WC-78-11	89.6	—	5.2	—	5.2	100.0
WC-78-13	—	59.9	8.8	31.3	—	100.0
WC-78-14	76.0	14.4	3.2	—	6.4	100.0
WC-78-17	72.0	16.1	—	—	11.9	100.0
WC-78-20	60.2	10.2	16.9	12.7	—	100.0
W78-CMD-	—	90.3	4.8	4.9	—	100.0
W78-CMD-2	—	24.7	0.9	74.4	—	100.0
W78-CL2-3	62.0	10.9	13.2	13.9	—	100.0
W78-CL2-4	—	92.8	1.6	5.6	—	100.0

*Mica includes chlorite + biotite + talc

Photo 1. Subhedral disseminated chromite with finely serrated edges and circular serpentine lizardite inclusions. Plane light. X44.

served in some thinner layers where isoclinally folded fragments occur. Thicker chromitite layers (4 to 6 cm) exhibit boudinage-type structures. Shearing has caused brittle fracture of the thicker chromitite layers with serpentinite filling the fractures. Fractures cut the thicker chromitite layers in subparallel sets which intersect the plane of layering and foliation at approximately 30°.

The thicker chromitite layers are formed of subhedral medium-grained chromite. Chromite adjacent to shear zones is granulated to very fine grained fragments which define a braided shear pattern cutting the chromite layers. Undeformed chromite defines a tightly packed cumulate texture with a matrix of approximately 2% to 3% intercumulate black-green serpentinite.

At the east end of the intrusion (Figure 9), chromite was mined from two underground levels. Samples from the tailings dump represent disseminated chromite and massive chromitite. Massive chromitite at this eastern locality is blocky and typical of podiform-style mineralization. Chromitite is massive, and breaks with a hackly fracture, revealing a metallic black lustre.

PETROGRAPHY

Chromite- and magnetite-bearing ultramafic rocks of the Puddy Lake-Chrome Lake body have been serpentinized to an assemblage of lizardite (flat-layer structure) + antigorite (corrugated structure) + mica. The micaceous phase is usually chlorite (after biotite), and brucite may also be present.

The most common process of serpentinization involves the addition of water to olivine. Johannes (1968) has shown that the reaction serpentine + brucite = 2 forsterite + $3H_2O$ occurs at 380°C and at 2 Kbars pressure. The reaction 5 serpentine = 6 forsterite + talc + $9H_2O$ occurs at 460°C (Scarfe and Wyllie 1967), or at 400°C (Chernosky 1971), all at 2 Kbars pressure. Wicks and Whittaker (1977) have summarized the temperature regimes of the various serpentine assemblages as shown in Figure 10. Modal analyses of some representative samples are given in Table 2.

CHROMITE

Chromite, in disseminated form, occurs as subhedral to anhedral grains in a predominantly lizardite matrix. Grain edges exhibit a deep reddish brown colour. Disseminated chromite is very fine grained (0.1 to 0.5 mm) and forms 5 to 15 modal percent of the rock. Disseminated grains may be isolated or form clusters of 10 to 20 grains. Some chromite grains in clusters coalesce and are surrounded by dust-sized chromite which becomes less abundant away from the clusters. Within sheared serpentinite, smaller grain fragments represent particles of chromite crushed during shearing. The fragments are concentrated in the plane of foliation and in pressure shadows adjacent to larger parent chromite grains.

Disseminated chromite grains have serrated, irregular borders (Photo 1) which suggest a stage of non-equilibrium. A period of non-equilibrium could occur during regional dynamo-thermal metamorphism which would promote corrosion of chromite.

Chromite from layered zones is subhedral to euhedral and tightly packed, forming 75 to 80 modal percent of the layer (Photo 2), with a matrix of lizardite. Grain borders are smooth and individual grains are unfractured. The "layer" environment has protected many chromite grains from corrosion and from shear-induced fractures. The largest chromite grains (1 mm) are approximately 10 times the size of the smaller grains (0.1 mm), with the smaller chromite grains forming 80% of the population in the layers. Mixing of all sizes is random, suggesting that chromite was nucleating for an extended period of time with grains from several generations settling as a single event to form mixed layers.

Polished sections of layered chromitite from the north end of Chrome Lake exhibit metamorphic features. Some grains are highly fractured and extensive alteration is reflected by the abundance of serpentine (lizardite) inclusions (Photos 3 and 4). The most extensive development of inclusions follows the most highly

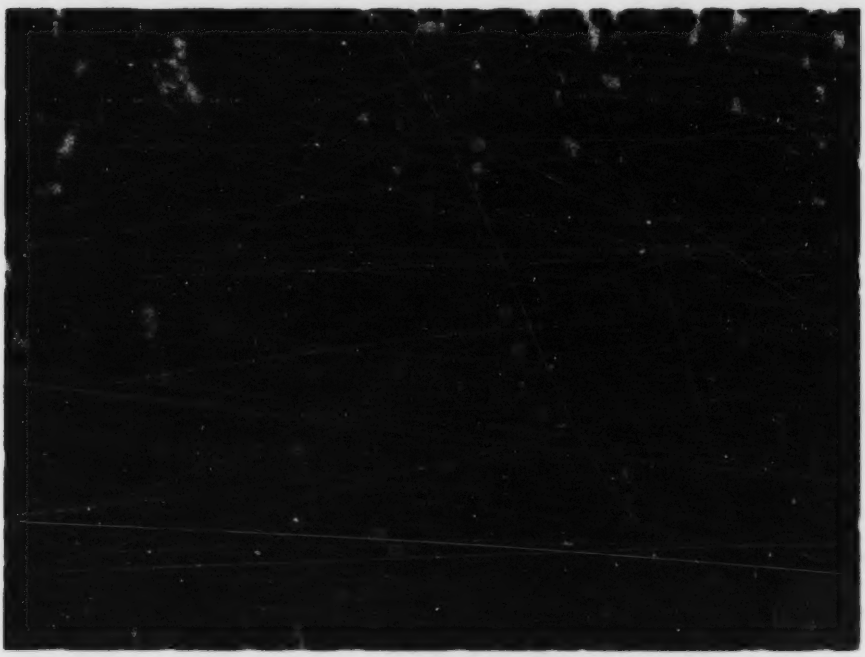

Photo 2. *Euhedral and subhedral chromite from layered occurrence, north end of Chrome Lake. Lizardite matrix. Crossed nicols. X44.*

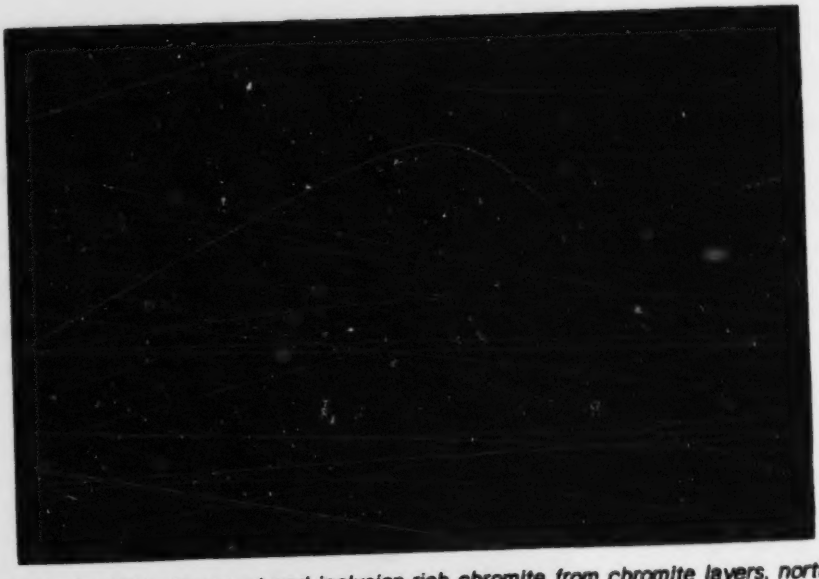

Photo 3. *Highly fractured and inclusion-rich chromite from chromite layers, north end of Chrome Lake. Reflected light. X125.*

Photo 4. *Inclusion-filled chromite with thin pale ferritchromit rim visible at top of grain. Reflected light. X125.*

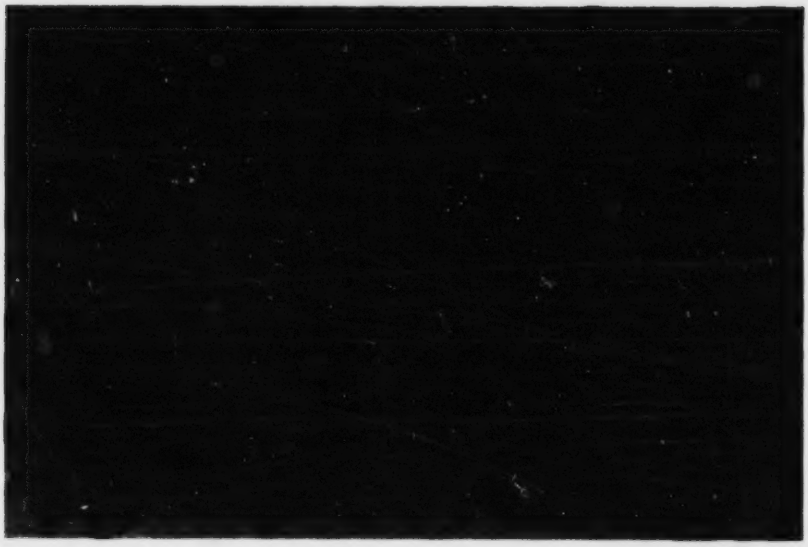

Photo 5. Massive chromite with intercumulus lizardite and magnetite. Reflected light. X125.

fractured zones within chromite grains. Relict primary chromite cores are rarely observed in inclusion-rich chromite.

Ferritchromit rims which envelop chromite grains as a result of regional metamorphism are, at Chrome Lake, masked by extensive fracturing and further alteration to chrome magnetite. One exception, described by Simpson and Chamberlain (1967), exhibits a distinct "ferritchromit" rim. Ferritchromit rims, a term first used by Spangenburg (1943) to denote a spinel composition intermediate between magnetite and chromite, have higher reflectivity than chromite cores. In metamorphic terranes, ferritchromit rims are usually dotted with inclusions of lizardite ± chlorite. The development of ferritchromit rims begins with the deposition of magnetite rims on chromite during serpentinization. Growth of the magnetite mantle incorporates serpentine inclusions to form an inclusion-rich rim. With prograde regional metamorphism, Fe^{+2}, Fe^{+3}, Ni, and Ti diffuse toward the core. The magnetite rim is thus altered to ferritchromit as Cr^{+3} migrates outwards and the sharp magnetite chromite contact is replaced by a diffuse ferritchromit-chromite border (Bliss and MacLean 1975).

Massive chromitite from the eastern mine shaft area represents a podiform style of deposit. The massive nature of the chromitite has protected it from metamorphism, resulting in homogeneous-appearing chromite (Photos 5 and 6). Serpentinite inclusions within the chromite occur as small dark grey dots and are relatively few in number (Photo 5). Serpentine (lizardite) represents the trapped intercumulus phase (dark grey) between coalesced chromite grains (pale grey) (Photo 5). Very fine, dark grey, suture lines outline relict chromite grain boundaries (Photo 6) in the now-massive chromitite. The black angular mineral occurring both in inclusion and interstitial form is magnetite. In Photo 5, at the centre of the photomicrograph, a trace amount of sulphide (chalcopyrite) is present as the pale greyish white, irregularly shaped mineral.

MAGNETITE

Magnetite and chromite coexist at the north end of Chrome Lake, and farther west, at Puddy Lake, magnetite becomes the exclusive oxide phase. A zone along the south shore of Puddy Lake, at the west end, contains nickeliferous magnetite (Figure 11; Commerce Nickel Mines Limited, Assessment Files, Resident Geologist's Office, Ontario Ministry of Northern Development and Mines, Thunder Bay).

Primary disseminated magnetite is anhedral with highly serrated borders and occurs as individual grains and in 2- to 4-grain clusters. Disseminated magnetite is very fine grained and in shear zones it is commonly fractured.

In sheared serpentinite, secondary magnetite occurs as an anastomosing fracture-filling phase (Photo 7). Magnetite in this form develops a comb texture where magnetite grew perpendicular to the fracture walls. Fractures range in thickness from 1 mm to 1 cm. Secondary magnetite also occurs as a product of serpentinization of primary olivine. Iron is released as olivine is serpentinized to lizardite and is oxidized to magnetite. Magnetite, thus formed, develops dusty rims outlining relict olivine phenocrysts.

LIZARDITE

Lizardite is the predominant serpentine mineral throughout the Puddy Lake-Chrome Lake serpentinite. In the east-central portion of the body, lizardite pseudomorphs cumulate olivine from the primary dunite. In thin section, the pseudomorphic texture reflects an initial massive, medium-grained, and equigranular ultramafic rock.

Westwards, in the Puddy Lake area, the serpentinite is in the form of a lizardite bastite which has developed a pseudomorphic texture after pyroxene (Photo 8). The bastite reflects initially subhedral to anhedral pyroxenes of a pyroxenite or possibly a peridotite. The bastite (after pyroxene) consequently reflects a change in rock type from dunite in the east (stratigraphically lower) to peridotite and/or pyroxenite in the central area of the body (stratigraphically central). Both areas are

Photo 6. Relict chromite boundaries defined by grey hairline sutures. Reflected light. X125.

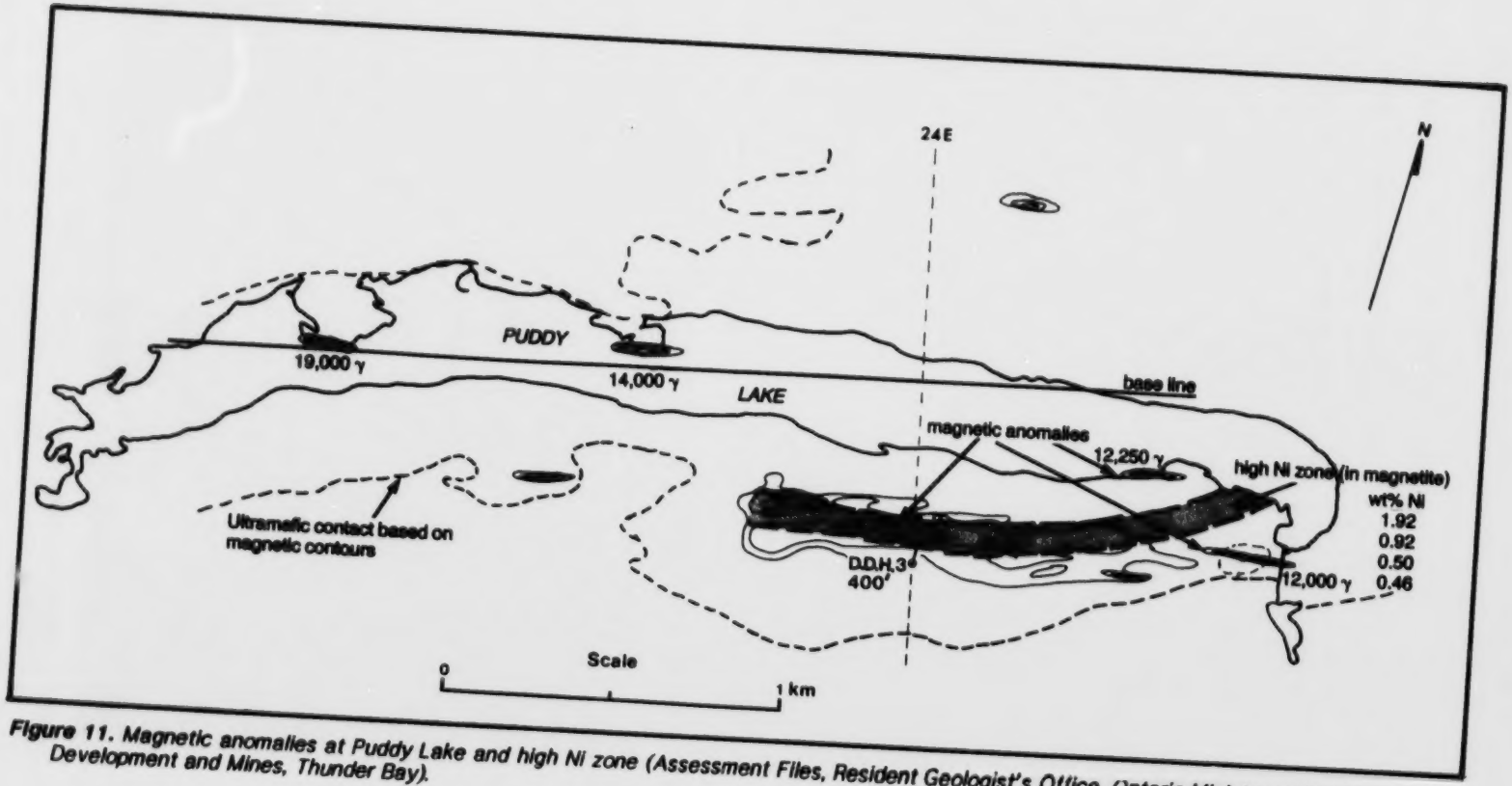

Figure 11. Magnetic anomalies at Puddy Lake and high Ni zone (Assessment Files, Resident Geologist's Office, Ontario Ministry of Northern Development and Mines, Thunder Bay).

Photo 7. *Secondary magnetite in anastomosing fractures. Matrix is pale green serpentinite. Reflected light. X44.*

Photo 8. *Lizardite bastite defining pseudomorphic texture after clinopyroxene. Lizardite columns developed along relict pyroxene cleavage traces. Crossed nicols. X44.*

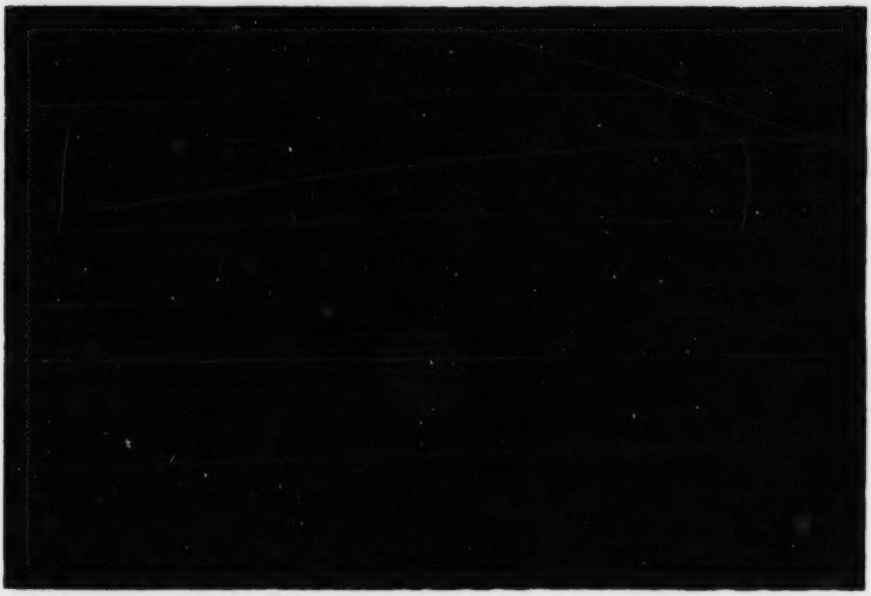

Photo 9. *Columnar fracture modifying lizardite mesh texture. Crossed nicols. X44.*

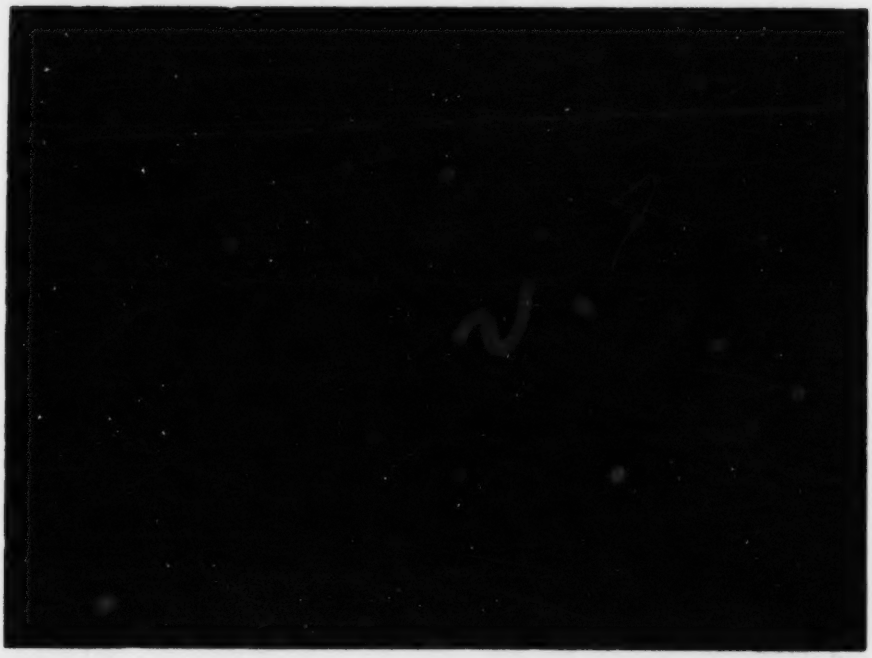

Photo 10. *Antigorite rimming relict olivine altered to lizardite. Crossed nicols. X44.*

Photo 11. Interlocking antigorite developed in random orientation. Crossed nicols. X44.

massive at the core and become increasingly foliated towards the northern contact. This could imply that the ultramafic body was cold at the time of emplacement.

Lizardite from olivine and pyroxene has, in both cases, formed a mesh texture. The mesh texture in the bastite is partly controlled by cleavage traces in the pre-existing pyroxene, which produces a more accentuated columnar structure in the mesh texture (Photo 9). The lizardite mesh texture is composed of mesh unit borders of ribbony lizardite with the core regions to each textural unit formed of intergrown lizardite. Intergrown lizardite is an aggregate of anhedral, approximately equant, randomly oriented lizardite grains. Towards the northern paragneiss contact, shearing has disrupted the initial pseudomorphic serpentine texture. The sheared lizardite consequently forms a non-pseudomorphic texture composed of interlocking subhedral to anhedral lizardite grains.

ANTIGORITE

Minor amounts of antigorite occur in the pseudomorphic unsheared lizardite at the edge of serpentinized olivine grains. Antigorite aids in defining the relict cumulate texture (Photo 10).

Towards the sheared serpentinite at the northern contact, antigorite becomes the predominant serpentine mineral. It progresses from an intergrown texture, composed of anhedral antigorite grains in the less sheared rocks, to an interlocking texture in the highly sheared rocks. Interlocking antigorite texture is defined by subhedral antigorite blades which grow in random orientation (Photo 11) and reflect relatively higher metamorphic conditions.

Within sheared serpentinite, tension and shear fractures are filled by intergrown antigorite oriented perpendicular to the fracture walls.

TABLE 3. MICROPROBE ANALYSES OF CHROMITE IN PERIDOTITE FROM PUDDY-CHROME LAKE (ANALYSES BY D.H. WATKINSON, CARLETON UNIVERSITY).

Wt % Oxide	1 (centre of grain)	2 (edge of grain)	3 (centre of grain)	4(centre of grain)	5 (centre of grain)
Na_2O	0.05	0.01	0.03	0.02	0.00
SiO_2	0.10	0.01	0.03	0.11	0.06
FeO	16.82	17.38	16.98	16.13	16.21
Fe_2O_3	4.28	4.51	4.89	4.93	5.71
CaO	0.00	0.04	0.00	0.00	0.00
MgO	10.86	10.23	10.73	10.85	11.03
Al_2O_3	14.12	13.30	13.75	13.88	13.56
NiO	0.10	0.00	0.00	0.07	0.00
K_2O	0.00	0.03	0.00	0.00	0.04
ZnO	0.39	0.20	0.21	0.00	0.14
TiO_2	0.11	0.28	0.18	0.21	0.23
Cr_2O_3	53.99	53.66	53.07	51.38	52.12
MnO	0.76	0.98	0.70	0.85	0.83
TOTAL	101.58	100.65	100.57	98.43	99.93
cations based on 24 oxygen					
Na	2.70	0.65	1.49	1.22	0.00
Si	2.44	0.89	0.71	2.93	1.54
Fe	358.73	376.38	366.20	353.68	351.26
Fe	82.04	87.86	94.87	97.30	111.28
Ca	0.00	0.97	0.00	0.00	0.00
Mg	412.53	395.05	412.64	423.88	425.75
Al	424.32	406.03	418.05	428.94	414.05
Ni	1.96	0.00	0.00	1.48	0.00
K	0.00	1.04	0.00	0.00	1.35
Zn	7.32	3.87	3.95	0.00	2.71
Ti	2.16	5.39	3.53	4.11	4.39
Cr	1088.47	1098.59	1082.05	1065.18	1067.49
Mn	16.47	21.40	15.33	18.96	18.31
TOTAL	2399.14	2398.13	2398.82	2397.67	2398.14

CHLORITE

Chlorite occurs in sheared serpentinites adjacent to the paragneiss contact. Chlorite also replaces biotite in paragneiss northwards from the contact (Kidd 1933). The growth of chlorite beyond the serpentinite contact suggests considerable fluid mobility outwards from the ultramafic body, possibly at the time of emplacement. Talc and brucite both occur as very fine grained, fibrous, platy aggregates.

Chlorite in serpentinite forms in two modes. The first includes formation of fine-grained aggregates of randomly oriented chlorite flakes. These chlorite aggregates grow amongst clusters of chromite and magnetite and in pressure shadows flanking opaque grains. The second mode of occurrence involves larger individual chlorite flakes which grow in the serpentinite between layers or clusters of chromite and magnetite.

The chlorite grains are generally undeformed and are distributed throughout foliation planes in proximity to opaque minerals. Their undeformed nature suggests post-kinematic growth. The foliation may have provided permeable planes through serpentinites along which fluids could more easily travel. Fluid transfer of elements could then facilitate the growth of chlorite in both serpentinite and paragneiss.

CHROMITE COMPOSITIONAL VARIATION

Electron microprobe analyses of chromite grains (Table 3) show that they are predominantly ferrian chromite to chromian magnetite (Figure 12). Ferrian chromite and chromian magnetite are fields representing altered chromite or "ferritchromit" and reflect metamorphic alteration. Ferritchromits from the Limassol Forest ultramafic complex in Cyprus similarly plot in the ferrian chromite field (Panayiotou 1978). Chromite from the north end of Chrome Lake is from a highly sheared part of the ultramafic intrusion. Consequently, alteration could be synkinematic. Two available analyses of chromite rims exhibit an affinity to be in or close to the chromian magnetite field. This reflects an iron enrichment in the rims which can be

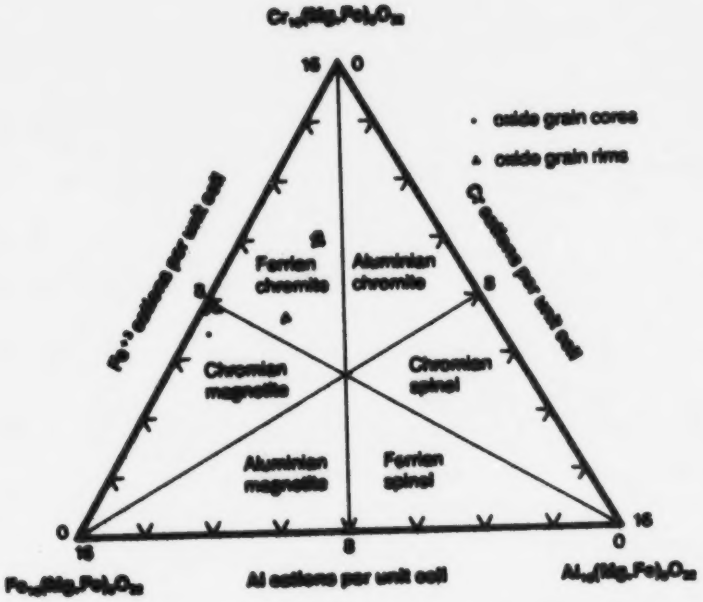

Figure 12. Composition of Puddy-Chrome Lakes chromite grains.

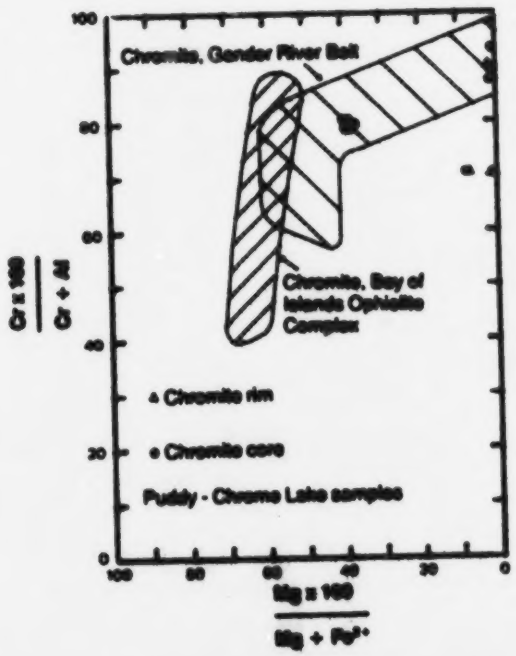

Figure 13. Plot of Cr and Mg ratios for Puddy-Chrome Lakes chromite grains.

seen in polished section. Rimming effects of magnetite on chromite, also described by Simpson and Chamberlain (1967), give further evidence of post-cumulus alteration. Work by Bliss and MacLean (1975) has shown that the outer rims of chromite and the margins along fractures which penetrate chromite grains have higher Fe and Cr, and lower Al and Mg relative to the unaltered core regions. The rims retain a spinel structure, but with a slightly larger lattice spacing, and the alteration rims and margins can be optically observed as selvages of fractionally higher reflectance. Chromite rim analyses illustrate the depletion of Mg in chromite margins (Figures 13 and 14).

Cr/Fe ratios at Puddy-Chrome Lakes (Table 4) are the highest encountered of the Ontario deposits examined and range between 2.38 and 2.56. The Puddy-Chrome Lakes chromite defines a high grade but apparently low volume, podiform and layered deposit.

Comparative plots with chromite from the Bay of Islands Ophiolite Complex and from the Gander River Belt in Newfoundland were compiled to illustrate the affinity of Chrome Lake chromite for an "alpine field" (Figure 15). In Figures 13, 14, and 15, several chromite analyses plot beyond the fields outlined; this may reflect metamorphic alteration suggested by field and petrographic work. Figure 14 illustrates fields for ophiolitic chromites from the Bay of Islands Complex and for chromite from the Gander River Belt (Malpas and Strong 1975).

Compared to these crystallization environments in Newfoundland, Puddy-Chrome Lakes chromite plots within or proximal to the field outlined for Gander River Belt chromite, currently interpreted to be alpine-type ultramafics.

MAJOR ELEMENT CHEMISTRY

Rocks of the Puddy Lake-Chrome Lake ultramafic body exhibit distinct ultramafic composition (Table 5). On a plot of weight percent SiO_2 vs. weight percent FeO/MgO (Figure 16), the FeO/MgO ratio is low and the range of SiO_2 values, from 32 to 41 weight percent, is within a dunite to peridotite field. Figure 17 is an AFM

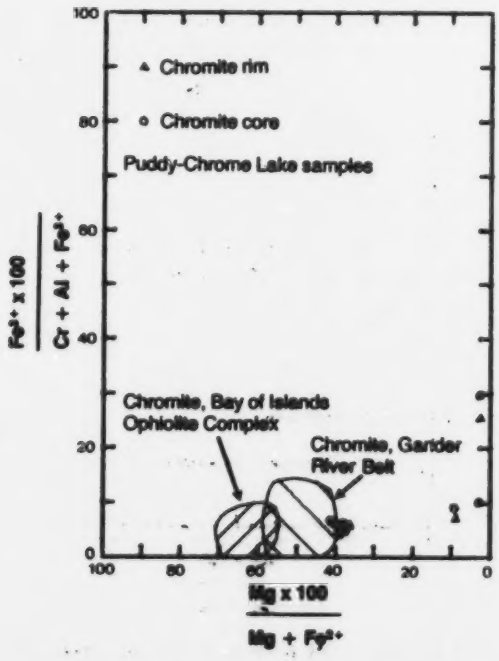

Figure 14. Plot of Fe^{+3} and Mg ratios for Puddy Chrome Lakes.

TABLE 4. Cr/Fe RATIOS FROM PUDDY-CHROME LAKES.

Sample Number	Sample Description	Cr/Fe
1.	Chromite in peridotite, centre of grain	2.56
2.	Chromite in peridotite, edge of grain	2.45
3.	Chromite in peridotite, centre of grain	2.43
4.	Chromite in peridotite, centre of grain	2.44
5.	Chromite in peridotite, centre of grain	2.38

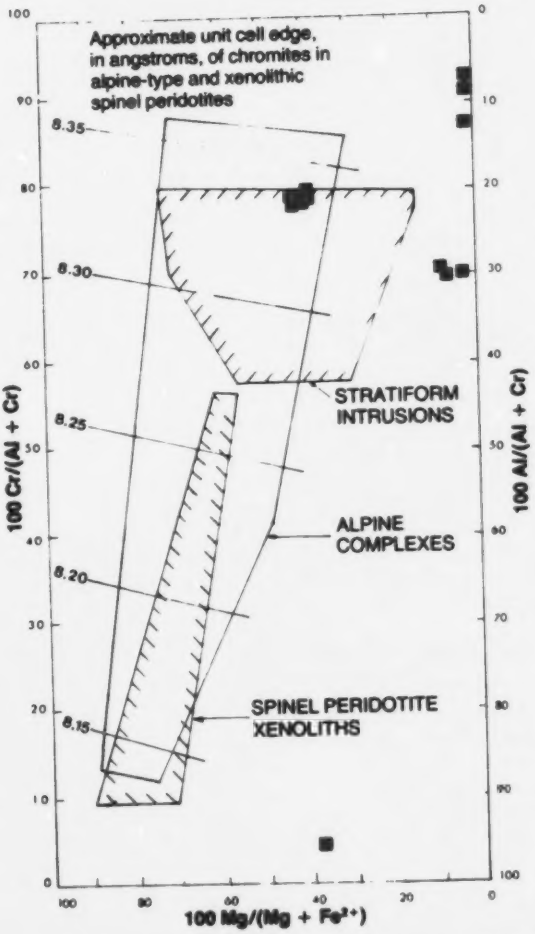

Figure 15. Plot of Puddy-Chrome Lakes chromite analyses (solid squares) illustrating their affinity for the combined Alpine Complex-Stratiform Intrusion field (from Irvine and Findlay 1972).

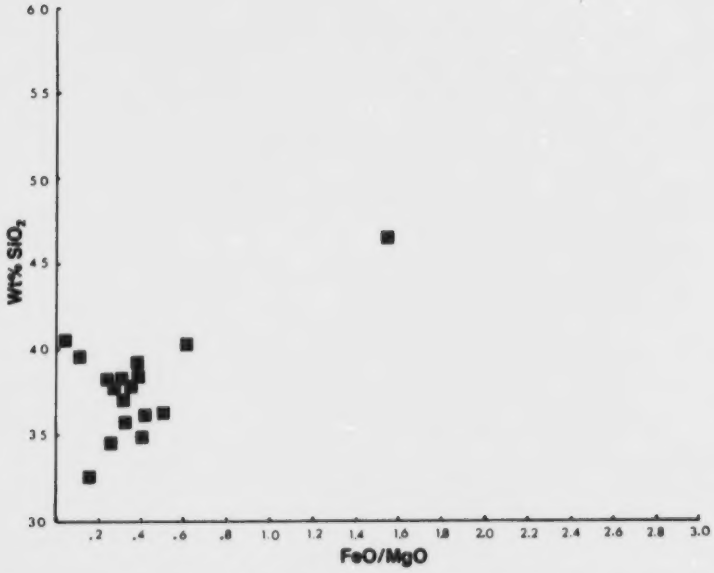

Figure 16. *Plot of Puddy-Chrome Lakes ultramafic rocks with characteristically low SiO_2 and low FeO/MgO ratio.*

plot of the same samples and this plot, in conjunction with the ternary plots of Figure 18, illustrates the high MgO content and ultramafic nature of this intrusion. Apart from two or three spurious points, most of the samples plot in a cluster. Ultramafic rocks at Puddy-Chrome Lakes represent a restricted fractionation interval.

The two or three points beyond the main cluster in each diagram represent samples from intensely sheared and altered parts of the ultramafic body. In Figure 16, the high SiO_2 a high FeO/MgO sample represents a Keweenawan diabase dike cutting the ultramafic rocks (Analysis 17, Table 5).

TRACE ELEMENT CHEMISTRY

Trace element data from the Puddy-Chrome Lakes ultramafic body suggest an alpine-type character. In Figure 19, a plot of NiO vs. Cr_2O_3 weight percent after Irvine and Findlay (1972) reveals that over half of the samples plot within the alpine-type peridotite field. These are ultramafic samples collected away from the layered and disseminated chromite showings. The data in Figure 20 exhibit a full range of values along the Ni-Cu join and only minor Co and Cu. The Co and Cu scales were multiplied by 20 to prevent cluttering the Ni-Cr join. The range in Ni-Cr values reflects Cr variation in the oxide phase from east to west. Chrome values are highest in the most easterly showing, are lower at Chrome Lake where magnetite occurs, and are lowest at Puddy Lake where magnetite alone forms the oxide phase. At Puddy Lake, magnetite is Ni-bearing and a nickelliferous magnetite zone has been outlined (Figure 11) from assays done on the property of S. Nelson (Assessment Files, Resident Geologist's Office, Ontario Ministry of Northern Development and Mines, Thunder Bay).

In Figure 21, the range in weight percent Cr_2O_3, NiO, and TiO_2 is given against weight percent MgO. The range of MgO, as shown earlier, is restricted within the ultramafic field. Cr_2O_3 varies from 0.10 to 0.90 weight percent; and NiO, from 0.10 to 0.45 weight percent. Values for Cr_2O_3 of samples taken from chromite-bearing outcrops (Table 6) give considerably higher Cr_2O_3 values. Since these are anomalous values for the ultramafic body, they are omitted from the more general plots.

In the classification of ultramafic rocks as alpine-type, one of the criteria is less than 0.03 weight percent TiO_2 (Irvine and Findlay 1972). TiO_2 values from Puddy-Chrome Lakes, as shown in Figure 21, exhibit some higher TiO_2 values than those attributed to alpine-type ultramafic. In this respect, there is disagreement in classifying the Puddy-Chrome Lakes ultramafic as an alpine-type intrusion.

SUMMARY

The Puddy-Chrome Lakes ultramafic intrusion exhibits many of the features typical of an alpine-type intrusion as outlined by Irvine and Findlay (1972). Chromite occurrences within the Puddy-Chrome Lakes body are similar to layered and podiform alpine-type chromite deposits. An increase in the intensity of the foliation as the ultramafic contact is approached suggests a relatively cold temperature during emplacement. In addition, the location of the Puddy-Chrome Lakes serpentinite along an east-trending fault zone would suggest an origin facilitated by faulting. All of these characteristics are compatible with alpine-type ultramafics. Whole-rock and chromite compositions together suggest an affinity for an alpine-type ultramafic host rock.

Chromite within alpine-type ultramafics occurs in disseminated, layered, and podiform style. In each style, the chromite-bearing zones are discontinuous and randomly distributed. Economic chromite deposits, where they occur, are usually in larger volume metallurgical grade pods. Chromite occurrences in the Puddy-Chrome Lakes body represent all three styles of mineralization and appear to be both small in scale and discontinuous. Despite the high Cr:Fe ratio, the restricted size of the overall intrusion could be a limiting factor for chromite exploration in the Puddy-Chrome Lakes ultramafic body.

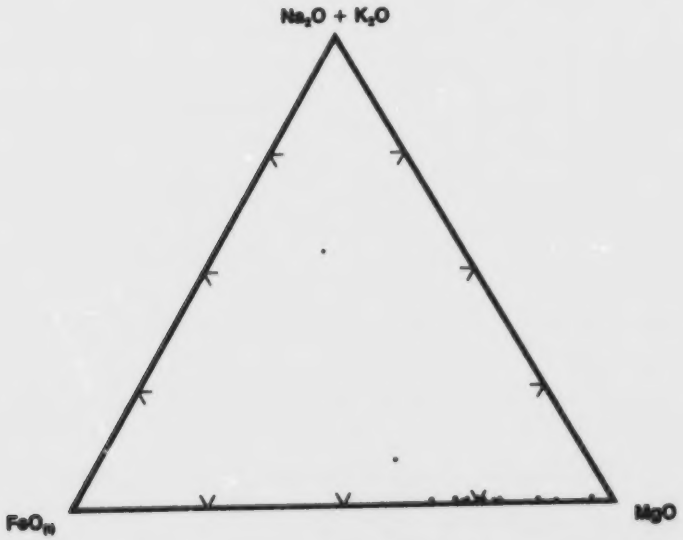

Figure 17. AFM plot of whole rock analyses from the Puddy-Chrome Lakes area.

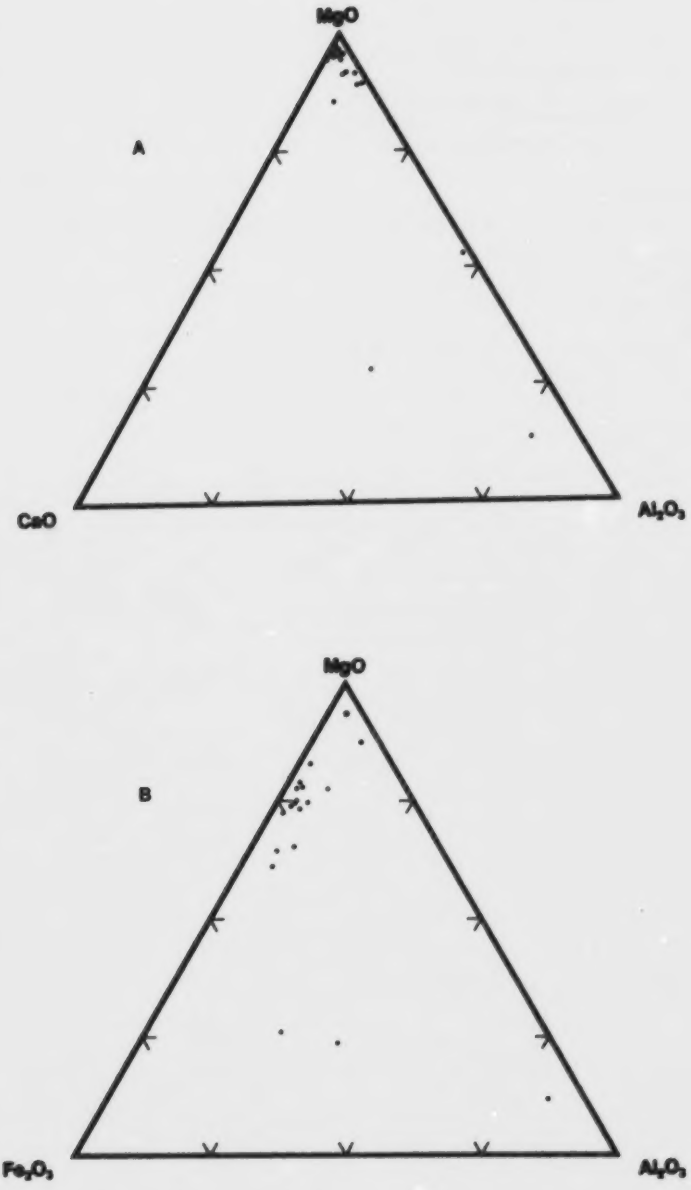

Figure 18. Ternary diagrams illustrating the restricted fractionation of the Puddy-Chrome Lakes ultramafic body. The two highest Al_2O_3 values are from Keweenawan diabase dikes.

TABLE 5. MAJOR AND TRACE ELEMENT ANALYSES FROM PUDDY-CHROME LAKES AREA.

Wt % Oxides	1 Serp.	2 Serp.	3 Serp.	4 Serp.	5 Q-F P	6 Q-F P	7 Serp.	8 Serp.	9 Serp.	10 Serp.	11 Serp.	12 Serp.	13 Serp.	14 Serp.	15 Serp.	16 Serp.	17 Gabbro
SiO_2	35.50	34.90	38.20	38.00	65.70	36.20	37.00	34.50	39.20	32.50	38.00	40.40	36.20	39.50	37.80	37.90	46.70
Al_2O_3	1.09	1.14	1.18	1.30	16.50	1.89	0.80	2.50	3.41	0.58	0.69	0.50	0.73	0.60	3.31	2.22	13.40
Fe_2O_3	8.51	10.51	10.10	9.54	1.09	14.00	8.86	8.72	5.63	6.71	8.61	1.29	11.40	3.59	13.20	10.50	14.30
FeO	3.86	3.94	0.63	2.12	2.18	1.48	2.54	0.63	6.90	0.21	1.34	0.35	2.75	0.71	0.00	0.00	0.00
MgO	37.00	36.10	35.20	35.20	2.58	31.10	36.00	35.50	33.40	42.00	38.20	40.40	34.50	38.30	34.50	37.40	9.25
CaO	0.05	0.21	0.10	0.30	1.89	0.73	0.03	2.61	0.30	0.03	0.25	1.60	0.70	1.01	0.51	0.70	10.20
Na_2O	0.00	0.00	0.11	0.06	3.64	0.11	0.06	0.06	0.11	0.06	0.06	0.06	0.06	0.06	0.00	0.00	1.67
K_2O	0.00	0.00	0.07	0.05	3.06	0.05	0.05	0.05	0.05	0.05	0.05	0.05	0.05	0.05	0.00	0.00	0.82
H_2O^+	10.30	10.50	11.90	11.30	2.10	11.40	11.70	10.20	10.00	15.40	12.00	12.00	10.70	12.00	10.60	11.60	2.20
H_2O^-	2.43	1.79	1.03	0.92	0.45	1.01	1.06	0.83	0.35	1.02	1.17	0.86	1.29	1.32	0.00	0.00	0.00
CO_2	1.44	1.70	0.22	0.41	0.21	0.50	0.18	2.74	0.33	1.60	0.35	1.20	0.46	1.07	0.56	0.86	0.07
TiO_2	0.03	0.03	0.10	0.06	0.39	0.12	0.06	0.06	0.20	0.04	0.04	0.03	0.06	<0.01	0.17	0.09	1.02
P_2O_5	0.00	0.00	<0.01	<0.01	0.07	<0.01	<0.01	<0.01	<0.01	<0.01	<0.01	<0.01	<0.01	<0.01	0.04	0.03	0.10
S	0.02	0.02	<0.01	<0.01	0.02	0.02	<0.01	<0.01	0.12	<0.01	<0.01	<0.01	<0.01	<0.01	0.03	<0.01	0.03
MnO	0.04	0.04	0.09	0.06	0.05	0.13	0.06	10.27	0.17	0.07	0.08	0.04	0.07	0.19	0.16	0.14	0.23
TOTAL	100.30	100.80	98.90	99.40	100.00	98.70	98.50	98.70	100.20	100.30	100.90	98.80	99.00	98.40	100.30	100.60	99.90
LOI	13.30	12.50													10.60	11.60	2.20
ppm																	
Ba	20	20	20A	30	70	20	20	20	40	20	30	30	40	40	20	20	140
Co	61	65	80A	9	35	40	43	9	110	20	85	200	25	880	101	152	48
Cr	850	990	.0860	.1400	.0025	.4100	.1360	.3500	.6040	.0480	.0880	.0600	.1340	.0800	5240	2000	109
Cu	<5	<5	<5	35	10	10	<5	10	50	<5	<5	65	<5	320	10	6	7
Li	<3	<3	<3A	<3	45	<3	<3	<3	<3	<3	<3	<3	<3	<3	<3	<3	79
Ni	2350	2280	.2440	.2140	.0040	.1580	.2080	.1620	.1320	.2520	.2680	.2000	.2000	.3360	1060	920	64
Pb	<10	<10	35A	10	10	30	<10	<10	<10	<10	<10	10	<10	440	<10	<10	17
Zn	15	15	30A	20	45	30	20	10	30	110	40	170	20	320	26	26	122

Q-F P — Quartz-Feldspar Porphyry
Serp. — Serpentinite
Analyses #3 to #14 provided by C. Kustra, Ontario Geological Survey. All other analyses by Geoscience Laboratories, Ontario Geological Survey, Toronto.

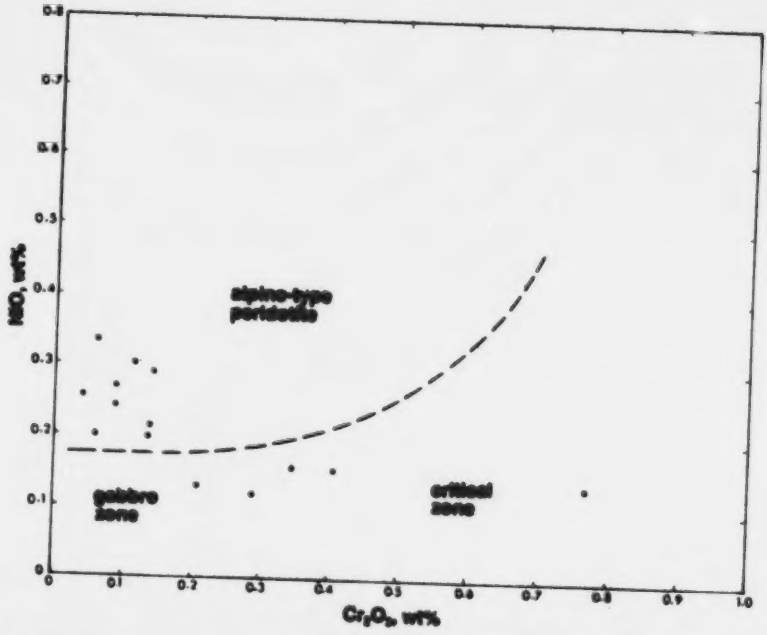

Figure 19. Decreasing Ni with increasing Cr in samples from the Puddy-Chrome Lakes area. Greater than half the samples plot in the alpine-type peridotite field (after Irvine and Findlay 1972).

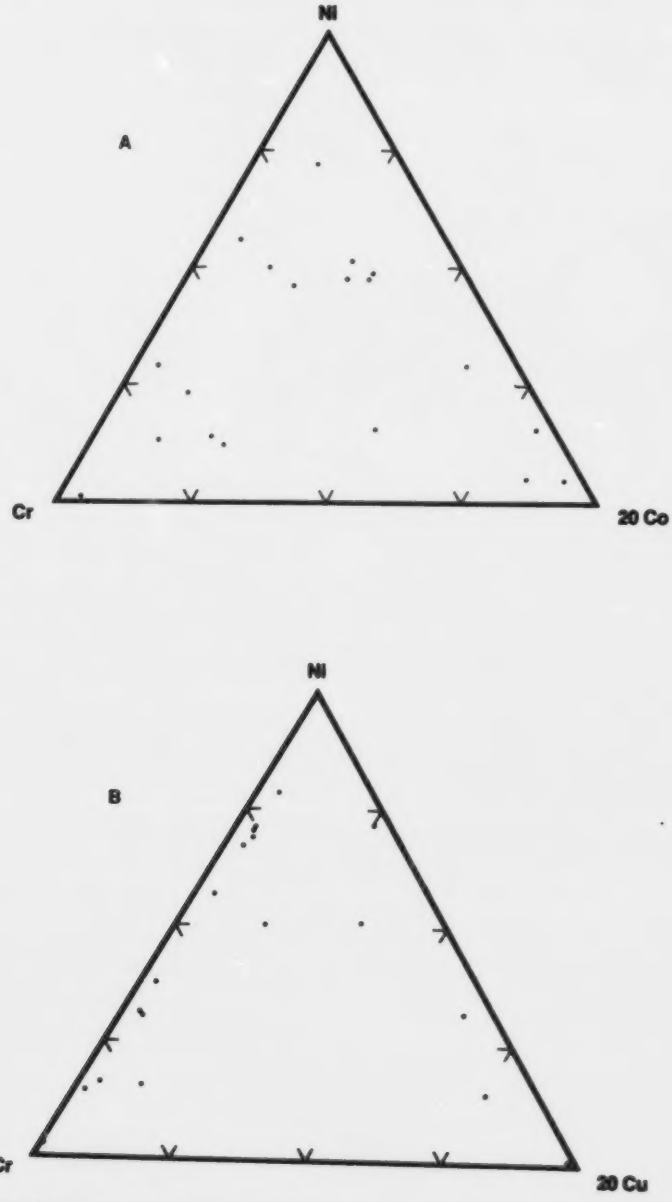

Figure 20. Puddy-Chrome Lakes Cr-Ni values, showing a wide range of values with minor Co and Cu. Co and Cu scales have been amplified to avoid congestion of points on or close to the Cr-Ni join.

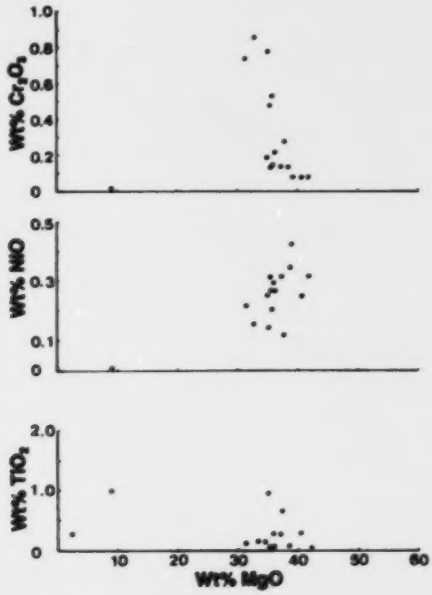

Figure 21. Variation of Cr_2O_3, NiO, and TiO_2 with MgO in Puddy-Chrome Lakes serpentinite.

TABLE 6. Cr VALUES FROM PUDDY-CHROME LAKES CHROMITE OCCURRENCES.

	Description	Cr (ppm)
1.	Serpentinized peridotite, mine dump	5,240
2.	Chromitiferous serpentinite, mine dump	75,100
3.	Massive chromitite, mine dump	410,000

Big Trout Lake Deposit

LOCATION AND ACCESS

Big Trout Lake is located 420 km northeast of Red Lake (Figure 22), and is accessible by float-equipped aircraft from either Red Lake or Pickle Lake. A landing strip on Post Island at the community of Trout Lake accommodates wheel-equipped aircraft.

PREVIOUS WORK

Early mapping was carried out by J.B. Tyrrell (1913) and brief descriptions of the major rock types are included in his report. Scattered information from prospecting activity can be found in the files of the Resident Geologist's Office, Ontario Ministry of Northern Development and Mines, Sioux Lookout. Reconnaissance geological mapping was conducted by Hudec (1964) for the Ontario Department of Mines and additional regional mapping was carried out by Thurston *et al.* (1971, 1979).

GENERAL GEOLOGY

The Big Trout Lake area is underlain by an Early Precambrian sequence which includes sedimentary, volcanic, and intrusive rocks (Figure 23). Much of the area is covered with till and outcrops are widely scattered. Intrusive rocks of prime interest to this study include anorthositic gabbro which outcrops on the northeast shoreline of Big Trout Lake, gabbroic anorthosite along the southeast shoreline of Big Trout Lake, and serpentinized peridotite described from diamond drilling south of Leopard Point.

Anorthositic gabbro and gabbroic anorthosite outline the limbs of an eastward plunging anticline (Hudec 1964; Thurston *et al.* 1971). The anorthositic suite is intrusive into an Archean metabasalt-andesite complex. South of the gabbroic anorthosite at Leopard Point, diamond drill information reveals a sheet-like serpentinite body consisting of dunite and peridotite (Figure 23). The intrusion dips steeply to the east, is up to 400 m thick, and is in fault contact with quartz diorite

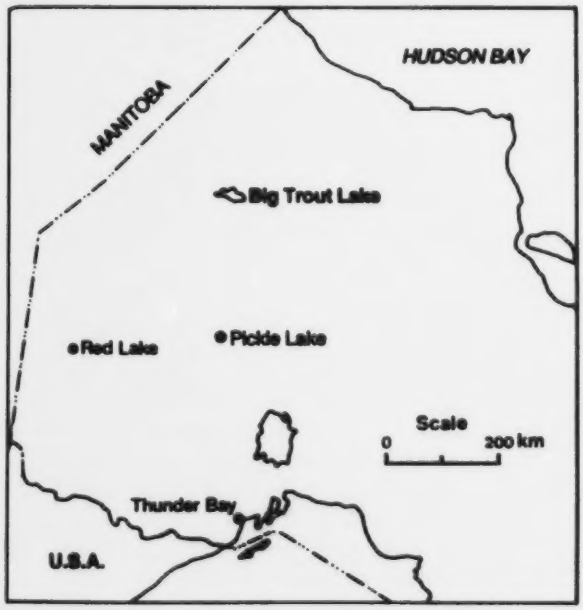

Figure 22. *Location Map, Big Trout Lake, Ontario.*

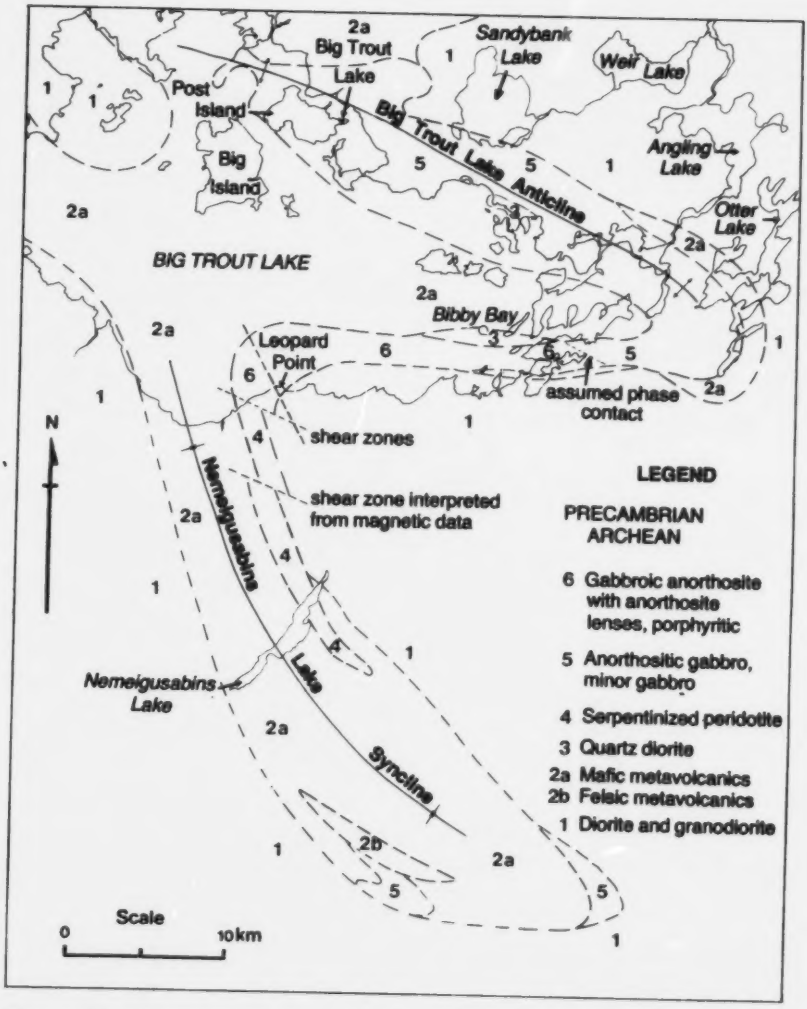

Figure 23. *General geology of the Big Trout Lake area (after Thurston et al.* 1971).

Photo 12. *Porphyritic gabbroic anorthosite on the southeast shore of Big Trout Lake, lens cap for scale.*

Photo 13. *Layered gabbro and anorthositic gabbro at Leopard Point.*

and diorite to the east. Shearing at the contact and within the serpentinite becomes increasingly more intense northwards towards Leopard Point. A fault contact is suggested between the gabbroic anorthosite at Leopard Point and the serpentinite and is shown as shear zones on Figure 23. The nearly perpendicular angle between the north-striking serpentinite and the east-striking south limb of the anorthositic anticlinorium represents a southeasterly dipping synclinal structure with the observed shearing in the anorthositic and ultramafic rocks representing an axial planar fault zone. This fault zone appears as parallel, southeast-striking shear zones in anorthositic rocks at Leopard Point.

ANORTHOSITIC ROCKS

Rocks of the anorthositic suite include anorthositic gabbro, gabbroic anorthosite, and sparsely distributed lenses of anorthosite. The anorthositic suite rocks are all very coarse grained, commonly porphyritic (Photo 12), and massive in structure. Large scale (several metres) layering is developed between the north and south limbs of the anticlinal structure with more leucocratic gabbroic anorthosite of the southeast shoreline area representing the lighter plagioclase-rich float fraction. The lenses of anorthosite occur in this zone and can be observed in the shoreline section south of Bibby Bay. Smaller scale layering is exposed at Leopard Point and strikes northwards with a steep easterly dip. The layers consist of alternating medium- to coarse-grained gabbroic anorthosite and fine- to medium-grained amphibolitic gabbro (Photo 13).

The layers are planar with minor boudinage-style undulations in the gabbro layers. The gabbroic layers, some of which bifurcate into thinner but parallel layers, are usually separated by 10 to 15 cm of gabbroic anorthosite. Layering is discontinuous along strike, eventually pinching out over lengths of 2 to 5 m. Contacts between layers are diffuse over distances of 0.5 to 1 cm, suggesting a co-nucleation of pyroxene and plagioclase for a short interval.

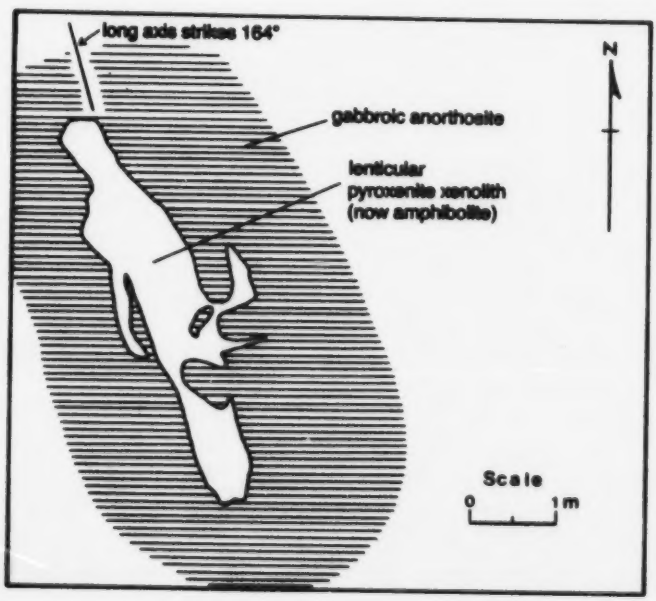

Figure 24. Diagram illustrating features of an ultramafic xenolith at Leopard Point.

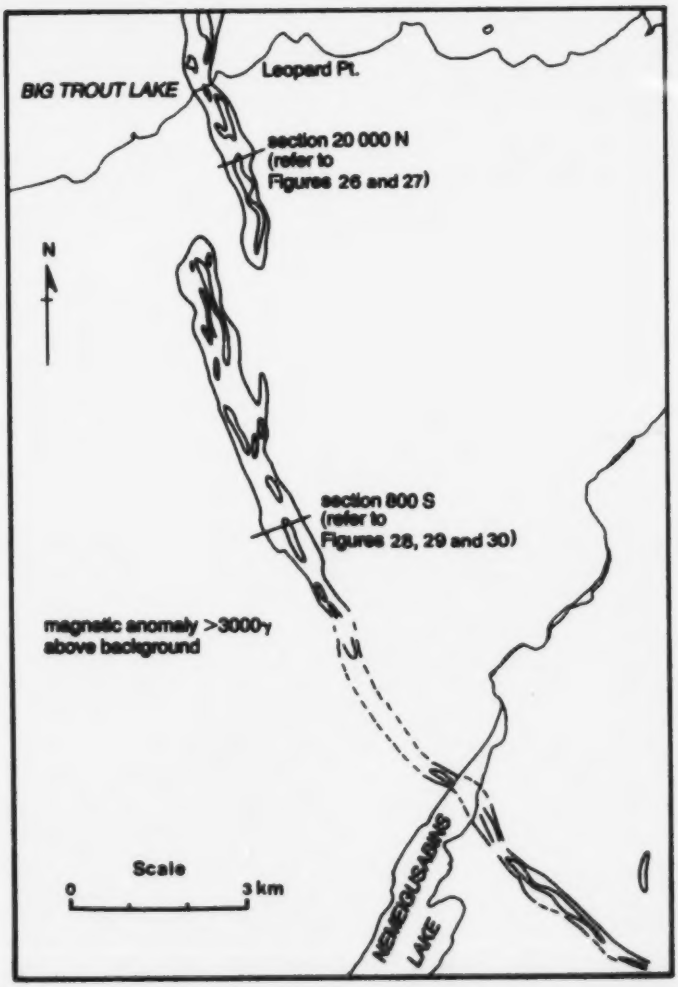

Figure 25. Drill sections through magnetic anomaly reflecting serpentinite body at Big Trout Lake.

TABLE 7. MODAL ANALYSES OF SERPENTINITES FROM BIG TROUT LAKE (1000 POINTS PER THIN SECTION).

Sample No.	2	7	28	30	40
Lizardite	75.4	—	45.0	74.8	90.3
Antigorite	19.0	38.8	29.7	12.0	5.3
Chromite	2.9	61.2	10.8	12.3	2.4
Actinolite	—	—	14.2	0.9	0.6
Carbonate	1.0	—	0.3	—	1.4
(magnesite?)	—	—	—	—	—
Chlorite (?)	1.7	—	—	—	—
TOTAL (%)	100.0	100.0	100.0	100.0	100.0

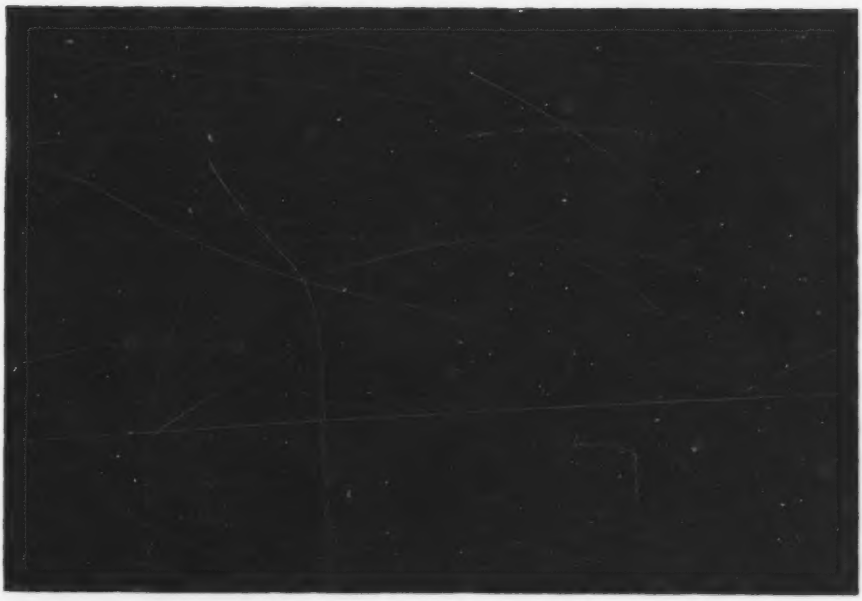

Photo 14. *Serpentinized olivine with lizardite cores and antigorite rims. Plane light. X28.*

Layered rocks at Leopard Point are cut by northwest-trending amphibolitic gabbro dikes, the largest observed being 8 m wide. These rocks are cut by two parallel, southeast-striking, vertically dipping, shear zones.

Ultramafic (amphibolitized pyroxenite) xenoliths occur at Leopard Point. The coarse-grained ultramafic xenoliths are irregular (amoeboid) in shape and up to 5 by 2 m in size (Figure 24). Smaller, 20 to 50 cm, irregularly shaped inclusions of gabbroic anorthosite are contained within the larger ultramafic xenoliths.

The occurrence of pyroxenitic xenoliths in the gabbroic anorthosite at Leopard Point, and the proximity of these rocks to the serpentinite body outlined from drilling, strongly suggest a genetic relationship. Faulting has disrupted the original fractionation sequence in the Leopard Point area, placing ultramafic rocks adjacent to the gabbroic anorthosite.

SERPENTINIZED ULTRAMAFIC ROCKS

The ultramafic rocks recovered from drill core extend from Leopard Point on the south shore of Big Trout Lake south to the Nemeigusabins Lake area, a distance of approximately 16 km (Figure 23). Chromite in both disseminated and layered form occur in these ultramafic rocks where they have been explored by drilling over a distance of 6.0 m (Figure 25).

The serpentinized ultramafic body is altered from peridotite. On a fresh surface, the serpentinite is a mottled black green to dark green with chromite grains giving a peppered texture in the chromitiferous zones. Serpentinization has resulted in a pseudomorphic texture which reflects a primary magmatic olivine and pyroxene cumulate. Primary olivine has been completely altered to lizardite and antigorite which appear as dark green cores (lizardite) and pale green rims (antigorite) after primary olivine (Photo 14). In some lizardite cores, the serpentinite is grey-blue to deep blue in colour. The common assemblage resulting from serpentinization of peridotite is:

lizardite + antigorite + chromite + actinolite + chlorite + carbonate (magnesite?)

SERPENTINITES

Serpentinite, in the drill holes illustrated in Figures 26, 27, 28, 29, and 30, is characterized by medium- to coarse-grained, massive, black-green rock with a well preserved primary cumulate texture. The cumulate phases are olivine and pyroxene, now mostly lizardite, and chromite (Table 7). Primary olivine has been completely altered to lizardite + antigorite, which in hand specimen can be observed as dark green (lizardite) cores and pale green (antigorite) rims. Grain size of primary olivine throughout the serpentinite is consistently medium to coarse. Chromite is consistently very fine grained throughout the intrusion.

Drill hole 57320 (section 20000 N; Figure 27), located approximately 1.6 m south of the anorthositic gabbro exposed at Leopard Point, first penetrates quartz diorite and diorite before cutting serpentinite. The diorite becomes increasingly sheared and foliated as the serpentinite contact is approached, with serpentinite at the contact also being sheared. The zone of intense shearing is 4 m wide and defines of a fault contact between country rock diorites and the serpentinite. An 86 m wide zone of shearing, strongly foliated and talcose, extends downwards from 222 m. A thinner shear zone extends for 22 m downwards from 313 m (Figure 27). Hole 57320 (Figure 27), which is the closest of all the holes examined to the country rock, exhibits the most highly sheared serpentinite. This would demonstrate an increasing intensity of shearing adjacent to the serpentinite-diorite fault contact. In hole 57321 of section 20000 N, which is 244 m from the contact, shearing is less well developed (Figure 25).

Brecciated serpentinite is present in hole 57321 of section 20000 N and in hole 57313 of section 800 S (Figure 30). The breccia in hole 57321 is associated with the chromitite layers (75% chromite) and may represent primary igneous brec-

ciation, as the brecciated chromitite layers are confined to massive non-sheared serpentinite. The breccia fragments are 1 to 2 cm in size and are plastically deformed. Breccia in hole 57313, in contrast, represents brittle deformation of massive serpentinite, followed by hematitic alteration.

LIZARDITE AND ANTIGORITE

Lizardite, the predominant serpentine mineral, forms both interlocking and interfingering textures replacing olivine and pyroxene. The pseudomorphic textures indicate primary subhedral to euhedral cumulate olivines and pyroxenes. Interlocking lizardite commonly forms mesh-textured units which together form a patchwork mosaic of lizardite within each olivine grain. The mesh-textured units are bounded by ribbony lizardite which, in many cases, forms a rim enveloping the olivine grain. Lizardite is also the common vein-filling serpentine mineral where individual blades (interlocking texture) or fingers (interfingering texture) grow perpendicular to fracture walls.

Antigorite is the second most commonly developed serpentinite mineral (Table 7). It occurs as thin rims (approximately 0.10 of the grain diameter) surrounding relict olivine and pyroxene. Antigorite also occurs in larger volumes where two or more olivine grains meet. In addition, veinlets of antigorite are observed to cut the predominantly lizardite serpentinite.

The higher proportion of lizardite, representing lower grade metamorphic conditions during serpentinization, to antigorite, reflecting higher metamorphic conditions, suggests prograde serpentinization under low to medium greenschist conditions, terminating in a relatively short period of upper greenschist-lower amphibolite conditions. Microfracturing at th peak of the prograde metamorphism would allow antigorite to form veinlet-filling material and, with later retrograde conditions, lizardite would become the vein-filling serpentine mineral.

CHROMITE

Chromite is confined to the serpentinite body and occurs in both disseminated and layered form. The massive serpentinite carries 1% to 3% disseminated chromite which is intercumulate in texture. Distinct chromitite layers are formed from greater than 75% accumulation of chromite and may form monomineralic chromitite layers.

Disseminated chromite occurs as subhedral to euhedral grains 0.5 to 1.0 mm in size. Proximal to shear zones, the chromite grains are fractured whereas in massive serpentinite they are whole. The chromite grains are opaque towards grain edges where they may exhibit a deep reddish brown colour. Inclusions of silicate minerals occur within approximately 25% of chromite grains. Silicate inclusions include lizardite, mica, and a possible amphibole. A sulphide inclusion phase is also present and is sparsely distributed in layered chromitite. Sulphide inclusions are 5 to 20 microns in diameter, euhedral and hexagonal, and are white with high reflectance. These are suggested to be platinum-group mineral inclusions in chromite.

Disseminated chromite forms an intercumulate phase where it outlines original olivine grain boundaries. This chromite has finely serrated borders, and in some areas it is penetrated by matrix antigorite (Photo 15). Corrosion of the disseminated chromite could result from interaction between the chromite and late serpentinizing fluids, where fO_2 would be low. Chromite grains with corroded borders tend to be surrounded by a greenish micaceous envelope. It is suggested that Fe^{++} from chromite interacted with the surrounding lizardite and/or antigorite plus fluids to form an Fe-chlorite.

Chromite within chromitite layers occurs as unfractured, subhedral to anhedral aggregates. Inclusions of silicate minerals occur within chromitè grains of the layered environment and are similar in proportion and features to inclusions in disseminated chromite. Chromites from the chromitite layers are generally in direct contact with each other.

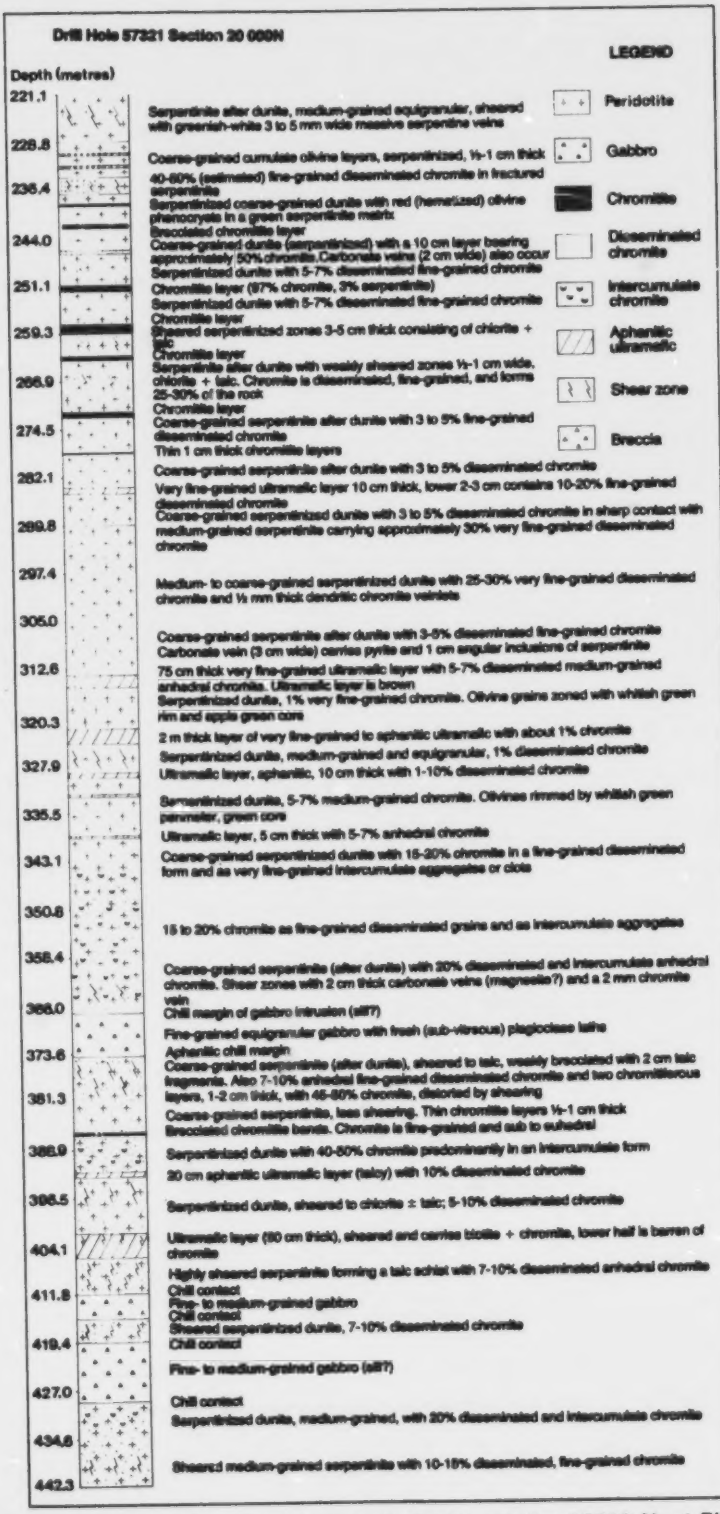
Drill Hole 57321 Section 20 000N
LEGEND
Depth (metres)
Peridotite
Gabbro
Chromitite
Disseminated chromite
Intercumulate chromite
Aphanitic ultramafic
Shear zone
Breccia
221.1
228.8
236.4
244.0
251.1
259.3
266.9
274.5
282.1
289.8
297.4
305.0
312.6
320.3
327.9
335.5
343.1
350.8
358.4
366.0
373.6
381.3
388.9
396.5
404.1
411.8
419.4
427.0
434.6
442.3
Serpentinite after dunite, medium-grained equigranular, sheared with greenish-white 3 to 5 mm wide massive serpentine veins
Coarse-grained cumulate olivine layers, serpentinized, ½-1 cm thick
40-60% (estimated) fine-grained disseminated chromite in fractured serpentinite
Serpentinized coarse-grained dunite with red (hematized) olivine phenocrysts in a green serpentinite matrix
Brecciated chromitite layer
Coarse-grained dunite (serpentinized) with a 10 cm layer bearing approximately 50% chromitite.Carbonate veins (2 cm wide) also occur
Serpentinized dunite with 5-7% disseminated fine-grained chromite
Chromitite layer (97% chromite, 3% serpentinite)
Serpentinized dunite with 5-7% disseminated fine-grained chromite
Chromitite layer
Sheared serpentinized zones 3-5 cm thick consisting of chlorite + talc
Chromitite layer
Serpentinite after dunite with weakly sheared zones ½-1 cm wide, chlorite + talc. Chromite is disseminated, fine-grained, and forms 25-30% of the rock
Chromitite layer
Coarse-grained serpentinite after dunite with 3 to 5% fine-grained disseminated chromite
Thin 1 cm thick chromitite layers
Coarse-grained serpentinite after dunite with 3 to 5% disseminated chromite
Very fine-grained ultramafic layer 10 cm thick, lower 2-3 cm contains 10-20% fine-grained disseminated chromite
Coarse-grained serpentinized dunite with 3 to 5% disseminated chromite in sharp contact with medium-grained serpentinite carrying approximately 30% very fine-grained disseminated chromite
Medium- to coarse-grained serpentinized dunite with 25-30% very fine-grained disseminated chromite and ½ mm thick dendritic chromite veinlets
Coarse-grained serpentinite after dunite with 3-5% disseminated fine-grained chromite
Carbonate vein (3 cm wide) carries pyrite and 1 cm angular inclusions of serpentinite
75 cm thick very fine-grained ultramafic layer with 5-7% disseminated medium-grained anhedral chromite. Ultramafic layer is brown
Serpentinized dunite, 1% very fine-grained chromite. Olivine grains zoned with whitish green rim and apple green core
2 m thick layer of very fine-grained to aphanitic ultramafic with about 1% chromite
Serpentinized dunite, medium-grained and equigranular, 1% disseminated chromite
Ultramafic layer, aphanitic, 10 cm thick with 1-10% disseminated chromite
Serpentinized dunite, 5-7% medium-grained chromite. Olivines rimmed by whitish green pennester, green core
Ultramafic layer, 5 cm thick with 5-7% anhedral chromite
Coarse-grained serpentinized dunite with 15-20% chromite in a fine-grained disseminated form and as very fine-grained intercumulate aggregates or clots
15 to 20% chromite as fine-grained disseminated grains and as intercumulate aggregates
Coarse-grained serpentinite (after dunite) with 20% disseminated and intercumulate anhedral chromite. Shear zones with 2 cm thick carbonate veins (magnesite?) and a 2 mm chromite vein
Chill margin of gabbro intrusion (sill?)
Fine-grained equigranular gabbro with fresh (sub-vitreous) plagioclase laths
Aphanitic chill margin
Coarse-grained serpentinite (after dunite), sheared to talc, weakly brecciated with 2 cm talc fragments. Also 7-10% anhedral fine-grained disseminated chromite and two chromitiferous layers, 1-2 cm thick, with 45-60% chromite, distorted by shearing
Coarse-grained serpentinite, less shearing. Thin chromitite layers ½-1 cm thick
Brecciated chromitite bands. Chromite is fine-grained and sub to euhedral
Serpentinized dunite with 40-50% chromite predominantly in an intercumulate form
20 cm aphanitic ultramafic layer (talcy) with 10% disseminated chromite
Serpentinized dunite, sheared to chlorite ± talc; 5-10% disseminated chromite
Ultramafic layer (50 cm thick), sheared and carries biotite + chromite, lower half is barren of chromite
Highly sheared serpentinite forming a talc schist with 7-10% disseminated anhedral chromite
Chill contact
Fine- to medium-grained gabbro
Chill contact
Sheared serpentinized dunite, 7-10% disseminated chromite
Chill contact
Fine- to medium-grained gabbro (sill?)
Chill contact
Serpentinized dunite, medium-grained, with 20% disseminated and intercumulate chromite
Sheared medium-grained serpentinite with 10-15% disseminated, fine-grained chromite

Figure 26. *Stratigraphic section from hole 57321, section 20000 N, at Big Trout Lake, plunge=45°W.*

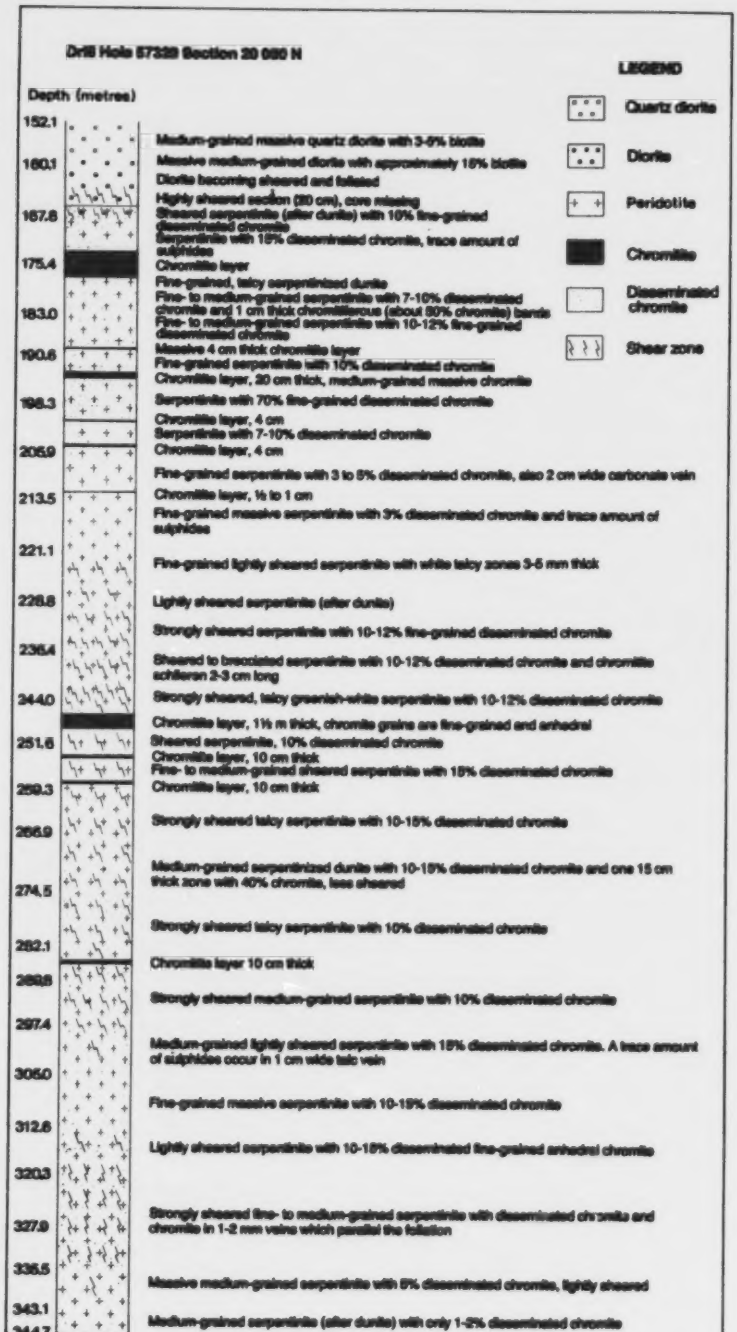
Drill Hole 57320 Section 20 000 N
Depth (metres)
LEGEND
Quartz diorite
Diorite
Peridotite
Chromitite
Disseminated chromite
Shear zone
152.1
160.1
167.8
175.4
183.0
190.6
198.3
205.9
213.5
221.1
228.8
236.4
244.0
251.6
259.3
266.9
274.5
282.1
289.8
297.4
305.0
312.6
320.3
327.9
335.5
343.1
344.7
Medium-grained massive quartz diorite with 3-5% biotite
Massive medium-grained diorite with approximately 15% biotite
Diorite becoming sheared and foliated
Highly sheared section (20 cm), core missing
Sheared serpentinite (after dunite) with 10% fine-grained disseminated chromite
Serpentinite with 15% disseminated chromite, trace amount of sulphides
Chromitite layer
Fine-grained, talcy serpentinized dunite
Fine- to medium-grained serpentinite with 7-10% disseminated chromite and 1 cm thick chromitiferous (about 80% chromite) bands
Fine- to medium-grained serpentinite with 10-12% fine-grained disseminated chromite
Massive 4 cm thick chromitite layer
Fine-grained serpentinite with 10% disseminated chromite
Chromitite layer, 20 cm thick, medium-grained massive chromite
Serpentinite with 70% fine-grained disseminated chromite
Chromitite layer, 4 cm
Serpentinite with 7-10% disseminated chromite
Chromitite layer, 4 cm
Fine-grained serpentinite with 3 to 5% disseminated chromite, also 2 cm wide carbonate vein
Chromitite layer, ½ to 1 cm
Fine-grained massive serpentinite with 3% disseminated chromite and trace amount of sulphides
Fine-grained lightly sheared serpentinite with white talcy zones 3-5 mm thick
Lightly sheared serpentinite (after dunite)
Strongly sheared serpentinite with 10-12% fine-grained disseminated chromite
Sheared to brecciated serpentinite with 10-12% disseminated chromite and chromitite schlieren 2-3 cm long
Strongly sheared, talcy greenish-white serpentinite with 10-12% disseminated chromite
Chromitite layer, 1½ m thick, chromite grains are fine-grained and anhedral
Sheared serpentinite, 10% disseminated chromite
Chromitite layer, 10 cm thick
Fine- to medium-grained sheared serpentinite with 15% disseminated chromite
Chromitite layer, 10 cm thick
Strongly sheared talcy serpentinite with 10-15% disseminated chromite
Medium-grained serpentinized dunite with 10-15% disseminated chromite and one 15 cm thick zone with 40% chromite, less sheared
Strongly sheared talcy serpentinite with 10% disseminated chromite
Chromitite layer 10 cm thick
Strongly sheared medium-grained serpentinite with 10% disseminated chromite
Medium-grained lightly sheared serpentinite with 15% disseminated chromite. A trace amount of sulphides occur in 1 cm wide talc vein
Fine-grained massive serpentinite with 10-15% disseminated chromite
Lightly sheared serpentinite with 10-15% disseminated fine-grained anhedral chromite
Strongly sheared fine- to medium-grained serpentinite with disseminated chromite and chromite in 1-2 mm veins which parallel the foliation
Massive medium-grained serpentinite with 5% disseminated chromite, lightly sheared
Medium-grained serpentinite (after dunite) with only 1-2% disseminated chromite

Figure 27. *Stratigraphic section from drill hole 57320, section 20000 N, at Big Trout Lake, plunge = 45° W.*

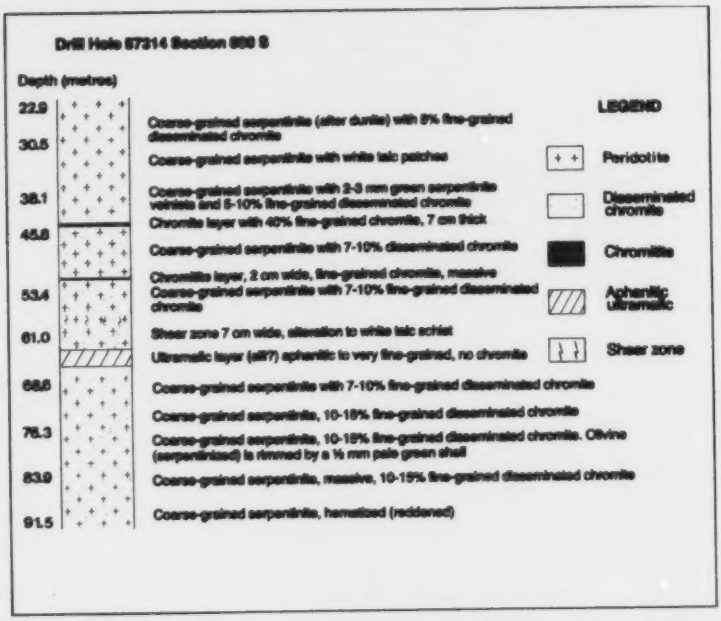
Drill Hole 57314 Section 800 S
Depth (metres)
22.9
30.5
38.1
45.8
53.4
61.0
68.6
76.3
83.9
91.5
Coarse-grained serpentinite (after dunite) with 5% fine-grained disseminated chromite
Coarse-grained serpentinite with white talc patches
Coarse-grained serpentinite with 2-3 mm green serpentinite veinlets and 5-10% fine-grained disseminated chromite
Chromite layer with 40% fine-grained chromite, 7 cm thick
Coarse-grained serpentinite with 7-10% disseminated chromite
Chromitite layer, 2 cm wide, fine-grained chromite, massive
Coarse-grained serpentinite with 7-10% fine-grained disseminated chromite
Shear zone 7 cm wide, alteration to white talc schist
Ultramafic layer (sill?) aphanitic to very fine-grained, no chromite
Coarse-grained serpentinite with 7-10% fine-grained disseminated chromite
Coarse-grained serpentinite, 10-15% fine-grained disseminated chromite
Coarse-grained serpentinite, 10-15% fine-grained disseminated chromite. Olivine (serpentinized) is rimmed by a ½ mm pale green shell
Coarse-grained serpentinite, massive, 10-15% fine-grained disseminated chromite
Coarse-grained serpentinite, hematized (reddened)
LEGEND
Peridotite
Disseminated chromite
Chromitite
Aphanitic ultramafic
Shear zone

Figure 28. Stratigraphic section from drill hole 57314, section 800 S at Big Trout Lake, plunge=45° W.

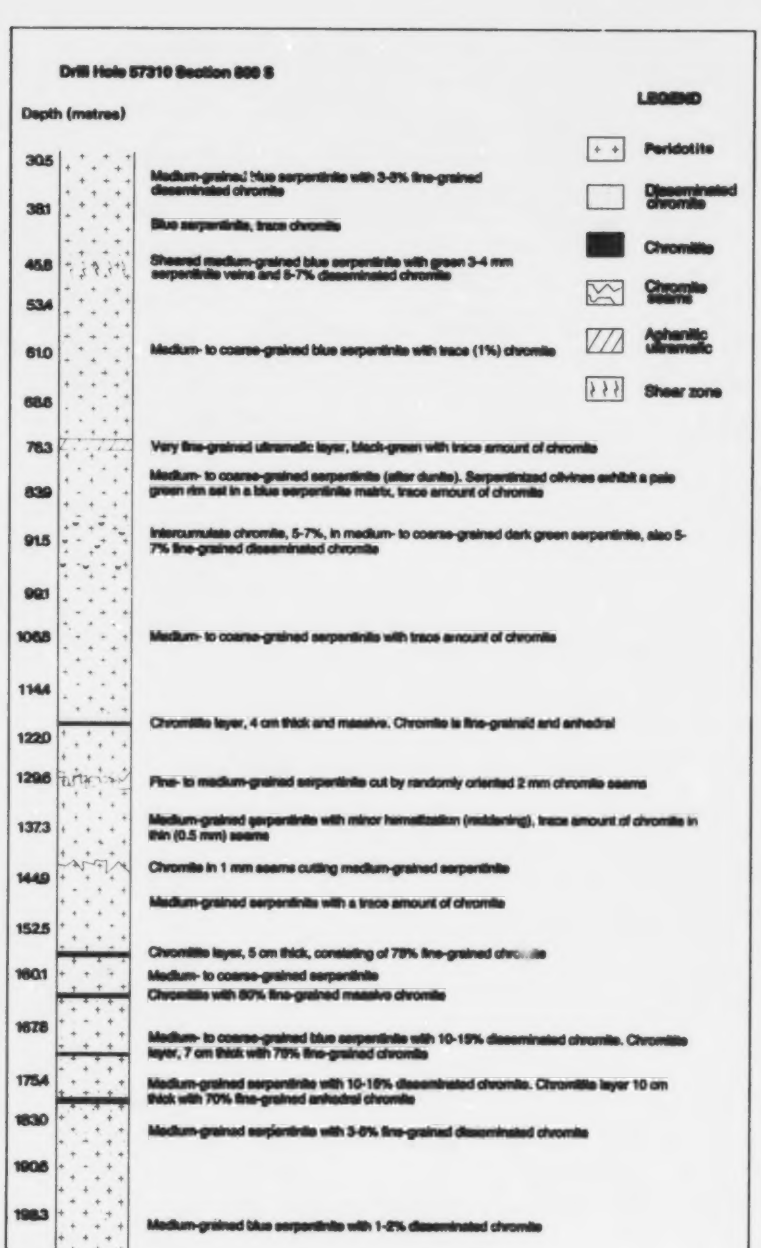
Drill Hole 57310 Section 800 S
Depth (metres)
LEGEND
Peridotite
Disseminated chromite
Chromitite
Chromite seams
Aphanitic ultramafic
Shear zone
305
381
458
534
610
686
763
839
915
991
1068
1144
1220
1296
1373
1449
1525
1601
1678
1754
1830
1906
1983
2059
2135
Medium-grained blue serpentinite with 3-5% fine-grained disseminated chromite
Blue serpentinite, trace chromite
Sheared medium-grained blue serpentinite with green 3-4 mm serpentinite veins and 5-7% disseminated chromite
Medium- to coarse-grained blue serpentinite with trace (1%) chromite
Very fine-grained ultramafic layer, black-green with trace amount of chromite
Medium- to coarse-grained serpentinite (after dunite). Serpentinized olivines exhibit a pale green rim set in a blue serpentinite matrix, trace amount of chromite
Intercumulate chromite, 5-7%, in medium- to coarse-grained dark green serpentinite, also 5-7% fine-grained disseminated chromite
Medium- to coarse-grained serpentinite with trace amount of chromite
Chromitite layer, 4 cm thick and massive. Chromite is fine-grained and anhedral
Fine- to medium-grained serpentinite cut by randomly oriented 2 mm chromite seams
Medium-grained serpentinite with minor hematization (reddening), trace amount of chromite in thin (0.5 mm) seams
Chromite in 1 mm seams cutting medium-grained serpentinite
Medium-grained serpentinite with a trace amount of chromite
Chromitite layer, 5 cm thick, consisting of 75% fine-grained chromite
Medium- to coarse-grained serpentinite
Chromitite with 80% fine-grained massive chromite
Medium- to coarse-grained blue serpentinite with 10-15% disseminated chromite. Chromitite layer, 7 cm thick with 75% fine-grained chromite
Medium-grained serpentinite with 10-15% disseminated chromite. Chromitite layer 10 cm thick with 70% fine-grained anhedral chromite
Medium-grained serpentinite with 3-5% fine-grained disseminated chromite
Medium-grained blue serpentinite with 1-2% disseminated chromite

Figure 29. *Stratigraphic section from drill hole 57310, section 800 S, at Big Trout Lake, plunge = 50° W.*

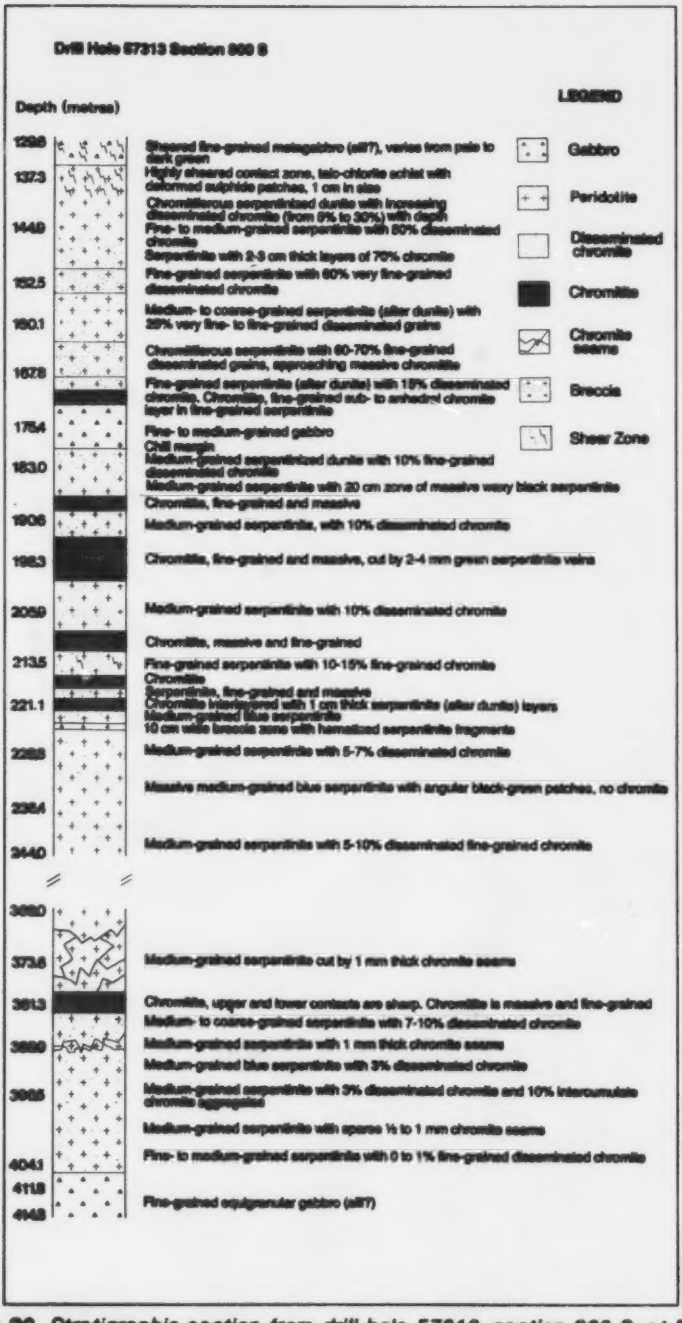
Drill Hole 57313 Section 800 S
Depth (metres)
LEGEND
Gabbro
Peridotite
Disseminated chromite
Chromitite
Chromite seams
Breccia
Shear Zone
1298
Sheared fine-grained metagabbro (sill?), varies from pale to dark green
1373
Highly sheared contact zone, talc-chlorite schist with deformed sulphide patches, 1 cm in size
Chromitiferous serpentinized dunite with increasing disseminated chromite (from 5% to 30%) with depth
1449
Fine- to medium-grained serpentinite with 60% disseminated chromite
Serpentinite with 2-5 cm thick layers of 70% chromite
1525
Fine-grained serpentinite with 60% very fine-grained disseminated chromite
Medium- to coarse-grained serpentinite (after dunite) with
1601
25% very fine- to fine-grained disseminated grains
Chromitiferous serpentinite with 60-70% fine-grained disseminated grains, approaching massive chromitite
1678
Fine-grained serpentinite (after dunite) with 15% disseminated chromite. Chromitite, fine-grained sub- to anhedral chromite layer in fine-grained serpentinite
1754
Fine- to medium-grained gabbro
Chill margin
1830
Medium-grained serpentinized dunite with 10% fine-grained disseminated chromite
Medium-grained serpentinite with 20 cm zone of massive waxy black serpentinite
Chromitite, fine-grained and massive
1906
Medium-grained serpentinite, with 10% disseminated chromite
1983
Chromitite, fine-grained and massive, cut by 2-4 mm green serpentinite veins
2059
Medium-grained serpentinite with 10% disseminated chromite
Chromitite, massive and fine-grained
2135
Fine-grained serpentinite with 10-15% fine-grained chromite
Chromitite
Serpentinite, fine-grained and massive
221.1
Chromitite interlayered with 1 cm thick serpentinite (after dunite) layers
Medium-grained blue serpentinite
10 cm wide breccia zone with hematized serpentinite fragments
2288
Medium-grained serpentinite with 5-7% disseminated chromite
2364
Massive medium-grained blue serpentinite with angular black-green patches, no chromite
2440
Medium-grained serpentinite with 5-10% disseminated fine-grained chromite
3680
3736
Medium-grained serpentinite cut by 1 mm thick chromite seams
3813
Chromitite, upper and lower contacts are sharp. Chromitite is massive and fine-grained
3889
Medium- to coarse-grained serpentinite with 7-10% disseminated chromite
Medium-grained serpentinite with 1 mm thick chromite seams
Medium-grained blue serpentinite with 3% disseminated chromite
3965
Medium-grained serpentinite with 3% disseminated chromite and 10% intercumulate chromite aggregates
Medium-grained serpentinite with sparse ½ to 1 mm chromite seams
4041
Fine- to medium-grained serpentinite with 0 to 1% fine-grained disseminated chromite
4118
4148
Fine-grained equigranular gabbro (sill?)

Figure 30. Stratigraphic section from drill hole 57313, section 800 S, at Big Trout Lake, plunge=45°W.

Photo 15. *Serrated edges on corroded chromite grains, Big Trout Lake. Plane light. X128.*

Polished section studies reveal that both spherical and negative crystal cavity inclusions are common in most chromite grains. Negative crystal cavities are outlined by angular, inward-facing, chromite crystal faces enclosing dark grey silicate inclusions (Photo 16). The largest proportion of silicate inclusions is concentrated around chromite grain edges and along fractures (Photo 16). These peripheral inclusion zones represent ferritchromit rims altered from original magnetite rims. The high density of inclusions in many of the inclusion zones suggests a rapid growth rate of the rims (Spry 1969).

Sulphide mineralization occurs as individual "droplets" of chalcopyrite in serpentinite and as thin, discontinuous rims on, or separating, chromite grains (Photo 17). Sulphides, defining the above textures, have been described by Hiemstra (1979) in some of the chromite zones from the Bushveld Complex. In the Bushveld environment, Hiemstra reports these sulphides as being rich in platinum group elements (PGE). Chromite acted as the collecting agent to trap sulphide droplets, thus concentrating them in the chromite zones. Consequently the PGE potential of the chromitiferous serpentinite should be examined.

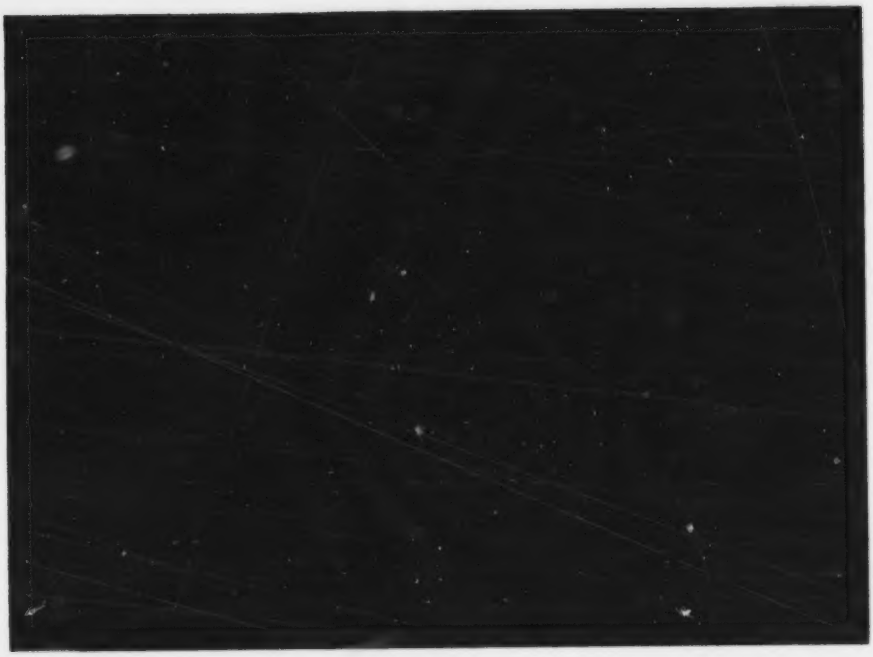

Photo 16. *Silicate inclusion-rich rim and negative crystal cavity fillings in chromite, Big Trout Lake. Reflected light. X125.*

Photo 17. *Sulphide (chalcopyrite, white) trapped between chromite grains, Big Trout Lake. Reflected light. X125.*

Major and Trace Element Chemistry

Samples for both major and trace element chemistry were selected to represent the major ultramafic rock types; analyses are given in Table 8. The anomalous chromitiferous zones were avoided as being atypical with respect to the overall composition of the ultramafic sequence.

An AFM plot (Figure 31) of serpentinite samples illustrates the ultramafic character of the chromitiferous portion of the Big Trout Lake complex. The samples exhibit only trace amounts of total alkalies and high MgO contents. Figure 32, which is a plot of SiO_2 vs. FeO/MgO, reflects the high MgO content (low FeO/MgO) and the low SiO_2 values which range from approximately 34 weight percent to 37 weight percent, typical of dunitic ultramafic rocks. The ultramafic samples were collected from widely separated positions in different drill holes. The close grouping of these analyses indicates that the ultramafic portion of the Big Trout Lake intrusion is chemically relatively homogeneous.

CHROMITE CHEMISTRY

Chromite grains from both layered and disseminated environments were analyzed and exhibit a restricted fractionation trend. Chromite cores, assumed to represent primary compositions, have limited iron enrichment and occupy the ferrian chromite field (Figure 33). Chromite rims plot within the chromian magnetite field and reflect their original magnetite composition, both by the high iron and low alumina contents. Microprobe data is given in Table 9.

In Figure 34, the plot of NiO weight percent vs. Cr_2O_3 weight percent shows a scattering of the data between the gabbro and critical zones, with no data points in the alpine-type peridotite zone. The gabbro and critical zones refer to the Bay of Islands ophiolitic complex which occupies the field below the dashed line in Figure 34. This lower field is also representative of dunite and olivine clinopyroxenite (wehrlite) from the lower half of the layered series of the Muskox Intrusion. Dunites and feldspathic peridotites from the Muskox Intrusion are concentrated between the dashed line and the level of 0.1 weight percent NiO. Below 0.1 weight percent NiO, olivine clinopyroxenite is predominant. The ultramafic rocks from Big Trout Lake are dunitic to peridotitic and plot in the same field as Muskox dunitic and feldspathic peridotitic rocks. Both intrusions on an overall scale are fractionated layered complexes. Within the ultramafic body at Big Trout Lake, the limited degree of fractionation is further shown by the close grouping of points for Cr_2O_3, NiO, and TiO_2 vs. MgO in Figure 35.

A plot of Cr/Fe ratios vs. Mg (weight percent) is shown in Figure 36 and outlines limited fractionation reflected by chromite grains. The Cr/Fe ratios have a low mean value of 0.88 (standard deviation = 0.26), which is compatible with the compositional plots (Figure 33) showing some ferrian chromite and mostly chromian magnetite. The Cr/Fe ratios are given in Table 10.

Chromite compositions are in agreement with the NiO vs. Cr_2O_3 plot where Big Trout Lake analyses are shown to be in fields occupied by ultramafic rocks of the Muskox Intrusion. These data show an affinity for the field outlined for stratiform intrusions (Figure 37; Irvine and Findlay 1972).

SUMMARY

Ultramafic and anorthositic rocks at Big Trout Lake represent a hypabyssal intrusion penetrating Archean metavolcanic rocks. The sequence of ultramafic to mafic rocks begins with peridotite which has been thoroughly serpentinized and ends with anorthositic gabbro to gabbroic anorthosite. Anorthosite lenses are sparsely developed. Fractionation has ended at anorthosite with no apparent granophyric phase. Layering is developed on a large (km) scale between anorthositic gabbro exposed along the north shore of Big Trout Lake and gabbroic anorthosite along the south shore. Within the ultramafic section the serpentinized peridotite exhibits layering defined by fine- to medium-grained chromite. Chromite layers are encountered in all drill holes and outline planar and laterally extensive layer development. These features are similar to the structure and composition of large layered, shallow level intrusions such as the Muskox and Bushveld Complexes. Trace

TABLE 8. MAJOR AND TRACE ELEMENT ANALYSES FROM BIG TROUT LAKE (ALL ANALYSES BY THE GEOSCIENCE LABORATORIES, ONTARIO GEOLOGICAL SURVEY, TORONTO).

Wt % Oxides	1 P.D.	2 D.	3 P.	4 P.D.	5 G.A.	6 A.G.	7 A.G.	8 G.A.	9 G.A.	10 G.A.	11 G.A.	12 A.D.	13 G.D.	14 G.A.	15 G.A.	16 D.D.	17 M.	18 A.	19 G.A.	20 G.A.
SiO_2	35.90	33.80	37.40	35.30	47.20	47.80	47.50	45.90	47.70	46.70	46.40	47.90	48.90	48.10	47.00	64.70	43.20	47.00	49.10	49.70
Al_2O_3	2.23	2.26	2.65	4.10	24.40	17.40	24.30	21.30	27.00	27.40	30.00	7.80	14.50	26.00	28.70	16.50	13.40	32.20	25.70	17.30
Fe_2O_3	4.33	6.15	4.40	6.48	5.10*	11.40*	6.60*	9.32*	4.57*	4.02*	3.56*	14.80*	12.40*	3.56*	2.66*	5.15*	18.30*	1.06*	3.74*	7.62*
FeO	7.06	7.25	7.65	5.96	n/d	n/d	n/d	n/d	n/d	n/d	n/d	n/d	n/d	n/d	n/d	n/d	n/d	n/d	n/d	n/d
MgO	36.20	34.60	34.40	33.00	4.94	8.00	4.15	6.69	3.00	2.70	2.60	13.50	6.68	4.51	1.97	1.91	4.77	0.57	4.43	9.54
CaO	0.24	0.70	0.45	1.72	13.90	11.60	13.80	12.20	14.20	14.20	14.20	12.50	12.30	14.80	15.50	4.83	6.32	15.10	13.80	12.90
Na_2O	0.03	0.00	0.00	0.00	1.72	1.22	1.48	2.20	2.01	2.15	2.29	0.66	2.37	1.82	1.53	4.07	2.64	2.30	1.42	2.37
K_2O	0.00	0.00	0.00	0.00	0.00	0.09	0.04	0.14	0.01	0.01	0.32	0.04	0.08	0.00	0.01	1.26	0.92	0.00	0.05	0.01
H_2O^+	9.47	9.25	10.90	9.71	n/d	n/d	n/d	n/d	n/d	n/d	n/d	n/d	n/d	n/d	n/d	n/d	n/d	n/d	n/d	n/d
H_2O^-	0.53	0.43	0.50	0.65	n/d	n/d	n/d	n/d	n/d	n/d	n/d	n/d	n/d	n/d	n/d	n/d	n/d	n/d	n/d	n/d
CO_2	4.23	5.77	1.26	2.94	0.25	0.14	0.13	0.19	0.16	0.27	0.20	0.20	0.20	0.24	0.62	0.13	3.65	0.23	0.12	0.22
TiO_2	0.07	0.08	0.15	0.07	0.15	0.75	0.62	0.73	0.26	0.28	0.24	0.96	0.91	0.16	0.33	0.64	1.98	0.14	0.11	0.31
P_2O_5	0.00	0.00	0.00	0.00	0.02	0.04	0.04	0.01	0.03	0.03	0.03	0.13	0.09	0.03	0.03	0.17	0.17	0.03	0.02	0.03
S	0.03	0.35	0.05	0.02	0.02	0.04	0.03	0.03	0.04	0.06	0.03	0.02	0.02	0.02	0.10	0.03	0.04	0.05	0.01	0.03
MnO	0.08	0.12	0.15	0.17	0.09	0.18	0.12	0.15	0.07	0.06	0.06	0.21	0.18	0.06	0.05	0.07	0.28	0.01	0.07	0.14
TOTAL	100.40	100.80	100.10	100.10	96.70	100.20	100.00	100.10	100.20	96.50	100.80	99.90	100.20	100.40	100.30	100.90	99.10	99.20	100.20	100.30
ppm																				
Ba	10	20	20	20	50	60	50	60	40	50	60	20	50	40	50	240	130	60	50	50
Co	94	90	124	115	23	42	22	37	16	16	15	71	38	16	9	18	56	7	17	35
Cr	3600	1850	1070	820	259	170	67	113	77	72	52	730	207	211	30	26	34	5	146	372
Cu	12	1740	22	8	17	119	67	60	24	43	20	74	19	16	9	200	230	24	48	39
Li	3	3	3	3	4	10	10	118	86	52	62	39	4	3	7	11	12	5	10	8
Ni	1690	730	1350	1110	60	95	44	154	32	28	43	610	59	60	31	21	53	13	56	115
Pb	42	29	10	10	11	10	16	13	14	10	10	10	23	11	13	22	13	10	10	10
Zn	18	18	31	25	41	80	45	76	36	34	33	92	80	24	14	86	210	10	28	49

A. — Anorthosite
A.D. — Amphibolite dike
A.G. — Anorthositic gabbro
D. — Dunite
D.D. — Diorite dike
n/d — not determined
G.A. — Gabbroic anorthosite
G.D. — Gabbro dike
M. — Metabasalt (pillowed)
P. — Peridotite
P.D. — Peridotitic dunite
* — total iron as Fe_2O_3

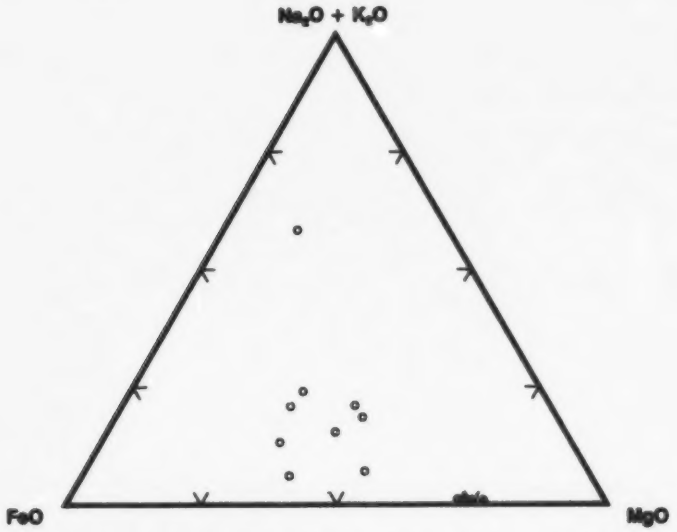

Figure 31. AFM plot of serpentinite (solid circles) and anorthositic rocks (open circles) from Big Trout Lake.

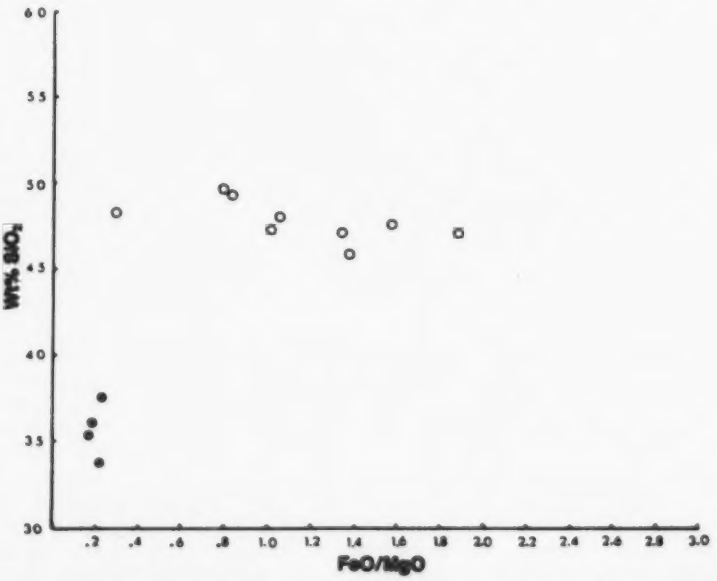

Figure 32. Plot of SiO_2 vs. FeO/MgO illustrating the low SiO_2 content of the serpentinite (solid circles) and anorthositic rocks (open circles) from Big Trout Lake.

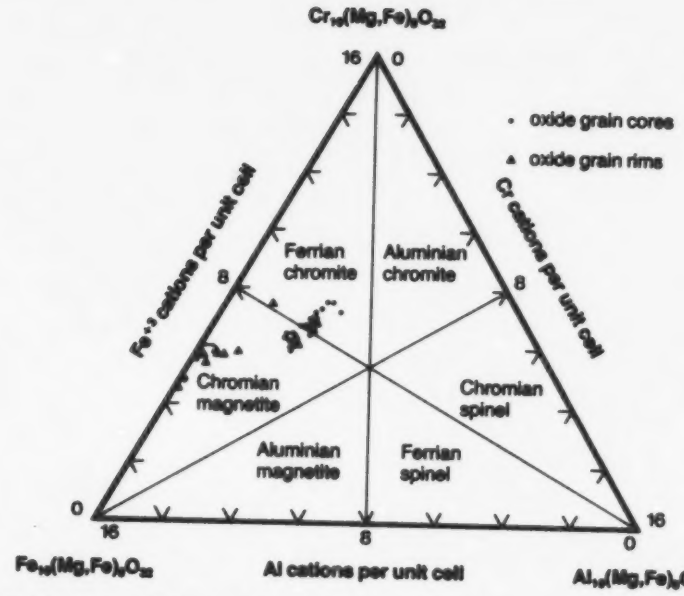

Figure 33. Compositional plots of chromite rims and cores from Big Trout Lake (after Panayiotou 1978).

element and chromite chemistry give further characteristics indicative of the Big Trout Lake body being a layered stratiform-type intrusion. With the field and chemical characteristics discussed, it is suggested that the development of chromite layers may extend the full length of the ultramafic outlined as a magnetic anomaly in Figure 25. The chromite forming the layers has a mean Cr/Fe ratio of 0.88 and this, together with its remoteness, makes this deposit economically unattractive at this time. Perhaps the feature of most economic interest is the presence of sulphide droplets, which in other similar situations such as in the Bushveld chromite layers are high in Pt and PGEs. Detailed examination of drill core to investigate the distribution of PGE values associated with trapped sulphide droplets and chromite mineralization should be carried out.

TABLE 9. MICROPROBE ANALYSES OF CHROMITE FROM BIG TROUT LAKE (ANALYSES BY D.H. WATKINSON, CARLETON UNIVERSITY).

Wt % Oxide	1 C.S. (c)	2 C.S. (b)	3 C.S. (c)	4 C.S. (b)	5 C.S. (c)	6 C.S. (b)	7 C.S. (b)	8 C.S. (c)	9 M.S. (c)	11 C.S. (c)	12 C.S. (c)	13 C.S. (b)	14 C.S. (c)	15 C.S. (b)	16 C.S. (c)	17 C.S. (b)	18 C.S. (c)	19 C.S. (b)
Na_2O	0.01	0.00	0.00	0.00	0.00	0.02	0.03	0.00	0.00	0.02	0.00	0.02	0.00	0.00	0.01	0.03	0.01	0.04
SiO_2	0.00	0.00	0.00	0.09	0.00	0.00	0.01	0.00	0.36	0.00	0.03	0.10	0.00	0.00	0.00	0.10	0.00	0.01
FeO	21.50	28.06	26.40	29.39	22.38	29.72	30.20	29.76	29.13	29.01	29.29	29.51	29.66	29.25	29.75	29.69	25.21	27.45
Fe_2O_3	14.94	13.74	13.39	14.24	14.90	27.98	23.61	26.91	67.82	11.14	12.70	31.52	11.92	29.09	12.38	32.70	9.86	8.88
CaO	0.00	0.02	0.04	0.00	0.00	0.00	0.00	0.03	0.38	0.00	0.00	0.00	0.00	0.00	0.03	0.04	0.00	0.00
MgO	8.23	3.22	4.99	2.44	7.16	0.46	0.76	0.55	0.65	1.92	1.95	0.27	1.74	0.51	2.11	0.30	5.29	3.26
Al_2O_3	16.29	15.31	16.02	15.59	15.72	3.07	7.07	4.45	0.06	14.93	14.95	0.95	16.01	3.07	16.54	0.72	17.55	17.38
NiO	0.26	0.03	0.05	0.19	0.21	0.00	0.15	0.15	0.00	0.00	0.00	0.00	0.10	0.27	0.00	0.00	0.18	0.00
K_2O	0.00	0.00	0.02	0.00	0.00	0.00	0.00	0.01	0.00	0.00	0.01	0.00	0.00	0.00	0.00	0.00	0.00	0.00
ZnO	0.00	0.05	0.00	0.33	0.09	0.00	0.00	0.00	0.00	0.13	0.58	0.00	0.55	0.64	0.21	0.25	0.05	0.07
TiO_2	1.28	1.33	1.37	1.30	1.53	1.71	1.32	1.52	0.00	2.50	2.78	0.63	0.96	0.41	0.99	0.52	0.54	0.44
Cr_2O_3	38.43	36.68	36.79	36.30	36.73	34.04	35.19	34.01	0.04	35.80	35.40	33.91	36.70	35.25	36.14	33.61	40.32	38.83
MnO	0.48	1.00	0.82	0.96	0.41	1.03	1.06	1.04	0.00	0.98	0.94	1.18	1.06	1.10	0.97	0.83	1.21	1.27
TOTAL	101.41	99.44	101.90	100.83	99.13	98.03	99.38	98.44	98.44	96.42	98.63	98.09	98.71	99.61	99.14	98.77	100.22	97.44
cations based on 24 oxygens																		
Na	0.71	0.00	0.00	0.00	0.00	0.89	1.42	0.00	0.00	0.86	0.00	1.21	0.00	0.00	0.79	1.50	0.61	2.36
Si	0.00	0.00	0.00	2.50	0.00	0.00	0.27	0.00	11.30	0.00	0.74	3.00	0.00	0.00	0.00	3.04	0.00	0.37
Fe^{+2}	463.87	640.28	580.01	665.23	497.17	747.66	732.60	740.15	755.65	685.52	678.03	753.99	687.22	727.84	682.61	754.93	557.62	631.93
Fe^{+3}	290.00	282.13	264.72	289.66	297.89	633.34	515.33	602.02	1582.93	236.85	264.42	724.74	248.42	651.34	255.59	748.10	196.20	179.74
Ca	0.00	0.52	1.24	0.00	0.00	0.00	0.00	1.11	12.61	0.00	0.00	0.00	0.00	0.00	0.75	1.32	0.00	0.01
Mg	316.62	130.90	195.50	98.42	283.34	20.42	32.85	24.33	30.26	80.82	80.29	12.26	71.86	22.64	86.45	13.57	208.57	133.57
Al	495.29	492.30	495.91	497.25	492.29	108.95	241.69	155.90	2.03	497.08	487.56	34.34	522.78	107.71	534.94	25.75	547.24	563.74
Ni	5.29	0.71	0.99	4.08	4.59	0.00	3.61	3.59	0.04	0.00	0.00	0.00	2.20	6.58	0.00	0.00	3.73	0.11
K	0.00	0.00	0.54	0.09	0.00	0.00	0.00	0.35	0.00	0.00	0.26	0.00	0.00	0.00	0.09	0.00	0.00	0.00
Zn	0.00	0.99	0.00	6.59	1.80	0.00	0.00	0.00	0.00	2.70	11.93	0.00	11.27	14.05	4.33	5.51	1.06	1.39
Ti	24.79	27.28	27.11	26.39	30.56	38.59	28.71	33.96	0.00	53.18	57.86	14.52	19.91	9.28	20.43	11.79	10.78	9.18
Cr	783.81	791.37	805.53	776.71	771.53	809.61	807.02	799.61	0.86	799.73	774.74	819.24	803.82	829.28	784.05	807.91	843.15	845.06
Mn	10.45	23.14	18.34	21.94	9.24	26.27	26.02	26.22	0.00	23.51	22.15	30.46	24.91	27.66	22.49	21.47	27.09	29.68
TOTAL	2390.83	2389.63	2389.90	2389.06	2388.40	2385.74	2389.54	2387.27	2395.68	2380.24	2377.96	2393.76	2392.40	2396.40	2392.53	2394.88	2396.04	2397.16

C.S. — Chromite in serpentinite
M.S. — Magnetite in serpentinite
(b) — border of grain
(c) — centre of grain

TABLE 9. CONTINUED

Wt % Oxide	20 C.S. (c)	21 C.S. (b)	22 C.S. (c)	23 C.S. (b)	24 Fe.C.	25 C.S. (c)	26 C.S. (c)	27 C.S. (c)	28 C.S. (b)	29 C.S. (c)	30 C.S. (b)	31 C.S. (c)	32 C.S. (b)	33 C.I. (c)	34 C.I. (b)	35 C.S. (c)	36 C.S. (c)
Na_2O	0.00	0.03	0.04	0.04	0.00	0.00	0.00	0.00	0.05	0.00	0.16	0.00	0.00	0.00	0.00	0.05	0.08
SiO_2	0.00	0.04	0.06	0.01	0.03	0.00	0.00	0.00	0.00	0.47	1.27	0.67	0.25	0.15	0.30	0.17	0.11
FeO	25.84	28.11	28.06	28.95	29.42	27.86	27.77	28.57	28.80	20.54	27.97	27.50	27.42	29.53	29.06	29.28	29.46
Fe_2O_3	7.68	8.06	8.17	8.96	33.67	15.52	15.27	36.94	37.48	13.96	29.12	14.17	13.18	8.90	11.94	7.76	7.98
CaO	0.04	0.00	0.00	0.02	0.00	0.00	0.00	0.10	0.00	0.00	0.00	0.00	0.00	0.03	0.01	0.06	0.03
MgO	4.58	2.96	3.14	2.26	0.67	2.96	3.26	0.62	0.61	8.29	0.62	2.79	3.40	1.93	0.74	2.05	2.09
Al_2O_3	17.56	18.28	17.96	17.62	0.33	14.01	13.88	0.33	0.31	16.30	2.70	15.57	16.14	18.22	9.01	18.13	18.82
NiO	0.04	0.00	0.00	0.07	0.13	0.03	0.01	0.17	0.28	0.09	0.03	0.34	0.00	0.11	0.00	0.06	0.15
K_2O	0.01	0.00	0.00	0.00	0.00	0.00	0.00	0.00	0.00	0.00	0.00	0.00	0.00	0.00	0.00	0.03	0.00
ZnO	0.16	0.19	0.15	0.28	0.00	0.52	0.00	0.44	0.00	0.00	0.24	0.00	0.00	0.14	0.14	0.00	0.00
TiO_2	0.53	0.52	0.54	0.70	2.62	1.36	1.38	2.77	3.06	1.68	1.51	1.74	1.28	0.53	0.39	0.57	0.52
Cr_2O_3	40.44	38.39	39.38	38.03	32.11	36.29	36.54	27.65	26.52	36.17	30.31	32.31	34.37	36.36	41.94	37.34	37.43
MnO	0.94	1.26	1.31	1.33	1.00	0.98	0.95	0.79	0.70	0.50	1.07	0.98	0.78	1.10	1.36	1.05	1.29
TOTAL	97.83	97.84	98.82	98.27	98.98	99.52	99.06	98.38	97.80	98.00	94.99	96.09	96.81	97.01	94.88	96.54	97.94
cations based on 24 oxygens																	
Na	0.00	1.76	2.01	1.87	0.00	0.00	0.00	0.00	2.79	0.00	9.34	0.00	0.00	0.00	0.00	2.67	4.04
Si	0.10	1.17	1.70	0.34	1.02	0.00	0.00	0.00	0.00	12.45	39.16	18.86	6.81	4.29	8.94	4.68	3.05
Fe^{+2}	586.32	643.21	636.73	665.11	734.40	640.91	640.24	726.31	735.82	454.31	719.97	645.19	636.74	685.90	726.82	681.91	675.43
Fe^{+3}	156.78	165.87	166.58	185.17	756.00	321.19	316.71	844.79	861.34	277.95	674.35	299.16	275.44	186.07	268.73	162.59	164.57
Ca	1.10	0.00	0.00	0.60	0.00	0.00	0.00	3.38	0.00	0.00	0.15	0.00	0.00	0.94	0.27	1.69	0.90
Mg	185.28	120.66	126.73	092.42	29.72	121.43	133.75	28.09	27.84	326.81	28.47	116.80	140.74	80.09	33.08	84.90	85.23
Al	562.05	589.29	573.77	570.65	11.62	454.28	451.04	11.66	11.19	508.21	97.86	514.64	528.14	596.21	317.46	595.20	607.93
Ni	0.96	0.00	0.00	1.61	3.05	0.75	0.18	4.17	6.85	1.84	0.80	7.75	0.00	2.47	0.00	1.42	3.22
K	0.18	0.00	0.00	0.00	0.00	0.00	0.00	0.00	0.00	0.00	0.00	0.00	0.00	0.00	0.00	1.00	0.00
Zn	3.26	3.90	2.97	5.77	0.00	10.61	0.00	9.89	0.00	0.00	5.36	0.00	0.00	2.85	3.16	0.00	0.00
Ti	10.75	10.60	11.00	14.38	58.76	28.08	28.62	63.23	70.19	33.36	34.85	36.73	26.71	11.17	8.69	12.00	10.68
Cr	867.55	830.46	844.19	826.15	757.57	789.34	796.39	664.44	640.35	756.48	737.53	716.61	754.43	798.30	991.67	822.18	811.25
Mn	21.53	29.17	30.18	30.95	25.32	22.74	22.21	20.22	18.23	11.27	27.79	23.27	18.28	25.77	34.42	24.73	29.91
TOTAL	2395.85	2396.10	2395.85	2395.04	2377.46	2389.33	2389.13	2376.18	2374.61	2382.68	2375.63	2379.02	2387.29	2394.06	2393.25	2394.98	2396.22

C.I. — Chromite with inclusions
C.S. — Chromite in serpentinite
Fe.C. — Fe-rich chromite
(b) — border of grain
(c) — centre of grain

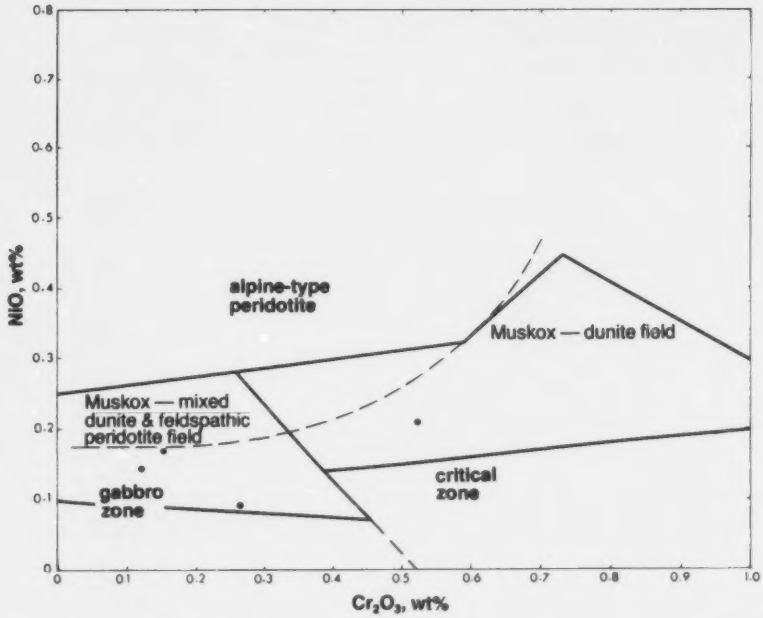

Figure 34. *Comparative plot of Big Trout Lake samples (solid circles) to the dunite-peridotite fields defined by rocks of the lower layered series, Muskox Intrusion (after Irvine and Findlay 1972).*

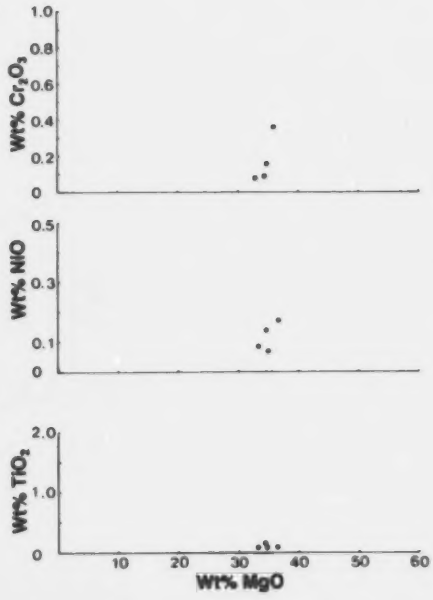

Figure 35. *Plot of Cr_2O_3, NiO, and TiO_2 vs. MgO for Big Trout Lake samples.*

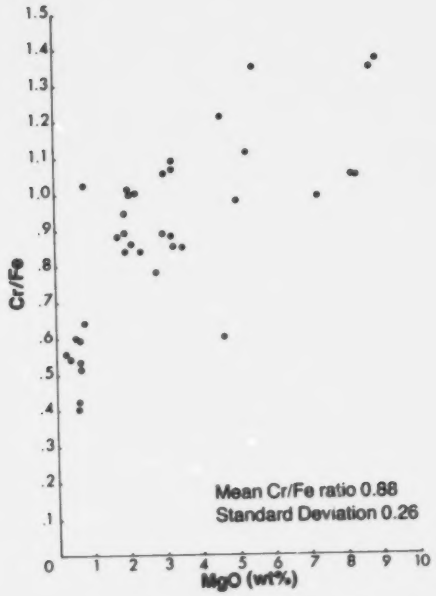

Figure 36. *Cr/Fe ratios vs. MgO (weight percent) of chromites from Big Trout Lake.*

TABLE 10. Cr/Fe RATIOS FROM BIG TROUT LAKE.

Sample Number	Sample Description	Cr/Fe	Sample Number	Sample Description	Cr/Fe
1.	Chromite in serpentinite	1.06	19.	Chromite in serpentinite	1.07
2.	Chromite in serpentinite	0.88	20.	Chromite in serpentinite	1.21
3.	Chromite in serpentinite	0.97	21.	Chromite in serpentinite	1.06
4.	Chromite in serpentinite	0.83	22.	Chromite in serpentinite	1.09
5.	Chromite in serpentinite	0.99	23.	Chromite in serpentinite	1.00
6.	Chromite in serpentinite	0.59	24.	Fe-rich chromite	0.51
7.	Chromite in serpentinite	0.62	25.	Chromite in serpentinite	0.84
8.	Chromite in serpentinite	0.60	26.	Chromite in serpentinite	0.85
9.	Magnetite in serpentinite	0.004	27.	Chromite in serpentinite	0.42
11.	Chromite in serpentinite	0.89	28.	Chromite in serpentinite	0.40
12.	Chromite in serpentinite	0.84	29.	Chromite in serpentinite	1.05
13.	Chromite in serpentinite	0.56	30.	Chromite in serpentinite	0.53
14.	Chromite in serpentinite	0.88	31.	Chromite in serpentinite	0.78
15.	Chromite in serpentinite	0.63	32.	Chromite in serpentinite	0.85
16.	Chromite in serpentinite	0.86	33.	Chromite with inclusions	0.95
17.	Chromite in serpentinite	0.54	34.	Chromite with inclusions	1.02
18.	Chromite in serpentinite	1.15	35.	Chromite in serpentinite	1.01
			36.	Chromite in serpentinite	0.99

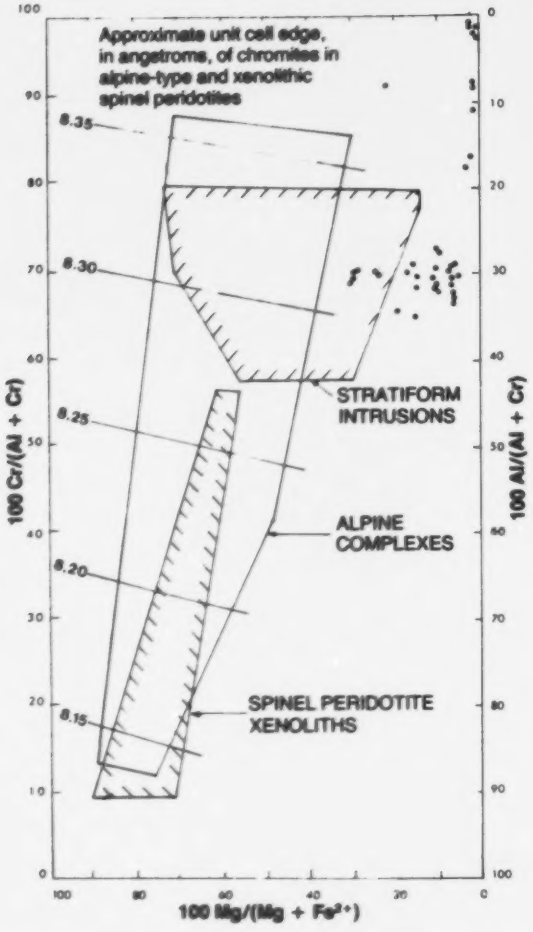

***Figure 37.** Plot of $^{100\ Cr}/_{(Al+Cr)}$ vs/ $^{100\ Mg}/_{(Mg+Fe^{+2})}$ of chromites from Big Trout Lake.*

Crystal Lake Gabbro

LOCATION AND ACCESS

The Great Lakes Nickel Limited property, within the Crystal Lake Gabbro, is located in Pardee Township, 47 km southwest of Thunder Bay, Ontario (Figure 38). An all-weather gravel-surfaced road, which leaves Highway 597 south of Thunder Bay, provides access to the area.

PREVIOUS WORK

Tanton (1931, 1935, 1936a, 1936b) was the first to describe the general geology of the area. Pye and Fenwick (1963, 1965) described the regional geology in Ontario Department of Mines Preliminary Map P.177 and Geological Compilation Map 2065.

A detailed geological map at 1 inch to 1/4 mile accompanies a report by J.J.C. Geul (1970) of the Ontario Department of Mines which deals in part with Pardee Township and the Crystal Lake Gabbro.

GENERAL GEOLOGY

The Crystal Lake Gabbro intrudes shales of the Proterozoic Rove Formation (Geul 1970). The metamorphic age of the Rove Formation shales is coincident with the Penokean Orogeny at 1.7 billion years (Peterman 1966). They were intruded by the olivine and quartz-bearing gabbros, which formed the Logan Sills, 1.4 billion years ago (DuBois 1962). Olivine diabase dikes were intruded at a later time, followed by emplacement of the Crystal Lake Gabbro, thought to be related to the Duluth Complex (1.1 billion years, Goldich *et al.* 1961). The presence of considerable olivine and of an anorthositic gabbro distinguish the Crystal Lake Gabbro from the older Logan Sills.

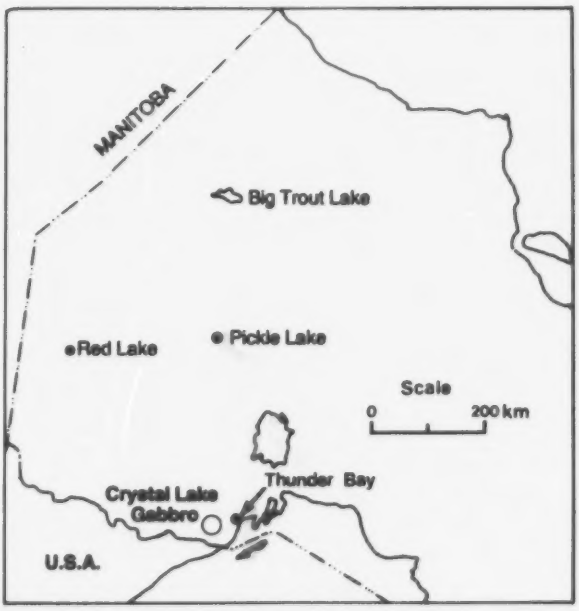

Figure 38. *Location map showing the Crystal Lake Gabbro.*

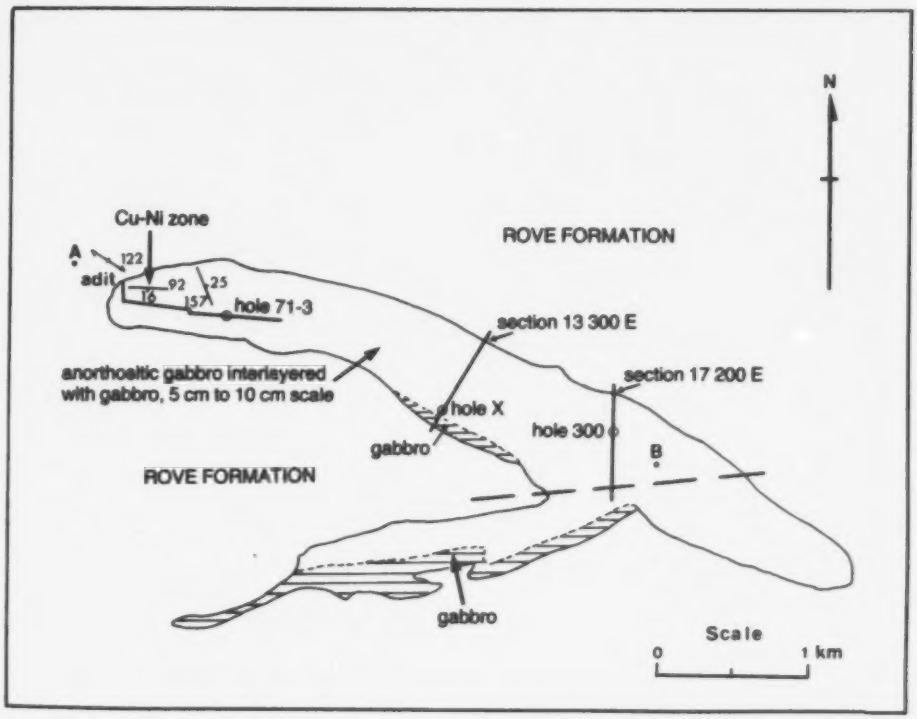

Figure 39. *The Crystal Lake Gabbro showing location of drill holes for sections in Figures 44a, b, and c, to Figures 47a, b, and c.*

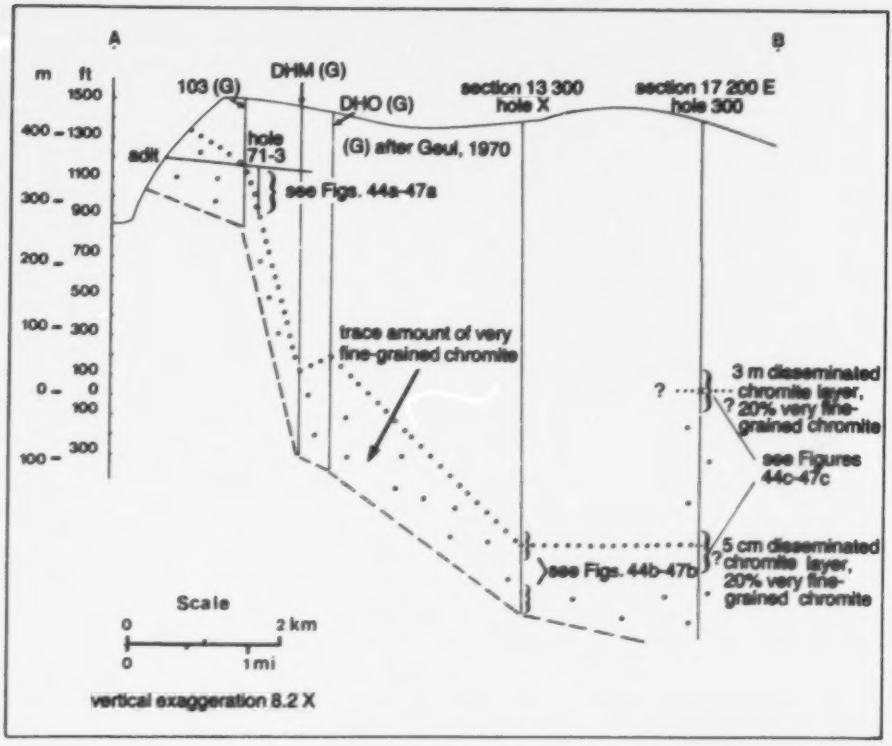

Figure 40. Distribution of disseminated chromite in the lower portion of the north limb of the Crystal Lake Gabbro. Drill hole data from Geul (1970) and from Great Lakes Nickel Limited drill core. Location of Figures 44a, b, and c, to Figures 47a, b, and c are also shown.

Photo 18. *Three- to five-centimetre layering in upper anorthositic gabbro zone. Dark layers are defined in part by disseminated chromite. Crystal Lake Gabbro.*

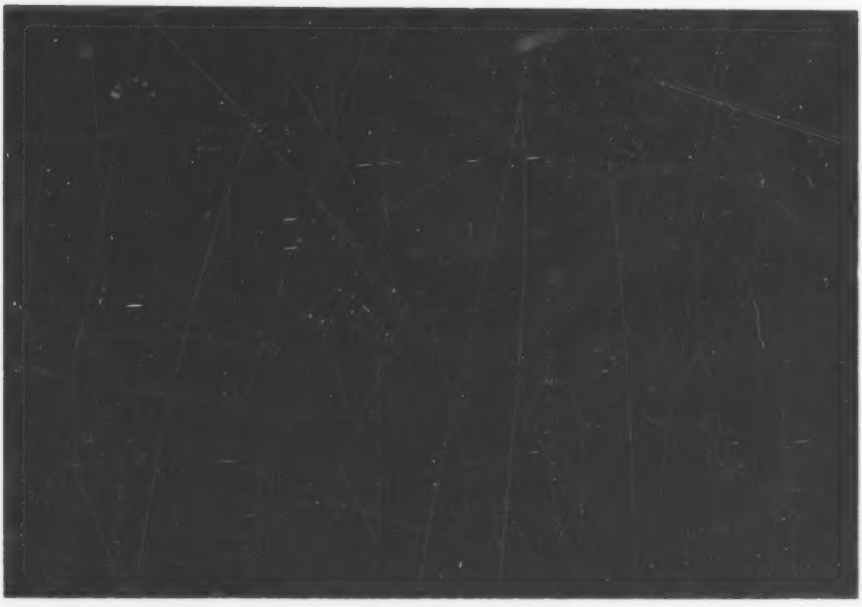

Photo 19. *Half-metre layering defined by alternating layers of anorthositic gabbro (pale grey) and gabbro (dark grey). Crystal Lake Gabbro.*

Photo 20. *Chromite poikilitically included within plagioclase, Crystal Lake Gabbro. Crossed nicols. X200.*

TABLE 11. MAJOR AND TRACE ELEMENT ANALYSES FROM THE CRYSTAL LAKE GABBRO (ALL ANALYSES BY THE GEOSCIENCE LABORATORIES, ONTARIO GEOLOGICAL SURVEY, TORONTO).

Wt % Oxides	1 A.G.	2 A.G.	3 A.G.	4 A.G.	5 A.G.	6 A.G.	7 A.G. (ss)	8 A.G. (f)	9 A.G. (f)	10 A.G. (f)	11 A.G. (mss)	12 A.G. (f)	13 A.G.	14 A.G.	15 A.G.	16 A.G. (f)	17 A.G. (mss)	18 A.G. (2%)	19 A.G.	20 A.G. (f)	21 A.G.	22 A.G.	23 A.G.
SiO_2	46.40	46.00	45.90	45.40	45.30	48.80	51.00	42.40	44.10	43.10	27.70	44.10	48.60	47.00	43.90	38.20	33.40	40.80	40.00	43.20	43.60	44.40	42.30
Al_2O_3	20.50	19.60	22.70	22.50	21.80	21.30	15.90	16.30	18.10	18.80	22.60	16.50	17.70	17.00	18.40	18.30	21.00	17.50	17.60	18.70	18.40	22.30	19.30
FeO*	11.40	12.40	8.44	8.88	8.15	8.56	15.10	12.30	10.30	10.00	18.10	13.40	11.70	10.80	12.10	15.30	16.60	13.00	13.70	10.10	9.36	6.75	10.20
MgO	7.80	8.06	8.54	8.73	7.70	6.56	5.88	11.80	10.40	10.40	9.61	8.44	7.04	7.54	6.43	11.10	9.15	8.58	7.52	10.10	10.10	5.80	10.80
CaO	10.70	10.20	11.30	11.00	9.76	7.37	5.53	7.54	10.10	10.60	8.58	8.44	8.84	10.70	12.00	8.26	7.74	9.04	7.66	10.60	10.60	12.70	10.20
Na_2O	2.11	1.86	2.17	1.82	1.93	2.10	1.31	1.48	1.80	1.92	1.44	2.53	2.66	2.56	2.17	1.40	1.86	1.21	1.44	1.27	1.27	1.88	1.41
K_2O	0.57	0.34	0.32	0.23	0.42	2.18	2.01	1.13	0.70	0.79	1.84	1.61	1.55	1.48	3.21	1.35	0.50	0.33	0.84	0.88	0.84	0.76	0.17
TiO2	1.35	1.13	1.08	0.83	0.42	0.67	2.22	0.73	0.70	0.62	1.84	0.80	0.18	0.19	0.18	0.10	0.05	0.10	0.12	0.08	0.12	0.01	0.04
P_2O_5	0.17	0.13	0.15	0.12	0.07	0.11	0.22	0.13	0.11	0.16	0.55	0.18	0.18	0.15	0.18	0.18	0.18	0.14	0.12	0.14	0.13	0.04	0.04
MnO	0.14	0.18	0.12	0.10	0.10	0.10	0.15	0.18	0.14	0.13	0.19	0.17	0.18	0.19	0.18	0.10	0.05	0.10	0.13	0.12	0.12	0.10	0.08
LOI	0.03	0.05	0.08	0.04	0.04	0.05	0.11	0.23	0.14	0.05	0.08	0.07	0.08	0.08	0.00	0.05	0.15	0.11	0.08	0.14	0.13	0.08	0.11
TOTAL	0.13	0.11	0.08	0.04	0.03	0.05	0.20	0.34	0.08	0.08	0.08	0.08	0.08	0.07	0.06	0.15	0.18	0.43	0.11	0.19	0.04	0.01	0.06
	100.10	99.90	100.80	100.20	99.80	99.10	99.30	99.80	96.80	97.80	98.00	96.50	99.00	99.20	98.80	95.20	97.30	91.40	99.30	98.80	96.40	95.10	95.30
ppm																							
Sc	140	120	130	100	192	457	457	357	189	170	180	230	280	270	180	190	150	130	180	100	220	330	110
V	280	300	327	271	198	347	270	770	1300	2710	7440	3870	2911	1470	1041	2784	1540	5700	1274	144	1184	1184	1570
Cr	440	300	367	114	222	222	41	107	330	230	330	320	198	271	198	880	880	1980	330	151	316	316	220
Co	10	7	7	9	10	10	112	188	48	48	48	310	27	258	143	240	240	1001	400	250	370	142	1270
Ni	<10	80	40	10	67	115	68	348	78	78	110	137	105	89	114	150	10	14	17	68	16	28	14
Cu	<10	60	<10	88	122	121											149	127	104		72		72
Zn			77																				
Rb																							
Sr																							
Y																							
Zr																							
Nb																							
Ba																							
La																							
Ce																							
Nd																							
Pb																							
Th																							
U																							

A.G. — Anorthositic gabbro
A.G. — Anorthositic gabbro (at contact)
A.G. — Anorthositic gabbro (near chromite)
A.G. — Anorthositic gabbro (main chromite zone)
A.G. — Anorthositic gabbro (3% chromite)
Gabbro (near chromite)
Chromite zone
Gabbro

TABLE 11. (CONTINUED)

Wt % Oxides	34 C.Z.	35 A.G.	36 A.G.	37 A.G. (ac)	38 A.G. (ac)	39 A.G.	30 A.G.	31 A.G.	32 A.G.	33 A.G.	34 A.G.	35 A.G.	36 A.G.	37 A.G.	38 A.G.	39 A.G.	40 A.G.	41 A.G.	42 A.G.	43 A.G. (mcz)	44 A.G. (mcz)	45 A.G.	46 A.G.
SiO_2	31.20	46.40	44.60	50.20	47.10	44.50	43.30	40.40	45.00	44.60	42.50	40.70	38.80	39.20	46.00	44.70	43.50	44.20	45.80	40.60	40.70	44.80	44.70
Al_2O_3	22.30	19.20	13.80	13.20	13.10	20.10	16.20	16.00	19.80	19.00	19.70	20.60	14.30	18.40	17.20	17.40	18.10	16.10	17.50	17.80	18.70	19.70	18.80
Fe_2O_{3t}	15.30	9.34	18.60	15.80	16.90	9.44	12.80	12.90	11.50	13.30	11.20	11.40	21.00	13.30	11.20	11.10	12.00	12.00	11.70	14.30	13.40	9.36	10.80
MgO	9.60	10.00	5.13	3.51	4.21	9.19	8.19	2.75	6.31	5.67	8.55	9.47	7.82	11.70	8.73	8.19	9.07	12.00	7.99	5.10	8.32	10.20	9.84
CaO	8.25	11.10	8.11	7.30	7.76	9.01	5.20	8.28	8.48	8.52	10.20	9.99	8.06	8.87	10.20	10.80	9.72	9.72	9.88	9.21	9.34	10.80	10.20
Na_2O	1.25	1.82	2.55	2.89	2.56	1.87	1.24	4.01	2.41	2.58	1.33	1.70	1.75	1.71	2.48	2.43	2.20	2.06	2.85	2.32	2.16	2.06	2.60
K_2O	0.13	0.34	1.30	0.99	0.79	1.19	3.65	2.76	1.78	1.49	0.45	0.32	0.41	0.31	0.43	0.42	0.43	0.28	0.85	0.38	0.63	0.31	0.43
TiO_2	1.23	1.01	3.58	2.97	3.69	0.82	1.05	2.73	0.99	1.62	0.57	0.82	3.36	1.02	1.37	1.38	1.25	1.28	1.80	1.86	1.61	0.78	0.98
P_2O_5	0.08	0.11	0.48	0.47	0.41	0.11	0.15	0.39	0.13	0.23	0.08	0.11	0.11	0.10	0.18	0.17	0.18	0.14	0.19	0.18	0.14	0.12	0.14
MnO	0.15	0.12	0.22	0.18	0.20	0.12	0.15	0.16	0.12	0.14	0.12	0.13	0.19	0.16	0.14	0.14	0.14	0.15	0.16	0.18	0.16	0.12	0.15
CO_2	0.01	0.01	0.04	0.03	0.05	0.01	0.07	0.04	0.01	0.07	0.00	0.00	0.00	0.00	0.00	0.00	0.05	0.00	0.00	0.00	0.00	0.03	0.04
S	0.35	0.09	0.33	0.14	0.09	0.06	1.17	0.17	0.73	1.04	1.41	0.24	1.84	0.05	0.08	0.08	0.59	0.08	0.08	0.08	0.20	0.05	0.09
LOI	1.60	0.80	1.30	3.20	1.40	1.80	5.50	1.20	2.00	1.30	1.40	0.30	0.00	0.10	1.00	0.80	0.40	0.30	0.04	0.60	0.30	0.60	0.30
TOTAL	91.00	99.40	99.80	100.40	98.10	98.20	97.50	96.80	98.40	96.40	97.20	96.50	93.80	94.80	98.70	97.40	97.00	98.20	98.50	95.60	95.40	98.50	98.60
ppm																							
Ba	90	190	380	470	330	370	280	1100	380	430	190	120	130	100	190	180	190	170	240	180	160	130	140
Co	74	58	59	42	51	56	69	35	60	78	90	67	134	88	58	50	77	71	54	70	75	57	65
Cr	8.2%	362	112	46	61	750	305	15	192	181	3630	1.86%	2.50%	2.24%	660	630	750	950	1360	2.21%	2.0%	351	2130
Cu	540	102	860	200	290	159	1300	280	1900	1620	4080	670	3960	166	166	132	2280	124	196	230	280	59	352
Li	17	7	24	28	28	50	134	24	40	28	28	19	18	25	21	18	16	17	25	24	22	17	17
Ni	700	230	330	39	58	440	720	33	980	910	2050	760	2540	660	290	220	1430	466	210	400	540	280	360
Pb	85	55	53	85	45	16	46	14	15	20	103	109	34	39	38	12	17	12	28	66	80	127	139
Zn	126	71	176	171	196	76	108	139	82	114	80	85	210	132	102	114	109	99	120	161	156	71	98

A.G. — Anorthositic gabbro
A.G. (ac) — Anorthositic gabbro (at contact)
A.G. (mcz) — Anorthositic gabbro (main chromite zone)
C.Z. — Chromite zone
(t) — total

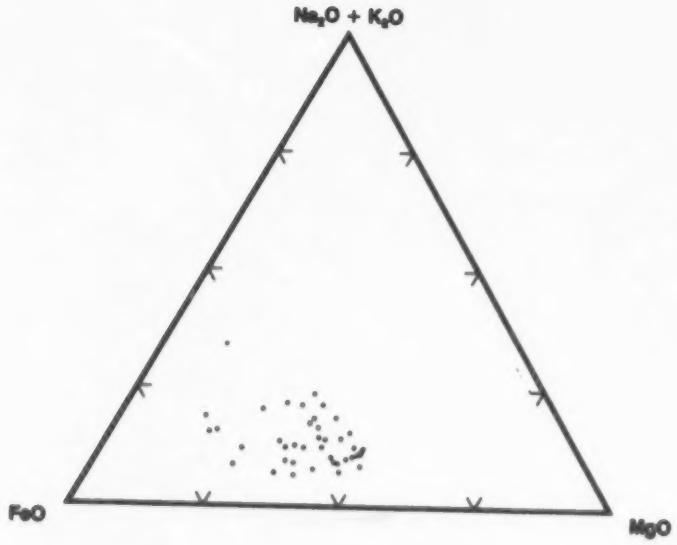

Figure 41. AFM plot of Crystal Lake Gabbro samples showing restricted fractionation.

CRYSTAL LAKE GABBRO

The Crystal Lake Gabbro is a conical intrusion open at its western end. In map view, the intrusion forms a "Y"-shaped body with the northern and southern limbs approximately 1 m and 0.8 m in outcrop width respectively (Figure 39). In the northern limb, where drilling has outlined chromitiferous zones, the rocks are predominantly anorthositic gabbro with pegmatitic gabbro patches. The lower portions of the intrusion adjacent to the Rove Formation contact are gabbroic in composition. Drilling by Great Lakes Nickel Limited (files of the Resident Geologist's Office, Ontario Ministry of Northern Development and Mines, Thunder Bay) and data from Geul (1970) indicate chromite distribution throughout the lower half of the northern limb (Figure 40). Intrusive rocks near the contact with the Rove Formation shales are medium-grained, equigranular, and gabbroic in composition. Away from the contact, coarse to very coarse grained anorthositic gabbroic rocks with pegmatitic gabbro patches predominate. Irregularly shaped pods of troctolite also occur as coarse-grained patches.

Planar layering is well developed within the north limb and in the area of the adit. Layers dip easterly at 20° to 30°, while disrupted layers are contorted and dip to the south (Figure 39). The disrupted layers may represent slumping, reflecting an unstable semi-crystallized zone between magma and consolidated layers.

The Crystal Lake Gabbro can be divided into three divisions: an upper portion formed of medium-grained massive gabbro to olivine gabbro, which is about 60 m thick at the western end and thickens to approximately 400 m, 1.2 km to the east; the middle zone, which extends to within 1 to 6 m of the basal contact, and consists of layered anorthositic gabbro with gabbro and pegmatitic olivine gabbro patches (Geul 1970); and the basal zone, varying from 1 to 6 m in thickness, and consisting of very fine grained to aphanitic gabbro in contact with the Rove Formation shales. Within the contact zone are hornfelsed angular fragments of laminated shales and fine-grained wackes of the Rove Formation.

The middle zone appears to be of greatest economic significance, as it contains the Cu-Ni ore zone developed by Great Lakes Nickel Limited and the top of the disseminated chromite zone (Geul 1970). Sulphide mineralization, consisting primarily of chalcopyrite ± pyrrhotite ± pentlandite, occurs in disseminated form in the anorthositic and olivine gabbro layers, and in the pegmatitic gabbro and olivine patches. Chromite first appears in the lower to central part of the middle zone and is sparsely disseminated throughout the various layers.

LAYERING

Phase layering is defined by fluctuations from anorthositic gabbro to gabbroic layers (Photos 18 and 19).

Layering within the lower one-third of the north limb of the sill is planar in form and occurs on a 0.5 m scale. Contacts between anorthositic gabbro and gabbroic layers are sharp, with variation in modal concentration of mafic minerals defining the two phases. Grain size and texture (medium-grained and sub-porphyritic) remain constant throughout the layers and across the stratigraphy.

Within the upper two-thirds of the north limb, the layering involves anorthositic gabbro and gabbroic layers which become thinner with increasing stratigraphic height. The upper layers remain planar and are 3 to 5 cm in thickness with sharply defined contacts.

PEGMATITIC PATCHES

Pegmatitic patches occur in the upper one-third of the north limb anorthositic gabbro. These are often elongate, striking 087°and dipping 42°S. The pegmatitic patches range in size from 10 cm to 2 m long by 20 cm thick. The elongate patches are generally planar but exhibit internal rippling which suggests flow disruption. They are anorthositic in composition, consisting of 5% to 7% euhedral amphibole blades 2 to 3 cm in length, and 93% to 95% sub- to euhedral plagioclase laths, also 2 to 3 cm in length. The plagioclase phenocrysts are

randomly oriented, while the amphibole blades are oriented normal to the boundaries of the pegmatite patches. Sulphide mineralization is often concentrated in pegmatitic patches.

CHROMITE

Chromite occurs primarily in disseminated and layered form in the anorthositic gabbro (Figure 40).

Disseminated subhedral to euhedral chromite forms 1% to 3% of the medium- to coarse-grained anorthositic gabbro. Chromite crystals are very fine grained (0.2 mm) and are poikilitically included within coarse- to medium-grained cumulate plagioclase and in finer grained intercumulate plagioclase (Photo 20). Disseminated chromite also occupies interstitial positions between silicate minerals.

Layered chromite concentrations from the main chromite zones occur in coarse-grained anorthositic gabbro and have well developed cumulate texture. These zones (7 to 10 cm thick) are dark grey as a result of higher chromite concentrations, from 10 to 20 modal percent. Disseminated chromite, forms 1 to 3 modal percent of the intervening rock (Figure 40).

PETROGRAPHY

FELDSPAR

Plagioclase occurs as euhedral lath-shaped phenocrysts, forming a sub-ophitic texture with clinopyroxene. Extinction angles give a mean value of 38° (An_{68} labradorite) and a maximum value, more indicative of the Ca content, of 43° (An_{78}, bytownite). Bytownite is representative of the basic anorthositic gabbro which, together with olivine-bearing gabbro, forms the bulk of the Crystal Lake Intrusion.

Grain boundaries between plagioclase laths are smoothly planar to smoothly and gently curved. In places, the grain boundary contacts are lobate, indicating grain boundary mobility responding to minor disequilibrium (Spry 1969). Boundaries between mafic minerals and plagioclase are irregular, indicating corrosion of the plagioclase by interstitial opaque minerals.

OLIVINE AND PYROXENE

Olivine is anhedral with embayed, altered, grain boundaries. Pyroxene occurs in approximately equal proportions to olivine and is subhedral to anhedral, tabular grains. The pyroxene is all clinopyroxene, with symmetrical extinction in basal sections. Clinopyroxene boundaries with olivine are commonly vague, giving evidence of deuteric alteration. Boundaries with clinopyroxene (augite) and plagioclase are generally sharply defined and planar. Very fine grained chromite euhedra are also observed poikilitically included in olivine and pyroxene.

OPAQUES

Magnetite and Cr-spinel are the oxide phases. Magnetite is completely opaque whereas Cr-spinel is various shades of reddish brown. The colour is best observed near the edge of the grain, or along a fracture, under high magnification with conoscopic illumination at full intensity. The darker shades correspond to higher iron contents, while paler reddish brown grains are closer to the chromite end member.

The opaque minerals occur as euhedral to subhedral inclusions within both plagioclase and mafic minerals and along fractures. In the mafic minerals, opaques are developed from alteration of the host grain, as well as occurring as primary poikilitic inclusions. In plagioclase, however, the opaques are primary inclusions trapped at the time of plagioclase growth (Photo 20). This is indicated by the generally fresh, unaltered condition of the plagioclase and the retention of optical continuity within the twin planes separated by the inclusion.

The opaque inclusions themselves host minute inclusions of olivine, clinopyroxene, and twinned plagioclase. An extensive interval of co-existing growth and nucleation of the major silicate and oxide phases is thus suggested.

Interstitial opaque minerals conform to the voids left between plagioclase laths, and bladed to spearhead-shaped opaque grains are common. The opaques appear to have been corroding plagioclase borders, leaving finely serrated edges and often a hairline micaceous (chloritic) seam between the opaque and plagioclase grains.

The medium- to coarse-grained rocks of the Crystal Lake Gabbro, together with subhedral to euhedral development of the two major silicate phases, olivine and pyroxene, suggest an undisturbed crystallization history. The anorthositic gabbro and the pegmatitic olivine gabbro represent a later stage product of mafic magma fractionation which would be expected in the upper portion of a larger magma chamber. Disseminated chromite at the Crystal Lake Gabbro is predominantly poikilitically trapped in the silicate phases and this texture indicates a eutectic magma composition. With these interpretations and the lithological similarities to the Duluth Complex it could be suggested that the Crystal Lake Gabbro may be related to this larger intrusion. Chromite has also been identified within the basal part the Duluth Complex (Paul Mainwaring, Research Associate, Carleton University, Ottawa, personal communication, 1979). Chromite in the Crystal Lake Gabbro supports the hypothesis of it forming from a magma similar to that of the Duluth Complex.

MAJOR ELEMENT CHEMISTRY

Samples were collected from the chromitiferous anorthositic gabbro zone which forms part of the exposed and drilled part of the intrusion. Major element analyses, given in Table 11, are plotted on an AFM diagram (Figure 41), and on ternary diagrams of CaO-MgO-Al_2O_3, and Fe_2O_3-MgO-Al_2O_3 in Figure 42. The analyses in these figures are closely grouped and show restricted fractionation, which is to be expected from the overall similarity of the intrusion. A plot of weight percent SiO_2 vs. FeO/MgO (Figure 43) again shows the restricted amount of fractionation, with some analyses giving relatively higher FeO/MgO ratios. Figures 44a, 44b, and 44c show the variation of FeO/MgO in the vicinity of chromitiferous anorthositic gabbro in three drill sections. The locations of these sections on the drill holes are shown in Figure 40. The FeO/MgO ratio remains generally constant with depth and falls within the same range, between 1.0 and 2.0, in all three drill sections. The major element chemistry of the anorthositic gabbro reveals a chemically homogeneous magma which is only anomalous due to the presence of very fine grained disseminated chromite.

TRACE ELEMENT CHEMISTRY

Figures 44a, 44b, 44c, 45a, 45b, 45c, 46a, 46b, 46c, 47a, 47b, and 47c show the stratigraphic variation of Cr, Ni, Cu, Co, Pb, and Zn with depth in the drill sections. The sections represented are centred upon the chromitiferous anorthositic gabbro. The highest Cr values are 7000 ppm from hole 71-3, representing the maximum amount of disseminated chromite encountered: approximately 20 modal percent, very fine grained chromite.

Cu, Co, Pb, and Zn values are low and all of them show only minor variation with depth. This would suggest a good mixing of oxide and sulphide minerals, and a chemically homogeneous magma as suggested by the major element data.

Figure 48 shows the pattern of Cr-Ni-Co, and Cr-Ni-Cu data. The widest range in values is between Cr and Cu, which would reflect a lesser amount of chromite in the Ni-sulphide-bearing zone, compared to the surrounding chromite-bearing anorthositic gabbro. The actual range of values of weight percent Cr_2O_3, NiO, and TiO_2 is plotted against weight percent MgO in Figure 49 and shows up to 11.0 weight percent Cr_2O_3, 0.33 weight percent NiO, and 3.75 weight percent TiO_2. A plot of weight percent NiO vs. weight percent Cr_2O_3 in Figure 50 (after Irvine and Findlay 1972) shows a close grouping of analyses in the gabbro zone with high Cr_2O_3

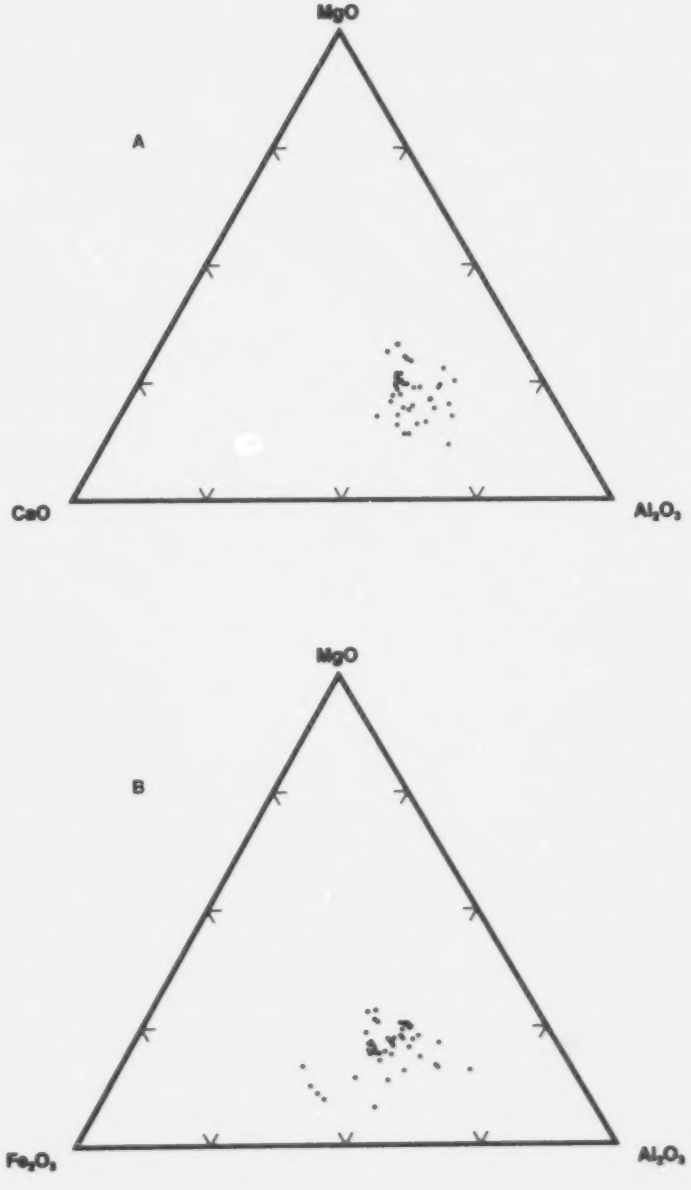

Figure 42. *Plot of MgO-CaO-Al_2O_3 and MgO-Fe_2O_3-Al_2O_3 from the Crystal Lake Gabbro showing restricted fractionation.*

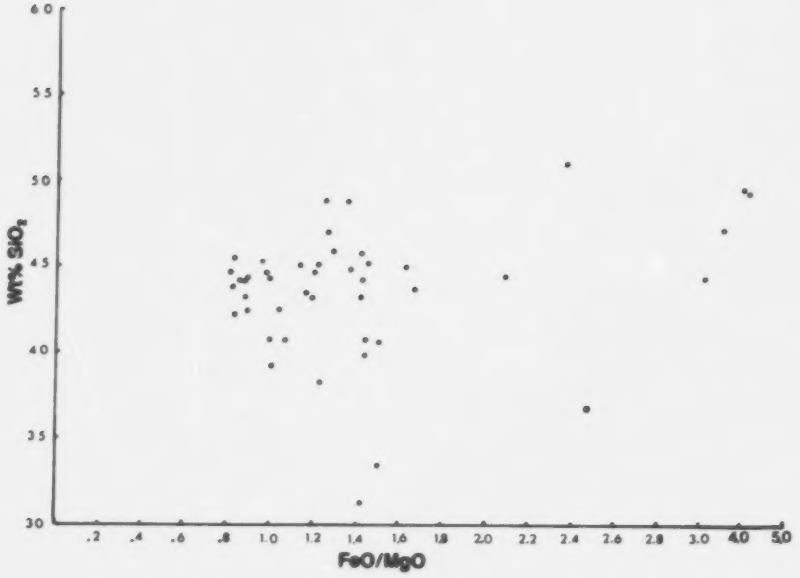

Figure 43. *Plot of SiO_2 vs. FeO/MgO ratios from Crystal Lake Gabbro analyses.*

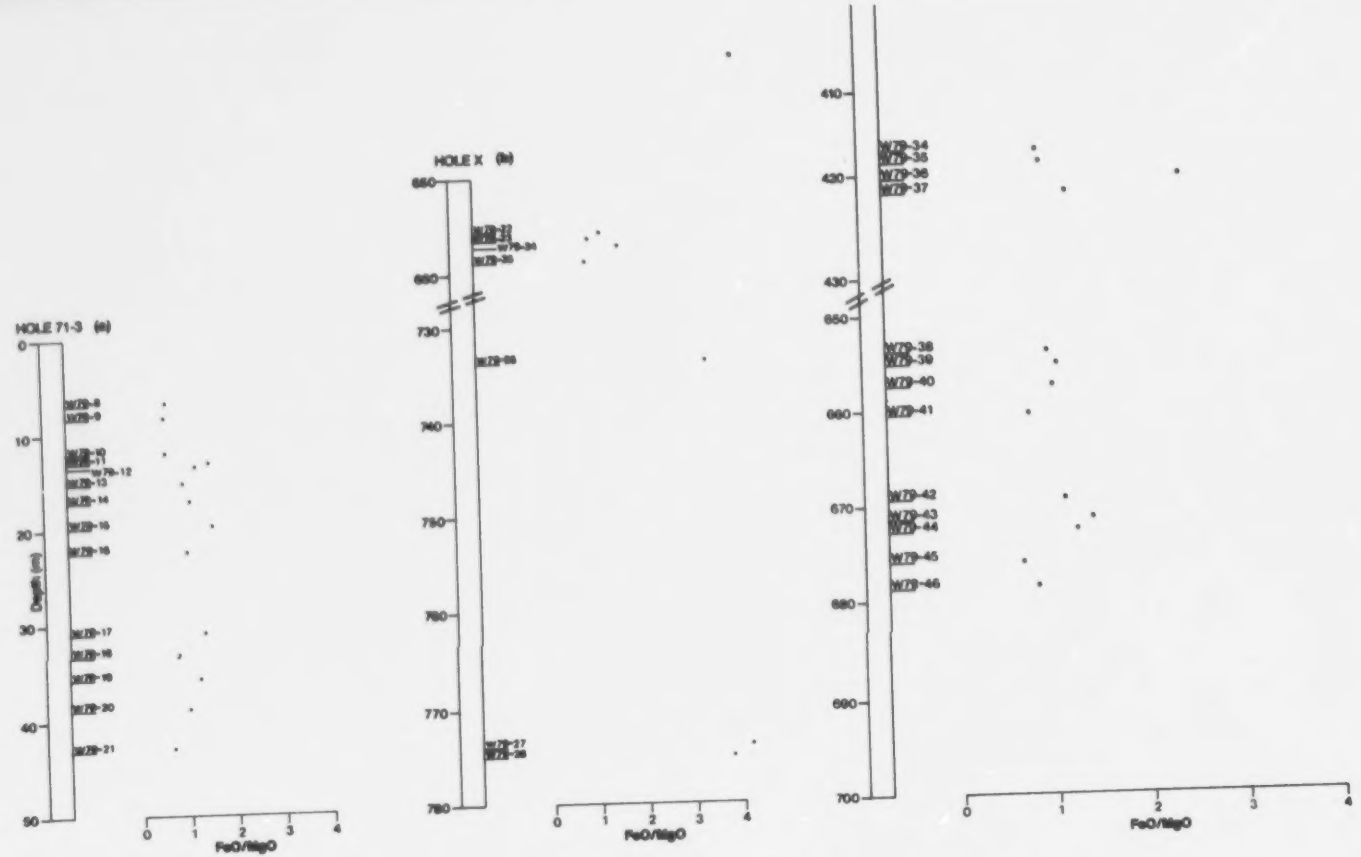

Figure 44a,b,c. *FeO/MgO in chromitiferous anorthositic gabbro, Crystal Lake Gabbro.*

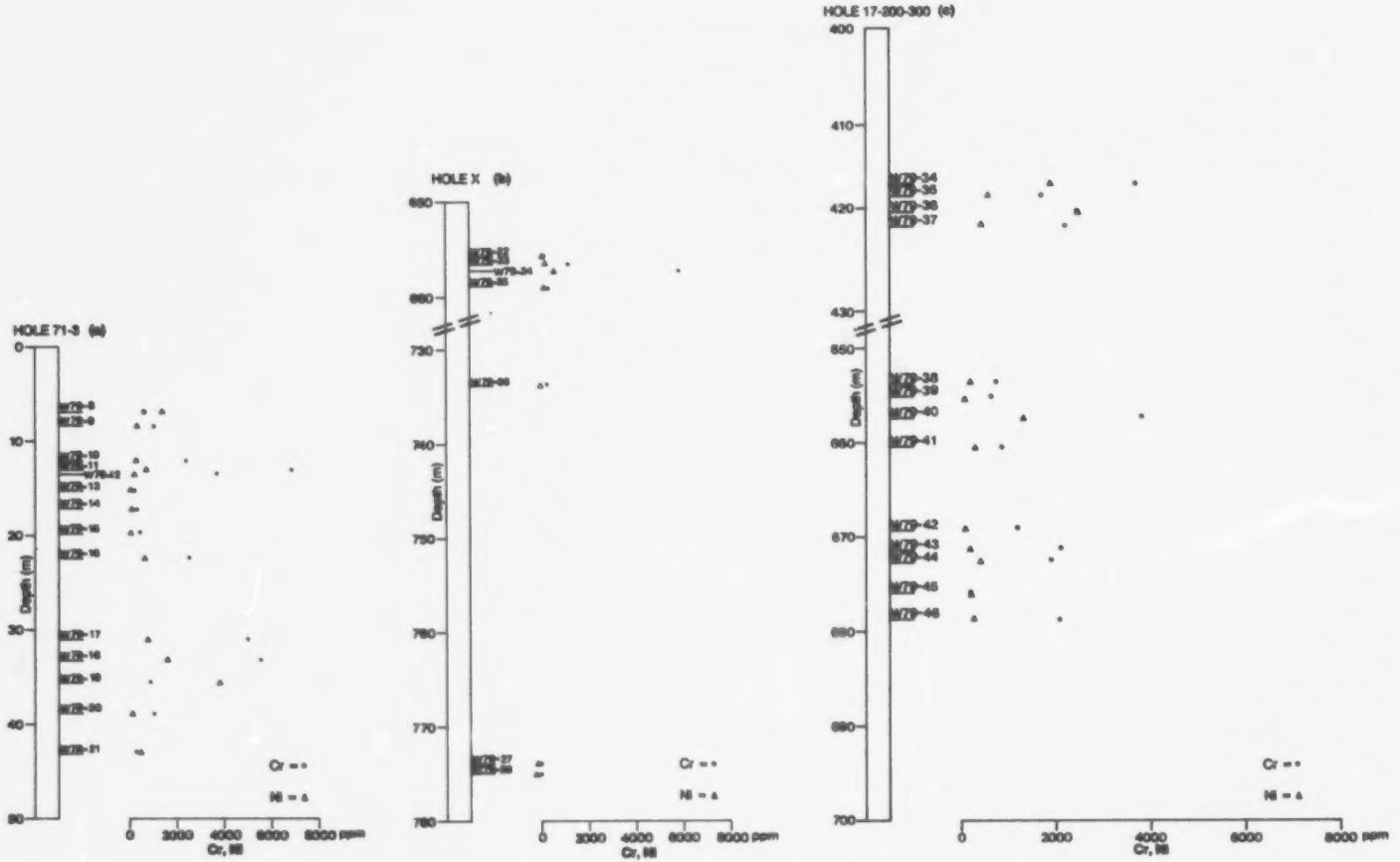

Figure 45a,b,c. *Cr and Ni values for samples from chromitiferous anorthositic gabbro, Crystal Lake Gabbro.*

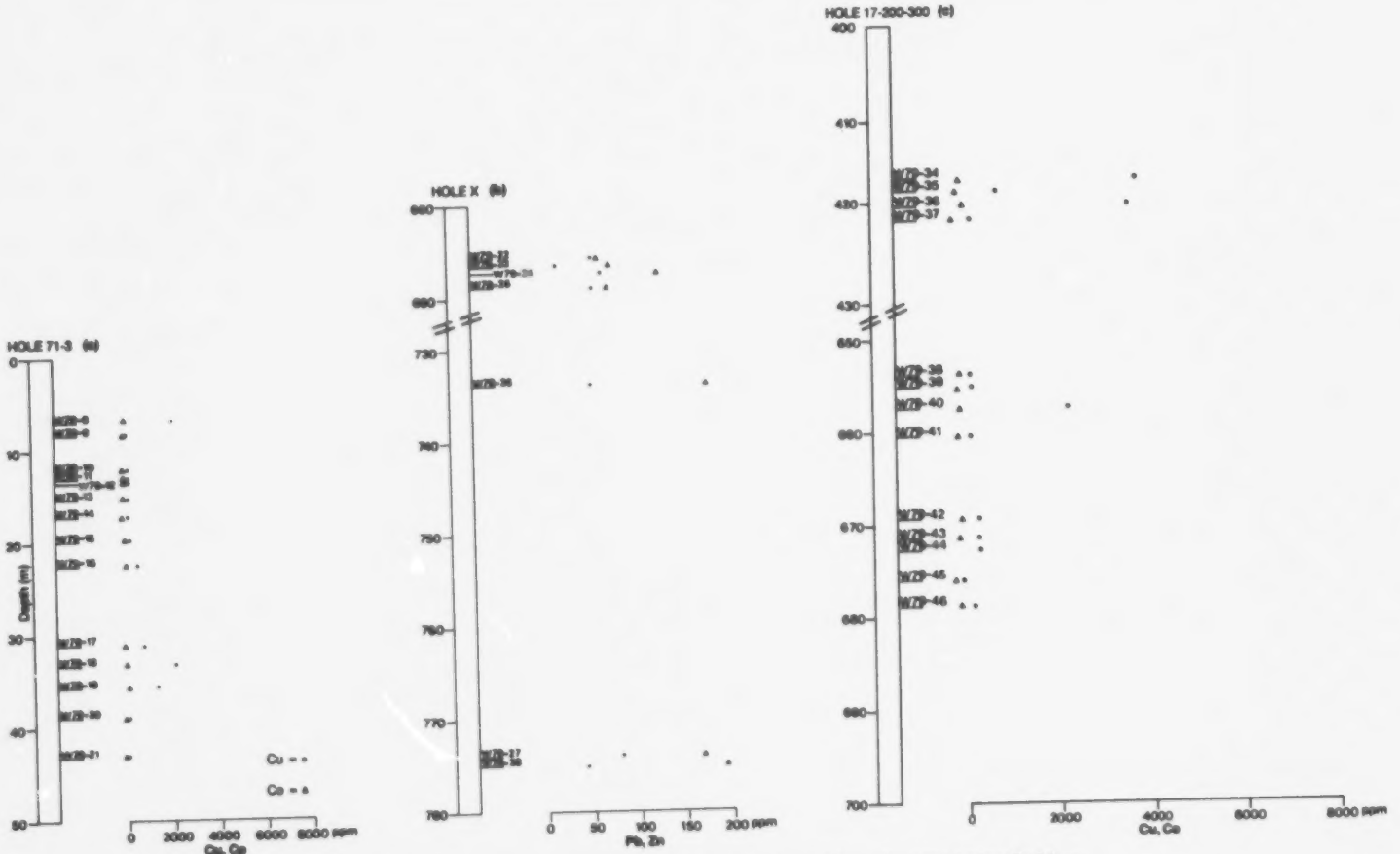

Figure 46a,b,c. *Cu and Co values for samples from chromitiferous anorthositic gabbro, Crystal Lake Gabbro.*

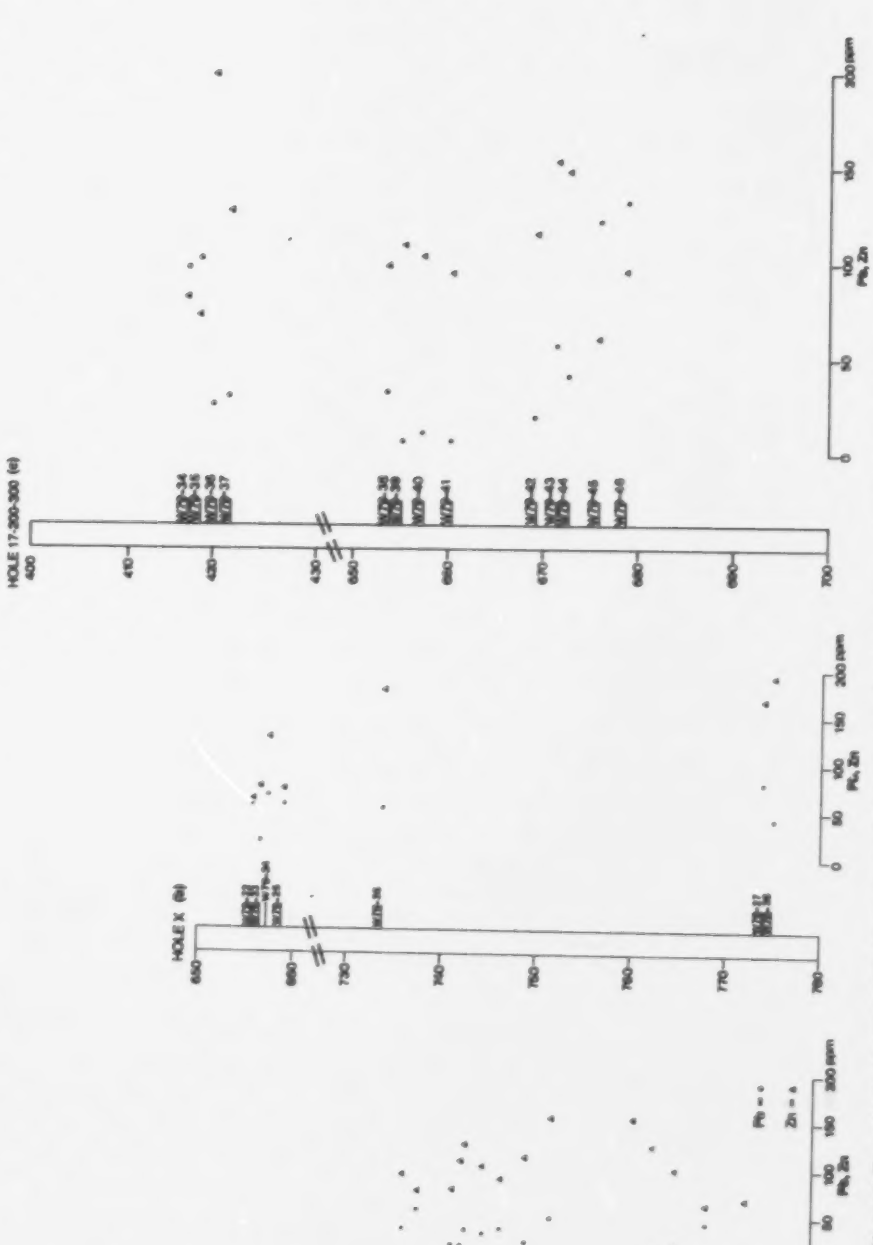

Figure 47a,b,c. Pb and Zn values for samples from chromitiferous anorthositic gabbro, Crystal Lake Gabbro.

values at the extreme end of the diagram. The gabbro zone grouping is in keeping with the bulk composition of this layered anorthositic gabbro to gabbroic intrusion.

SUMMARY

Both the major and trace element chemistry of the Crystal Lake Gabbro reflect the homogeneous nature of the sill. The sections sampled are characteristic of most of the exposed outcrop and of the rock encountered in drill core. The bulk chemical homogeneity is thus applicable only to this portion of the sill and the deeper, inaccessible roots of the intrusion would likely show more primitive compositions. The anomalous presence of chromite is reflected by the higher Cr analyses.

Chromite from the Crystal Lake Gabbro is of heterogeneous compositional character. The very fine grained chromite, which occurs poikilitically included within both plagioclase and the mafic silicates, has been analyzed by electron microprobe. The data reveal a wide variation in composition between individual chromite grains trapped within the same silicate mineral. In the case of TiO_2, a variation of 15 weight percent between adjacent chromite grains is not uncommon, and similar variations are shown by MgO, Cr_2O_3, and MnO. Similarly, intercumulate chromite grains are also chemically heterogeneous. In the Duluth Complex, chromite showing similar heterogeneity is encountered where contamination from country rock shales is evident and has resulted in the formation of V_2O_5-rich chromites (Paul Mainwaring, Research Associate, Carleton University, Ottawa, personal communication, 1979).

The potential of the Crystal Lake Gabbro to host major concentrations of chromite is considered to be low due to the apparent absence of chromitite layers. The limited size of the intrusions is also a consideration. However, it is of interest that chromite occurs associated with an anorthositic gabbro of Proterozoic age. This would suggest that exploration of other layered complexes with anorthositic phases should be considered as targets for chromite mineralization.

The similarities in lithology to the Duluth Complex and the presence of chromite in both intrusions suggests a genetic relationship between the Duluth and Crystal Lake intrusions.

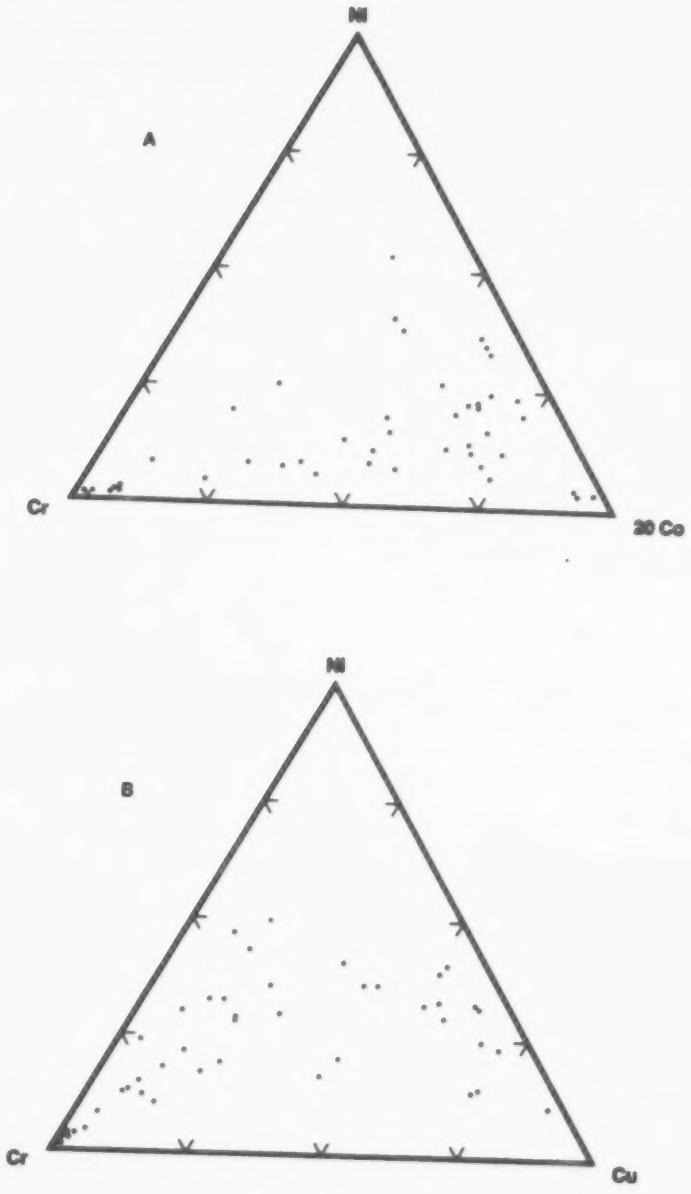

Figure 48. Plot of Ni-Cr-Co and Cu values from the Crystal Lake Gabbro showing a wide range between Co and Cu values. Co has been amplified X20 to avoid congestion on the Cr-Ni join.

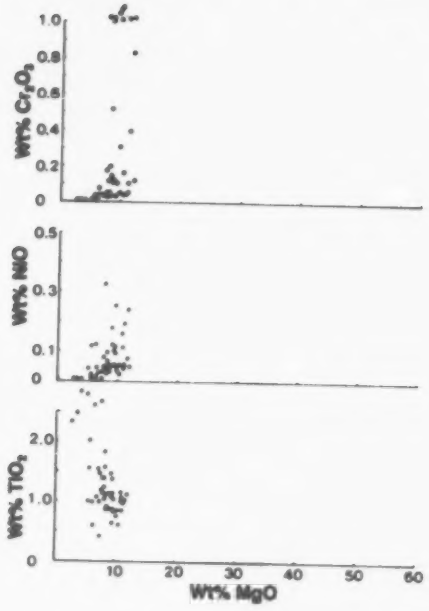

Figure 49. Plot of Cr_2O_3, NiO, TiO_2 (weight percent) vs. MgO (weight percent) from Crystal Lake Gabbro analyses.

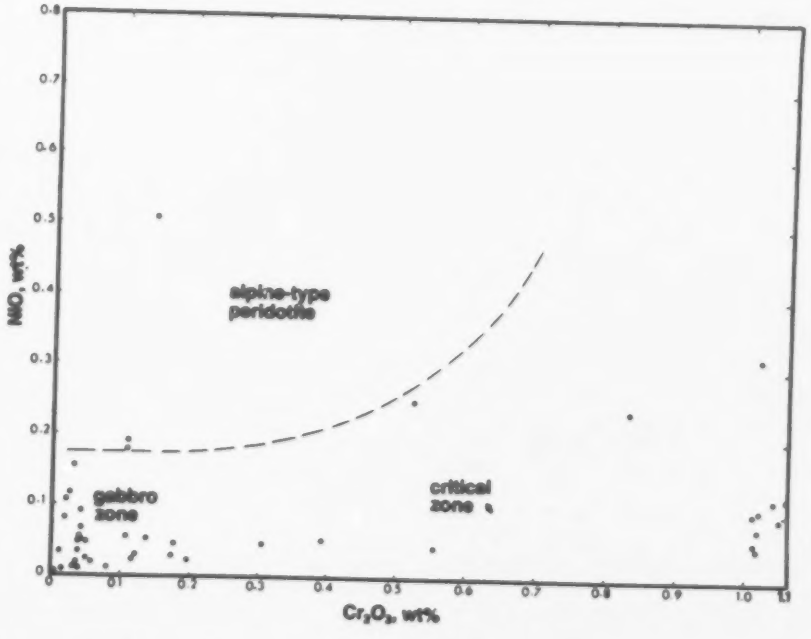

Figure 50. Plot of NiO (weight percent) vs. Cr_2O_3 (weight percent) of Crystal Lake Gabbro analyses predominantly within the gabbro zone (after Irvine and Findlay 1972). The high Cr_2O_3 points are from samples with approximately 15% to 20% disseminated chromite.

Other Chromite Occurrences

Other chromite occurrences considered during this study are representative of subvolcanic hypabyssal to extrusive environments. Chromite, associated with the Shebandowan Cu-Ni deposit, represents a hypabyssal subvolcanic environment, while chromite in ultramafic flows in the Timmins area represents a volcanic extrusive environment.

SHEBANDOWAN MINE

The Shebandowan Cu-Ni deposit is developed in a serpentinized ultramafic (peridotite) intrusion which has intruded as a sill-like body into a metavolcanic sequence (Morin 1973). The ultramafic body strikes approximately east, dips steeply south, and is in fault contact with andesitic pyroclastic rock to the south. This fault zone (Crayfish Creek Fault) is the locus of chromite mineralization in the serpentinite body. The distribution of chromite is given in plan view (Figure 51) and in vertical section (Figures 52 and 53). Intersections of the chromite zone (about 3 m wide) have been recorded in exploration drill holes in the 400-foot, 600-foot, 800-foot, and 1200-foot levels of the Shebandowan Mine.

CHROMITE ZONE

Finely disseminated chromite occurs over a 3 m wide zone in layered and brecciated form. The main chromite layer is 10 to 11 cm thick and has 40 to 50 modal percent very fine grained chromite. On either side of this main layer are found brecciated fragments of chromitiferous serpentinite. These fragments, along with the serpentinite matrix, which carries minor disseminated chromite, are strongly foliated. This intense schistosity defines the Crayfish Creek Fault zone which extends into the country rocks. Microprobe analyses of the core areas of the chromite grains by Morton (1979) suggest a primary magmatic origin for the chromite.

CHROMITE IN THE EXTRUSIVE ENVIRONMENT

Chromite occurs as an accessory mineral associated with komatiitic flows in Archean greenstone environments throughout Ontario. The Timmins area was chosen as an example of this environment.

In the Timmins area, numerous localities of komatiitic flows have been recognized (Muir 1975, Naldrett and Mason 1968, and Pyke *et al.* 1973). Within these flows, chromite often occurs as an accessory mineral and occasionally it may accumulate to form thin layers (MacRae 1965, 1969; Coad 1979). Chromite is usually very fine grained and euhedral (Arndt *et al.* 1977) and occurs as interstitial grains between olivine crystals. At the Langmuir nickel sulphide deposit, chromite occurs at the base and at the top of the massive sulphide layers. Within the massive sulphide zones of pyrrhotite and pentlandite, chromite rimmed by magnetite forms small discontinuous layers; chromium values from these rocks seldom exceed 0.5% Cr (Green 1978).

The early extrusive environment represented by komatiitic flows commonly has accessory chromite. Observed concentrations of chromite in komatiitic flows form thin discontinuous layers of no economic significance. Consequently, the Ontario Precambrian extrusive environment is not suggested as an important exploration target for chromite.

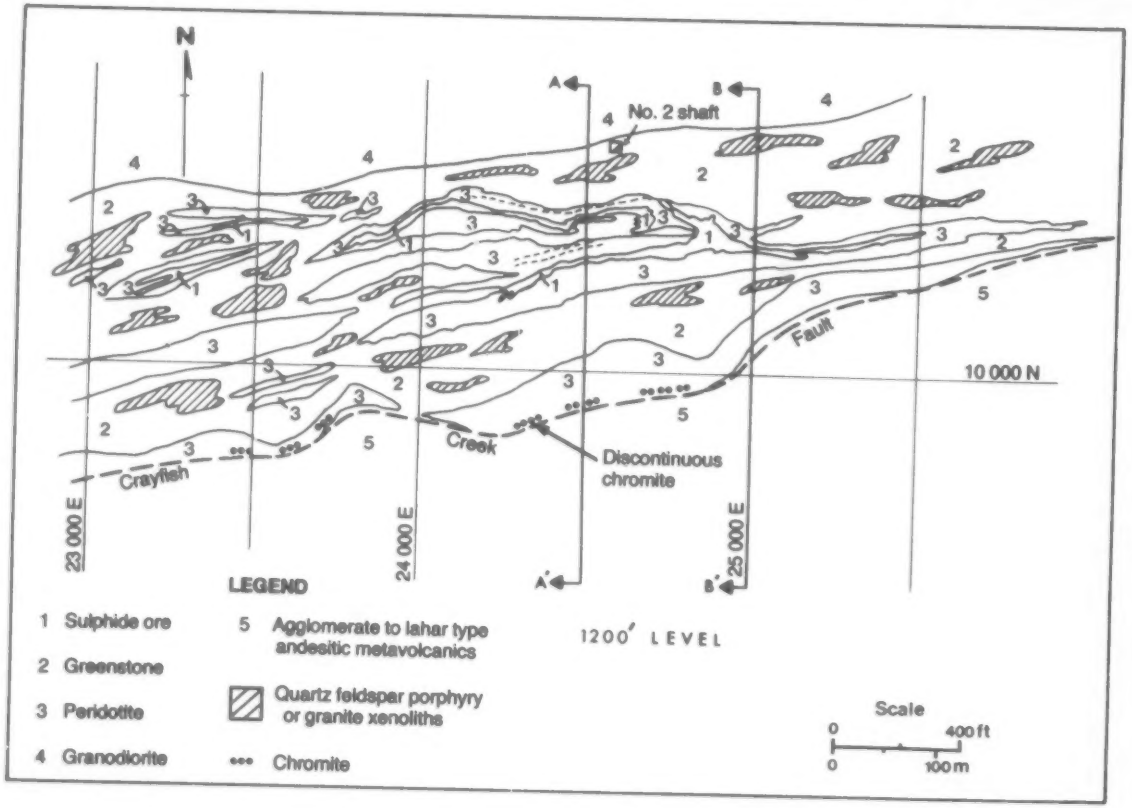

Figure 51. Simplified plan of ultramafics and ore at Shebandowan Mine on the 1200-foot level (modified after INCO plans). Details for Sections A-A' and B-B' are on Figures 52 and 53.

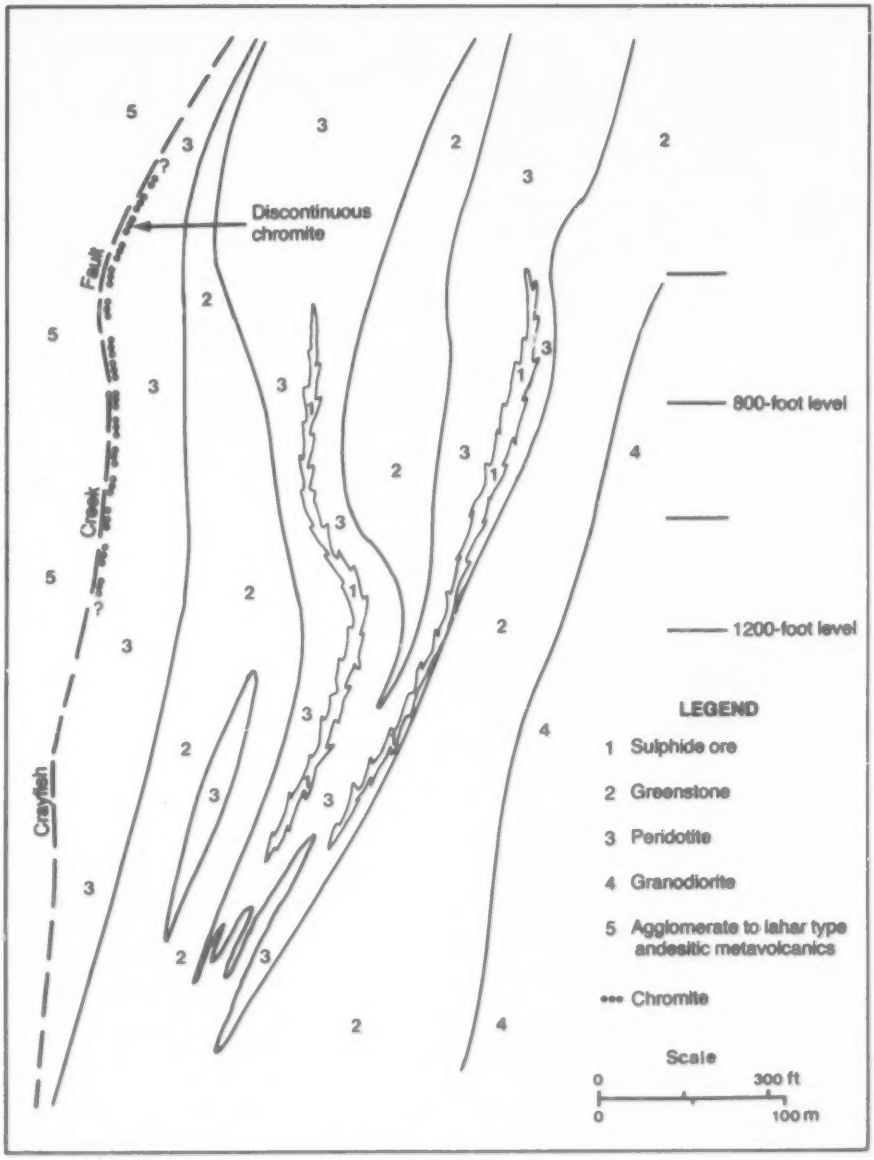

Figure 52. *Section A-A' looking west, Shebandowan Mine (modified after INCO sections).*

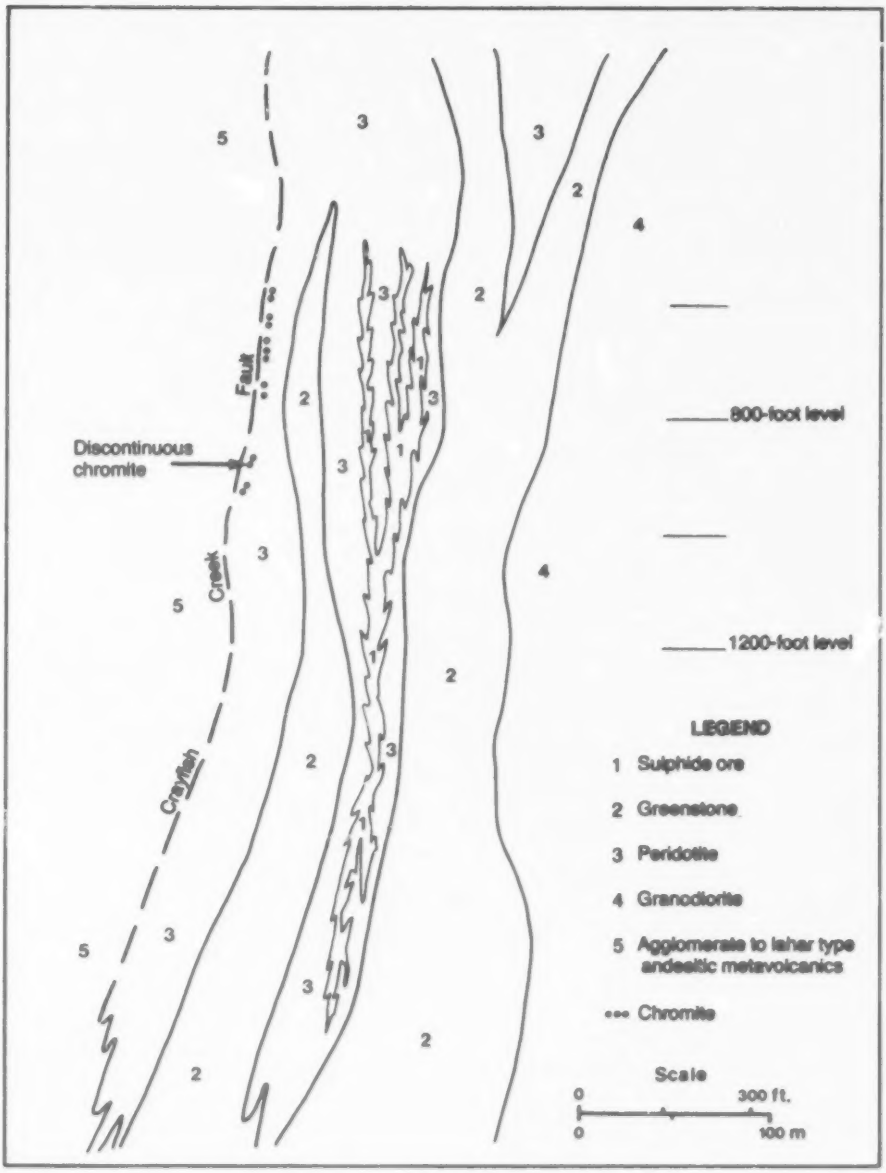

Figure 53. *Section B-B' looking west, Shebandowan Mine (modified after INCO sections).*

Summary and Conclusions

Chromite in Ontario occurs in ultramafic and mafic suite rocks which represent three distinct crystallization environments (Table 12): plutonic, hypabyssal, and extrusive. Minor chromite concentrations are also found in sedimentary rocks.

The plutonic environment is represented by serpentinites of the Puddy-Chrome Lakes serpentinite, which carries both layered and podiform chromite. The search for smaller ultramafic bodies may yield higher grade-lower tonnage deposits similar in style to ophiolitic podiform chromite where it has been economically recovered (e.g. Cyprus, Greenbaum 1977).

Hypabyssal rocks of ultramafic and mafic affinity contain variable amounts of chromite in both disseminated and thinly layer form. Chromite has been recognized in the lower portions of peridotitic-gabbroic sills in the Abitibi area (MacRae 1965) and in the Dundonald intrusion (Naldrett and Mason 1968). In both occurrences, chromite is present in amounts varying from trace to a maximum of 5 modal percent.

Another example of this environment is found at the Shebandowan Nickel Deposit where chromite in disseminated form occurs throughout most of the "Mine Ultramafic". Poorly defined chromite layers 1 to 2 cm thick, with 30 to 40 modal percent chromite, occur at the base of the ultramafic body in a zone approximately 0.5 m wide (Morton 1979).

Chromite is also developed in the Crystal Lake gabbro, a fractionated olivine gabbro to anorthositic gabbro (Geul 1970). Chromite layers developed within the anorthositic gabbro are diffuse and contain 1 to 20 modal percent very fine grained chromite. The layers are 1 to 2 cm thick and are widely separated (2 to 3 m) by anorthositic gabbro containing 5 to 10 modal percent of very fine grained disseminated and euhedral chromite. The disseminated chromite grains appear as fine black specks both within and interstitial to plagioclase phenocrysts. Disseminated chromite in irregular patches is also found from the lower portion of the anorthositic gabbro to the lower contact of the olivine gabbro with the underlying Rove Formation shales.

Gabbroic-anorthositic suite rocks, such as those described by Hudec (1964) at Big Trout Lake, may represent a similar environment for chromite. This hypabyssal environment for ultramafic-gabbroic-anorthositic suite rocks is similar to that of the Bushveld Complex in South Africa (Hunter 1979) and the Stillwater Complex in Montana (Hess 1960), where economic deposits of chromite and associated platinum group metals occur.

Past-producion of chromite ore at Puddy-Chrome Lakes (Figure 9) represents the only attempt at development of a chromit occurrence in Ontario.

Exploration for additional chromite deposits should be centred around Archean layered anorthositic bodies with mafic to ultramafic components. Ontario's best example of this is the Big Trout Lake layered complex. Other anorthositic complexes worthy of study include the Mulcahy Lake Stock (Blackburn 1978) and the Bad Vermilion Lake anorthositic rocks, some of which are texturally similar to anorthositic rocks at Big Trout Lake. Layered Archean anorthositic complexes generally are large enough to allow for the collection of substantial quantities of chromite, as is evidenced by the Stillwater Complex in Montana (Hess 1960; Page and Simon 1978).

Most Proterozoic and Late Precambrian anorthositic rocks, with the exception of the Crystal Lake Gabbro chromite deposit, exhibit only minor spinel concentrations. The large size and massively layered structure of complexes such as the East Bull Lake Complex (Born and James 1978), the Shakespeare-Dunlop Complex (James and Harris 1977), and the Shawmere Complex (Riccio 1979) are favourable for large concentrations of opaques. However, field work in the Shawmere and other complexes reveals a lack of either disseminated or layered opaque mineralization. These anorthositic rocks may be too evolved to carry Cr-spinel, which would be associated with the earlier more basic phases, perhaps hidden at depth.

Komatiitic rocks represent the extrusive ultramafic environment where trace amounts of chromite (up to 1 modal percent) occur. Very fine grained euhedral chrome spinel is described by Arndt *et al.* (1977) in the Munro Township

TABLE 12. SUMMARY OF CHROMITE—BEARING DEPOSITS IN ONTARIO.

Deposit	Type	Age	Oxide-Sulphide Assemblage	Style of Chromite Mineralization	Mean Cr/Fe Ratio (where available)
Puddy Lake	Plutonic	Archean	Chromite + Ni-magnetite + chalcopyrite + pentlandite	Layered, Podiform, Interstitial	2.45
Big Trout Lake	Hypabyssal	Archean	Chromite + magnetite + chalcopyrite	Layered, Interstitial	0.82
Crystal Lake Gabbro	Hypabyssal	Proterozoic	Chromite + magnetite + chalcopyrite + pentlandite	Layered, Interstitial	n/a
Shebandowan	Hypabyssal	Archean	Chromite + pentlandite + chalcopyrite	Interstitial, Layered	n/a
Timmins Area	Extrusive	Archean	Chromite + magnetite + chalcopyrite + pentlandite + pyrrhotite	Layered, Interstitial	n/a

komatiites. This environment offers negligible potential for economic concentrations of chromite.

Metallurgy is a prominent factor in chromium recovery and, at present, high Fe chromite is unsuitable for refining. Advances in metallurgical processes, however, can bring about the lowering of the Cr/Fe ratio as a limit to ore grade chromite. Near Kemi, Finland, an open pit chromite mine produces a low grade ore with a Cr/Fe ratio of 1.6:1 (The Northern Miner, September 1979). Ontario chromite, much of which has Cr/Fe ratios of 1.4:1 to 1.5:1 should therefore remain of interest.

References

Ahmed, Z.
1978: Chromite from Sakhakot-Qila Area, Malakand Agency, Pakistan; Mineralogical Magazine, Volume 42, p.155-157.

Ardnt, N.T., Naldrett, A.J., and Pyke, D.R.
1977: Komatiitic and Iron-Rich Tholeiitic Lavas of Munro Township, Northeast Ontario; Journal of Petrology, Volume 18, Part 2, p.319-369.

Blackburn, C.E.
1978: Populus Lake-Mulcahy Lake Area; p.36-39 *in* Summary of Field Work, 1978, by the Ontario Geological Survey, edited by V.G. Milne, Owen L. White, R.B. Barlow, and J.A. Robertson, Ontario Geological Survey, Miscellaneous Paper 82, 235p.

Bliss, N.W., and MacLean, W.H.
1975: The Paragenesis of Zoned Chromite from Central Manitoba; Geochimica et Cosmochimica Acta, Volume 39, p.973-990.

Born, P., and James, R.S.
1978: Geology of the East Bull Lake Layered Gabbro Anorthosite Intrusion, District of Algoma, Ontario; Current Research, Part A, Geological Survey of Canada, Paper 78-1A, p.91-95.

Buchanan, D.L.
1979: Chromite Production from the Bushveld Complex; World Mining, September, p.97-101.

Burns, V.M., and Burns, R.G.
1975: Mineralogy of Chromium; Geochimica et Cosmochimica Acta, Volume 39, p.903-910.

Card, K.D.
1978: Geology of the Sudbury-Manitoulin Area, Districts of Sudbury and Manitoulin; Ontario Geological Survey, Report 166, 238p. Accompanied by Map 2360, Scale 1:126 720 or 1 inch to 2 miles.

Card, K.D., and Palonen, P.A.
1976: Geology of the Dunlop-Shakespeare Area, District of Sudbury; Ontario Division of Mines, Geoscience Report 139, 52p. Accompanied by Map 2313, Scale 1:31 680 or 1 inch to 1/2 mile.

Chernosky, J.V.
1971: Minerals of the Serpentine Group; Carnegie Institution of Washington Year Book 70, Geophysical Laboratory, p.153-157.

Coad, P.R.
1979: Nickel Sulphide Deposits Associated with Ultramafic Rocks of the Abitibi Belt and Economic Potential of Mafic-Ultramafic Intrusions; Ontario Geological Survey, Study 20, 84p.

Coertze, F.J., Burger, A.J., Walraven, F., Marlow, A.G., and MacCaskie, D.R.
1978: Field Relations and Age Determinations in the Bushveld Complex; Transactions of the Geological Society of South Africa, Volume 81, Part 1, p.1-11.

Downing, J.H.
1971: Discussion of Paper: The Mechanism and Kinetics of Reduction of Transvaal Chromite Ores: Electric Furnace Conference Proceedings, Volume 29, p.93.

DuBois, P.M.
1962: Palaeomagnetism and Correlation of Keweenawan Rocks; Geological Survey of Canada, Bulletin 71, 75p.

Ethem, M.Y.
1979: Turkish Chromite Deposits, Geology, and Operations, World Mining, September, p.73-75.

Geul, J.J.C
1970 Geology of Devon and Pardee Townships and the Stuart Location; Ontario Department of Mines, Geological Report 87, 52p. Accompanied by Map 2207, Scale 1:31 680 or 1 inch to 1/2 mile.

Goldich, S.S., Nier, A.O., Baadsgaart, Halfdan, Hoffman, J.H., and Krueger, H.W.
1961: The Precambrian Geology and Geochronology of Minnesota; Minnesota Geological Survey, Bulletin 41.

Graham, A.R.
1931: Obonga Lake Chromite Area, District of Thunder Bay; Ontario Department of Mines, Annual Report for 1930, Volume 39, Part 2, p.51-60.

Green, A.H.
1978: Evolution of Fe-Ni Sulphide Ores Associated with Archean Komatiites, Langmuir Township, Ontario; Unpublished Ph.D. Thesis, University of Toronto, Toronto, Ontario.

Greenbaum, D.
1977: The Chromitiferous Rocks of the Troodos Ophiolite Complex, Cyprus; Economic Geology, Volume 72, Number 7, p.1175-1194.

Hess, H.H.
1960: Stillwater Igneous Complex, Montana. A Quantitative Mineralogical Study; Geological Society of America, Memoir 80, 230p.

Hiemstra, S.A.
1979: The Role of Collectors in the Formation of the Platinum Deposits in the Bushveld Complex; Canadian Mineralogist, Volume 17, Part 2, p.469-482.

Hudec, P.P.
1964: Big Trout Lake Area; Ontario Department of Mines, Geological Report 23, 35p. Accompanied by Map 2045, Scale 1:126 720 or 1 inch to 2 miles.

Hunter, D.
1978: The Bushveld Complex and its Remarkable Rocks; American Scientist, Volume 66, Number 5, p.551-559.

Hurst, M.E.
1931: Chromite Deposits of the Obonga Lake Area, District of Thunder Bay; Ontario Department of Mines, Annual Report for 1931, Volume 40, Part 4, p.111-119.

Irvine, T.N., and Findlay, T.C.
1972: Alpine-Type Peridotite with Particular Reference to the Bay of Islands Igneous Complex; Canadian Contribution Number Eight to the Geodynamics Project, p.97-140.

Irvine, T.N., and Smith, C.H.
1967: The Ultramafic Rocks of the Muskox Intrusion; p.38-49 *in* Ultramafic and Related Rocks, edited by P.J. Wyllie, New York, Wiley, 464p.

James, R.S., and Harris, B.J.
1977: Geology of Shakespeare-Dunlop Layered Gabbro-Anorthosite Intrusion, Ontario; p.411-414 *in* Report of Activities, Part A, Geological Survey of Canada Paper 77-1A.

Johannes, W.
1968: Experimental Investigation of the Reaction Forsterite + H_2O = Serpentine + Brucite; Contributions to Mineralogy and Petrology, Volume 19, p.309-315.

Kidd, D.F.
1933 Obonga-Kashishibog Area, Thunder Bay District, Ontario; Canada Department of Mines and Resources, Mines and Geology Branch, Summary Report for 1933, Part D, p.16-37.

Kustra, C.R.
1966: Obonga-Leigh Lakes Area, East Half, District of Thunder Bay; p.18-20 *in* Summary of Field Work, 1966, by the Geological Branch, edited by E.G. Pye, Ontario Department of Mines, Preliminary Report 1966-1, 65p.

Lumbers, S.B.
1975: Geology of the Burwash Area, Districts of Nipissing, Parry Sound, and Sudbury; Ontario Division of Mines, Geological Report 116, 160p. Accompanied by Map 2271, Scale 1:126 720 or 1 inch to 2 miles.

MacRae, N.D.
1965: Petrology and Geochemistry of Ultramafic-Gabbroic Intrusions in Abitibi Area, Ontario; Unpublished Ph.D. Thesis, McMaster University, Hamilton, Ontario, 118p.
1969: Ultramafic Intrusions of the Abitibi Area, Ontario; Canadian Journal of Earth Sciences, Volume 6, p.281-303.

Malpas, J., and Strong, D.F.
1975: A Comparison of Chrome-Spinels in Ophiolites and Mantle Diapirs of Newfoundland; Geochimica et Cosmochimica Acta, Volume 39, p.1045-1060

Meyn, H.D.
1979: Uranium Deposits of the Cobalt Embayment; p.218-221 *in* Summary of Field Work, 1979, by the Ontario Geological Survey, edited by V.G. Milne, Owen L. White, R.B. Barlow, and C.R. Kustra, Ontario Geological Survey, Miscellaneous Paper 90, 245p.

Morin, J.A.
1973: Geology of the Lower Shebandowan Lake Area, District of Thunder Bay; Ontario Division of Mines, Geological Report 110, 45p. Accompanied by Map 2267, Scale 1:31 680 or 1 inch to 1/2 mile.

Morton, P.
1979: Volcanic Stratigraphy in the Shebandowan Ni-Cu Mine Area, Ontario; Current Research, Part B, Geological Survey of Canada, Paper 79-1B, p.39-43.

Muir, T.L.
1975: A Petrological Study of the Ultramafic and Related Rocks of the Shaw Dome, Southeast of Timmins, Ontario; Unpublished M.Sc. Thesis, Queen's University, Kingston, Ontario, 271p.

Naldrett, A.J., and Mason, G.D.
1968: Contrasting Archean Ultramafic Igneous Bodies in Dundonald and Clergue Townships, Ontario; Canadian Journal of Earth Sciences, Volume 5, p.111-143.

Page, N.J., Rowe, J.J., and Haffty, J.
1976: Platinum Metals in the Stillwater Complex, Montana; Economic Geology, Volume 71, Number 7, p.1352-1363.

Page, N.J., and Simon, F.O.
1978: Differentiation of the Sulfides in the Basal Zone of the Stillwater Complex, Montana; Journal of Research of the United States Geological Survey, Volume 6, Number 4, p.473-482.

Panayiotou, A.
1978: The Mineralogy and Chemistry of the Podiform Chromite Deposits in the Serpentinites of the Limassol Forest, Cyprus; Mineralium Deposita, Volume 13, p.259-274.

Parsons, C.S.
1937: Investigations in Ore Dressing and Metallurgy, January to June, 1937; Canada Department of Mines and Resources, Mines and Geology Branch, Number 785, 158p.

Peterman, Z.E.
1966: Rb-Sr Dating of Middle Precambrian Metasedimentary Rocks of Minnesota; Geological Society of America Bulletin, Volume 77, Number 10, p.1031-1043.

Pye, E.G., and Fenwick, K.G.
1963: Lakehead-Shebandowan Sheet, District of Thunder Bay; Ontario Department of Mines, Preliminary Geological Map P.177, Geological Compilation Series, Scale 1:126 720 or 1 inch to 2 miles. Compilation 1962.
1965: Atikokan-Lakehead Sheet, Kenora, Rainy River, and Thunder Bay Districts; Ontario Department of Mines, Compilation Map 2065, Scale 1:253 440 or 1 inch to 4 miles. Compilation 1962-1963.

Pyke, D.R., Naldrett, A.J., Eckstrand, O.R.
1973: Archean Ultramafic Flows in Munro Township, Ontario; Geological Society of America Bulletin, Volume 84, Number 3, p.955-978

Raicevic, D.
1977: Methods for Chromium Recovery from Manitoba Bird River Chromite Deposits; Canadian Mining Journal, Volume 98, Number 11, November, p.61-68.

Riccio, L.
1979: Shawmere Anorthosite; p.100-103 *in* Summary of Field Work, 1979, by the Ontario Geological Survey, edited by V.G. Milne, Owen L. White, R.B. Barlow, and C.R. Kustra, Ontario Geological Survey, Miscellaneous Paper 90, 245p.

Robertson, J.A.
1976: Geology of the Massey Area, Districts of Algoma, Manitoulin, and Sudbury; Ontario Division of Mines, Geoscience Report 136, 130p. Accompanied by Maps 2308 and 2309, Scale 1:31 680 or 1 inch to 1/2 mile.

Scarfe, C.M., and Wyllie, P.J.
1967: Serpentinite Dehydration Curves and their Bearing on Serpentine Deformation in Orogenesis; Nature, Volume 215, p.945-946.

Shannon, R.D., and Prewitt, C.T.
1969: Effective Ionic Radii in Oxides and Fluorides; Acta Crystallographica, B25, p.925-946.

Simpson, P.R., and Chamberlain, J.A.
1967: Nickel Distribution in Serpentinites from Puddy Lake, Ontario; Proceedings of the Geological Association of Canada, Volume 18, p.67-91.

Spangenburg, K.
1943: Die Chromitlsagerstatte oon Tempedal in Zobten; Zeitschrift fur Praktische Geologie, Volume 51, p.13-35.

Spooner, E.T.C., Beckinsale, R.D., Fyfe, W.S., and Smewing, J.D.
1974: O^{18} Enriched Ophiolitic Metabasic Rocks From E. Liguria (Italy), Pindos (Greece), and Troodos (Cyprus); Contributions to Mineralogy and Petrology, Volume 47, p.41-62.

Spry, A.
1969: Metamorphic Textures; Pergamon Press, 350p.

Tanton, T.L.
1931: Fort William and Port Arthur, and Thunder Cape Map Areas, Thunder Bay District, Ontario; Geological Survey of Canada, Memoir 167, 222p.
1936a: Pigeon River Area, Thunder Bay District, Sheet 1; Canada Department of Mines Map 354A, Scale 1:63 360 or 1 inch to 1 mile.
1936b: Pigeon River Area, Thunder Bay District, Sheet 2; Canada Department of Mines Map 355A, Scale 1:63 360 or 1 inch to 1 mile.
1935: Copper-Nickel Mineral Occurrences in Pigeon River Area, Ontario; Geological Survey of Canada, Paper 35-1, 11p.

Thurston, P.C., Sage, R.P., and Siragusa, G.M.
1971: Operation Winisk Lake: Wunnummin Lake-Big Trout Lake Sheet, District of Kenora (Patricia Portion); Ontario Department of Mines and Northern Affairs, Preliminary Map P.712, Geological Series, Scale 1:126 720 or 1 inch to 2 miles. Geology 1971.
1979: Geology of the Winisk Lake Area, District of Kenora, Patricia Portion; Ontario Geological Survey, Report 193, 169p. Accompanied by Maps 2287 and 2292, Scale 1:253 440 or 1 inch to 4 miles.

Tyrrell, J.B.
1913: Hudson Bay Exploring Expedition, 1912; Ontario Bureau of Mines, Annual Report for 1913, Volume 22, Part 1, p.161-209.

Wicks, F.J., and Whittaker, E.J.W.
1977: Serpentine Textures and Serpentinization; Canadian Mineralogist, Volume 15, Part 4, p.459-488.

INDEX

Abitibi area 86
Actinolite 43
Alkalies, total 52
Alpine-type:
  Intrusion 31
  Peridotite 5,30
    Zone 52
  Trace element data 30
  Ultramafics 28
Alteration 15,18
  Dendritic 15
  Deuteric 71
  Hematitic 44
  Post-cumulus 28
  Synkinematic 26
  Variegated 15
Amphibole 11,44
  Blades 70,71
  Gabbro 40
    Dike 43
Analyses, electron microprobe 26,82
Andesite:
  Metabasalt complex 37
  Pyroclastic rock 82
Anomaly, magnetic 55
Anorthosite 5,40,52
  Gabbroic 37,40,43,52
    Leucocratic 40
Anorthositic gabbro 37,40,52,62,70-72,86
  Porphyritic rocks 40
Anticlines 37,40
Antigorite 15,17,25,43
  Rims 43
Aphanitic gabbro 70
Archean 86
  Greenstone 82
  Metavolcanic rocks 52
Augite 71

Bad Vermilion Lake 86
Basalt 7,9
  Komatiites 6
Bastite 25
  Lizardite 21
Bay of Islands Ophiolite Complex 28,52
Bibby Bay 40
Big Trout Lake Complex, chromitiferous portion 52
Big Trout Lake Intrusion 52
Boudinage-style undulations 40
Boudinage-type structures 17
Breccia 44,82
  Chromite 44
  Serpentinite 43
Bricks 5
Brucite 17,26
Burwash 7
Bushveld Complex, South Africa 5,6,50,52,55,86
  Ore reserves 6
  Steelport bed 6
Bytownite 71

Carbonate 43
Chalcopyrite 50,70
Chemistry:
  Major element 28
  Trace element 30
Chlorite 17,20,43
  Flakes 26
Chromian magnetite 26
  Field 27
Chromite:
  Aggregates 44
  Anhedral grains 18
  Breccia 44
  Clustered grains 18
  Cores 52
  Corrosion 18
  Ferrian 26
  Grades:
    Chemical 5
    Concentrate 11
    Metallurgical 5
    Refractory 5
  Grains:
    Relict boundaries 20
    Isolated 18
  Magnesiochromite 5
  Massive 15,17
  Podiform:
    Deposit 28
    Mineralization 15,17,20
    Ophiolitic 86
    Type 6
  Production:
    Pakistan 6
    Turkey 6
  Reserves, Turkey 6
  Rims 27,52
  Subhedral grains 18
  Ultramafic rocks 17
Chromitiferous portion, Big Trout Lake complex 52
Chromitite layers 17,18
Chromium concentration 6,9
Chromium Mining and Smelting Corp. Ltd. 11

Cleavage traces 25
Clinopyroxene 71,72
Columnar structure 25
Commerce Nickel Mines Ltd. 21
Contact:
  Quartzofeldspathic paragneiss-volcanogenic metasediment 11
Cr-spinel 71
Cr/Fe ratios 6,31
Crayfish Creek Fault 82
Critical zone 52
Crystal Lake Gabbro 79
Crystallization environment:
  Extrusive 86
  Hypabyssal 86
  Plutonic 86
Cumulate:
  Concentrations 15
  Olivine texture 15
Cyprus 86
  Limassol Forest ultramafic complex 26
  Tertiary Troodos complex 6

Deformation, brittle 44
Deuteric alteration 71
Diabase:
  Dikes 62
    Keweenawan 30
  Nipissing 7,9
Diamond drilling 11,37,70
Dikes:
  Amphibolitic gabbro 43
  Diabase 62
  Keweenawan diabase 30
Diorite 40,43
  Quartz 37,43
Drill core 43
Drill holes 43,52,72,82
Duluth Complex 62,72,79
Dundonald intrusion 86
Dunite 6,9,11,15,21,28,37,52
  Ultramafic rocks 52
Dunlop-Shakespeare body 7
Dynamo-thermal metamorphism 18

Early Precambrian sequence 37
East Bull Lake:
  Complex 7,86
  Intrusion 7
Electron microprobe analyses 26
Eutectic magma composition 72
Exploration shaft, Puddy-Chrome Lakes 11
Extrusive environment 82
  Volcanic 82

Faulting 43
  Zone 82
Feldspathic peridotite 6,52
Ferrian chromite 26
Ferritchromit 20,26
  Rims 20,50
Ferrochromium alloys 5
Flows:
  Disruption 70
  Komatiitic 9,82
  Ultramafic 82
Fluid mobility 26
Fluid transfer of elements 26
Foliation 17,31
Forsterite 17
Fractionation 30,52,72
Fractures 50,71
  Hackly 17

Gabbro 7,9,52,70
  Amphibolitic 40
    Dikes 43
  Anorthositic 37,40,52,62,70-72,86
  Aphanitic 70
  Basalt groups 9
  Crystal Lake 79
  Massive 70
  Olivine 62,70,71,86
  Pegmatitic 70
    Olivine 72
  Peridotite sills 86
  Quartz 62
  Zone 72
Gabbroic anorthosite 37,40,43,52
  Leucocratic 40
  Rocks 7,86
Gander River Belt, Newfoundland 28
Gangue material 5
Granophyre 5
  Phase 52
Great Lakes Nickel Ltd. 62,70
Greenschist conditions:
  Low to medium 44
  Lower amphibolite 44
Greenstone, Archean 82
Grenville Province 7

Hematitic alteration 44
Highway 597 62
Hornfelsed fragments 70

Huronian Supergroup 7,9
Hypabyssal intrusion 52
Hypabyssal rocks 86

Inclusions 71
  Opaque 72
  Poikilitic 71
  Serpentine 18,20
  Zones 50
Intrusions:
  Alpine-type 31
  Big Trout Lake 52
  Dundonald 86
  East Bull Lake 7
  Hypabyssal 52
  Layered stratiform-type 55
  Muskox 6,52
  Serpentinized ultramafic peridotite 82
  Silicate 50
  Stillwater 6
  Stratiform 52
    Layered 5
  Ultramafic 9,11
Intrusive rocks 37
Iron 11,21,71
  Enrichment 27,52
  See also: Magnetite

Kemi, Finland 88
Keweenawan diabase dike 30
Komatiites 9
  Basaltic 6
  Flows 9,82
  Munro Township 86
  Rocks 86
  Ultramafic 6
  Volcanic rocks 5

Labradorite 71
Langmuir nickel sulphide deposits 82
Late Precambrian rocks 86
Layered chromitite 17,18
Leopard Point 37,40,43
Leucocratic gabbroic anorthosite 40
Limassol Forest ultramafic complex, Cyprus 26
Lizardite 15,17,20,21,25,43
  Bastite 21
  Intergrown 25
  Matrix 18
  Ribbony 25
  Rims 44
Logan Sills 62

Mafic minerals 70,71
Mafic rocks 9,86
Magma 72
Magnesiochromite 5
Magnesite 15,43
Magnetic anomaly 55
Magnetic data 11
Magnetite 15,20,21,28,30,52,71
  Chromium 28
    Field 27
  Nickel-bearing 30
  Rims 20,50,82
  Veins 11
  Ultramafic rocks 17
Margins 28
McKim Formation 9
Metabasalt-andesite complex 37
Metallurgical processes 88
Metamorphism:
  Dynamo-thermal 18
  Features 18
Metapelite 9
Metapyroxenite 7
Metasediments 11
Metasiltstones, Mississagi Formation 9
Metavolcanic rocks:
  Archean 52
  Sequence 82
Micaceous (chloritic) seam 72
Micaceous phase 17
Mica 44
Microprobe analysis 82
Mineralization:
  Iron 11
Mississagi Formation metasiltstones 9
Mulcahy Lake Stock 86
Munro Township komatiites 86
Muskox Intrusion 6,52

Nelson, S., property 31
Nemeigusabins Lake 43
Nickel:
  Langmuir sulphide deposits 82
  Shebandowan Deposit 86
  Sulphide-bearing zone 72
Nickel-bearing magnetite 30
Nipissing Diabase 7,9

Olivine 5,15,17,21,25,43,44,62,72
Clinopyroxenite 52
Crystals 82
Cumulate 43
Gabbro 62,70,71
Fractionated 86
Phenocrysts 11,15
Relict 21
Relict 44
Opaque minerals 71,72
Interstitial 71
Ophiolite complexes 6
Bay of Islands 28,52
Ophiolitic podiform chromite 86
Ophiolitic suites 5
Optical continuity 71
Ore:
Friable 5
Hard lumpy 5
Reserves, Bushveld Complex 6
Orthopyroxenite 6
Oxide minerals 72
Oxide phase 30,72
Oxygen fugacity 11

Pakistan, Chromite production 6
Paragneiss 11,26
Xenoliths 11
Pardee Township 62
Pegmatite:
Gabbro 70
Olivine gabbro 72
Penokean Orogeny 62
Pentlandite 70,82
Peridotite 5,6,9,11,21,28,43,52
Alpine-type 5,30
Zone 52
Feldspathic 6,52
Gabbroic sills 86
Serpentinized 37
Petrogenetic indicator 5
Phenocrysts:
Olivine 11,15
Relict 21
Plagioclase 70
Interstitial 86
Pickle Lake 37
Plagioclase 5,40,71
Corrosion 71
Cumulate 71
Intercumulate 71
Laths 70-72
Phenocrysts 70
Interstitial 86
Twinned 72
Platinum 55
Platinum group elements (PGE) 50,55,86
Values 6
Podiform chromite:
Mineralization 15,17,20
Ophiolitic 86
Polkilitic 71,72
Inclusions 71
Porphyritic anorthositic rocks 40
Post Island 37
Post-cumulus alteration 28
Post-kinematic growth 26
Precambrian 82
Primary magmatic origin 82
Proterozoic 62,79
Rocks 86
Puddy-Chrome Lakes, exploration shaft 11
Pyroclastic rocks, andesitic 82
Pyroxene 5,15,21,25,44,72
Cumulate 43
Pyroxenite 11,21
Pyrrhotite 70,82

Quartz:
Diorite 37,43
Gabbro 62
Quartzofeldspathic paragneiss-volcanogenic metasediment, contact 11

Red Lake 37
Retrograde conditions 44
Rove Formation 62,70,86

Sault Ste. Marie 7
Schistosity 82
Schlieren structure 6
Schlieren-type concentrations 15
Sedimentary rocks 37
Semi-crystallized zone 70
Serpentine 17
Assemblages 18
Inclusions 18,20
Serpentinite 11,15,17,21,26,31,40,43
Brecciated 43
Serpentinized peridotite 37
Shakespeare-Dunlop Complex 86
Shales 62,70,86
Laminated 70

Shawmere Complex 86
Shear zones 43
  Proximal 44
Shearing 15
Shebandowan deposit 82
Shebandowan Mine 82
Shebandowan Nickel
  Deposit 86
Silicate:
  Intrusions 50
  Minerals 44,71
  Phase 72
Sill-like body 82
Sills, Peridotitic-gabbroic 86
Slumping 70
Spinel 5,20,86
  Chromium 71
  Structure 28
Steelport bed, Bushveld
  Complex 6
Stillwater Complex, Montana 86
Stillwater Intrusion 6
Stratiform intrusions 52
  Layered 5
Subvolcanic hypabyssal
  environment 82
Sudbury 7
Suites, ophiolitic 5
Sulphide 50,55
  Langmuir nickel deposits 82
  Mineralization 50,70,71,72
  Nickel-bearing zone 72
  Zones 82
    See also Chalcopyrite;
    Pentlandite; Pyrrhotite
Surface, maculose 11
Suture lines 20
Synclinal structures 40
Synkinematic alteration 26

Talcose 43
Talc 15,17,26
Temperature regimes 18
Tertiary Troodos complex,
Cyprus 6
Texture:
  Cumulate 71
    Olivine 15
    Relict 25
  Interfingering 44
  Interlocking 44
  Mesh 25
  Net 6
  Pseudomorphic 43,44
  Sub-ophitic 71
Thunder Bay 62
Till 37
Timmins 82
Trout Lake, community 37
Turkey:
  Chromite production 6
  Chromite reserves 6

Ultramafics 31
  Alpine-type 28
  Contact 31
  Flows 82
  Intrusions 9,11
  Komatiites 6
  Magnetite 17
  Rocks 86
    Dunitic 52
    Types 52

Veins, magnetite 11
Volatiles 15
Volcanic rocks 37
  Komatiites 5
Volcanic extrusive
  environment 82
Volcanogenic metasediment-
  quartzofeldspathic
    paragneiss, contact 11

Wackes 70
Wehrlite 52

Xenoliths 43
  Paragneiss 11